1983

Biocompatibility Investigations Of Surgical Implant Alloys.

Linda Chambers Lucas
University of Alabama at Birmingham

INFORMATION TO USERS

This reproduction was made from a copy of a document sent to us for microfilming. While the most advanced technology has been used to photograph and reproduce this document, the quality of the reproduction is heavily dependent upon the quality of the material submitted.

The following explanation of techniques is provided to help clarify markings or notations which may appear on this reproduction.

1. The sign or "target" for pages apparently lacking from the document photographed is "Missing Page(s)". If it was possible to obtain the missing page(s) or section, they are spliced into the film along with adjacent pages. This may have necessitated cutting through an image and duplicating adjacent pages to assure complete continuity.

2. When an image on the film is obliterated with a round black mark, it is an indication of either blurred copy because of movement during exposure, duplicate copy, or copyrighted materials that should not have been filmed. For blurred pages, a good image of the page can be found in the adjacent frame. If copyrighted materials were deleted, a target note will appear listing the pages in the adjacent frame.

3. When a map, drawing or chart, etc., is part of the material being photographed, a definite method of "sectioning" the material has been followed. It is customary to begin filming at the upper left hand corner of a large sheet and to continue from left to right in equal sections with small overlaps. If necessary, sectioning is continued again—beginning below the first row and continuing on until complete.

4. For illustrations that cannot be satisfactorily reproduced by xerographic means, photographic prints can be purchased at additional cost and inserted into your xerographic copy. These prints are available upon request from the Dissertations Customer Services Department.

5. Some pages in any document may have indistinct print. In all cases the best available copy has been filmed.

University Microfilms International
300 N. Zeeb Road
Ann Arbor, MI 48106

Lucas, Linda Chambers

BIOCOMPATIBILITY INVESTIGATIONS OF SURGICAL IMPLANT ALLOYS

The University of Alabama in Birmingham PH.D. 1983

PLEASE NOTE:

In all cases this material has been filmed in the best possible way from the available copy. Problems encountered with this document have been identified here with a check mark __✓__.

1. Glossy photographs or pages ✓
2. Colored illustrations, paper or print _____
3. Photographs with dark background ✓
4. Illustrations are poor copy _____
5. Pages with black marks, not original copy _____
6. Print shows through as there is text on both sides of page _____
7. Indistinct, broken or small print on several pages _____
8. Print exceeds margin requirements _____
9. Tightly bound copy with print lost in spine _____
10. Computer printout pages with indistinct print _____
11. Page(s) _____ lacking when material received, and not available from school or author.
12. Page(s) _____ seem to be missing in numbering only as text follows.
13. Two pages numbered _____. Text follows.
14. Curling and wrinkled pages _____
15. Other _____

BIOCOMPATIBILITY INVESTIGATIONS OF SURGICAL IMPLANT ALLOYS

BY

LINDA CHAMBERS LUCAS

A DISSERTATION

Submitted in partial fulfillment of the requirements for the degree of Doctor of Philosophy in the Department of Biomedical Engineering in the Graduate School, University of Alabama in Birmingham

Birmingham, Alabama

1982

ABSTRACT OF DISSERTATION

GRADUATE SCHOOL, UNIVERSITY OF ALABAMA IN BIRMINGHAM

Degree Ph.D. Major Subject Biomedical Engineering

Name of Candidate Linda Chambers Lucas

Title Biocompatibility Investigations of Surgical Implant Alloys

Three alloys used for surgical applications, 316L stainless steel (Fe-Cr-Ni, ASTM F138), Co-Cr-Mo (ASTM F75) and Ti-6Al-4V (ASTM F136) were investigated to determine the elemental constituents released during corrosion and to determine the tissue responses elicited under *in vitro* and *in vivo* conditions. *In vitro* testing involved exposing cell cultures to varying concentrations of synthetic solutions based on the alloy's chemical composition and independently to solutions of the elements comprising the alloy. *In vivo* testing involved implanting the alloys in rabbits and injecting synthetic solutions of corrosion products at the implant-to-capsule interface.

In vitro exposure of cell cultures to synthetic stainless steel corrosion product solutions demonstrated toxic responses (inhibited growth rates and altered cellular morphologies) at concentrations as low as 3.0 ppm (representing in ppm 2.0 Fe, 0.6 Cr, and 0.42 Ni). Cell cultures exposed to Co-Cr-Mo solutions demonstrated toxic responses at 1.5 ppm (representing in ppm

1.0 Co, 0.45 Cr, and 0.09 Mo). Individually Fe, Ni, Co, or Mo demonstrated nontoxic responses at these low concentrations. However, chromium was the most toxic. Cells exposed to chromium solutions demonstrated abnormal morphologies above a concentration of 0.375 ppm. Cell cultures exposed to Ti-6Al-4V solutions demonstrated toxic effects at 6.25 ppm (representing in ppm 5.6 Ti, 0.378 Al, and 0.25 V). Individually none of these elements were toxic at these concentrations where collectively a toxic response was observed. Vanadium was the most toxic element of this alloy, demonstrating toxicity above 0.75 ppm.

Histological examinations of fibrous tissue capsules by optical microscopy showed a relative difference between alloys but no direct correlations between tissue response and concentration of solutions injected at the interface. However, transmission electron microscopic analysis of the cellular capsules showed a direct correlation. With increasing concentration, representative cellular ultrastructures showed a decrease in rough endoplasmic reticulum, a more diffuse plasma membrane, an increase in cytoplasmic vaculozation, and a decrease in cellular organization. This trend was consistent for both the in vivo and in vitro cells. Thus, the overall tissue response was dependent on the types and quantities of ions released during biocorrosion.

Abstract Approved by: Committee Chairman 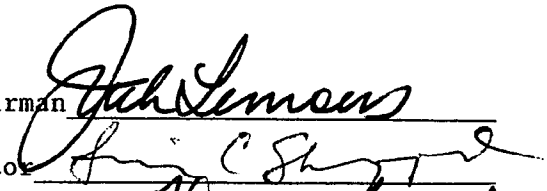

Program Director 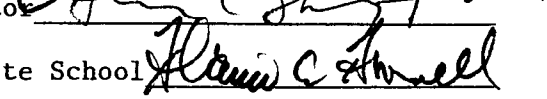

Date 3/18/83 Dean of Graduate School

DEDICATION

For My Mother

ACKNOWLEDGEMENTS

I wish to express my sincere appreciation to the following people: Dr. Jack Lemons for his continued assistance with all aspects of this investigation, Dr. Ray Buchanan for his support with the corrosion investigations and for introducing me to the area of biomaterials, Dr. Larry Bearden for his assistance with the initial TEM investigations, Ms. Patsy Henson and Dr. Glen Malone for their assistance with the animal studies, Ms. Donna Wilson with Alabama Power Company for her support with the atomic absorption analyses, Mr. Frank Denys and Mr. Ron Austin for assistance with the tissue preparations and TEM examinations, Mr. Rick Comptom for printing the many photographs used in this manuscript and to my family and friends for their kind words of encouragement at times when they were really needed.

TABLE OF CONTENTS

TABLE OF CONTENTS (Continued)

TABLE OF CONTENTS (Continued)

LIST OF TABLES

LIST OF FIGURES

LIST OF FIGURES (Continued)

LIST OF FIGURES (Continued)

LIST OF FIGURES (Continued)

LIST OF FIGURES (Continued)

FIGURE PAGE

CHAPTER I

INTRODUCTION

The three major alloys used for surgical applications are iron-chromium-nickel (316L stainless steel, ASTM F138), cobalt chromium-molybdenum (ASTM F75), and titanium-6aluminum-4vanadium (ASTM F136). The stainless steel and cobalt-base alloys were introduced in the late 1920's and early 1930's respectively; the titanium base alloy was not adopted for surgical applications until the 1960's. Thus, the application of these alloys for implantable devices now spans two to five decades, depending on the alloy. During this time much effort was expended to enhance both their mechanical and corrosion resistance properties for surgical applications.

The following sections of this introduction will address the question of biocompatibility for these alloys and examine the current understanding that has developed through their continued use. Biocompatibility involves two criteria: firstly, the response of the material to the host and secondly, the response of the host to the material. For an implant material to be functional both criteria have to be satisfied. Considering the response of the material, the corrosion characteristics of each of the alloys will be examined and considering the response of the host, both

local and systemic tissue responses to ionic constituents released from the implant alloys will be examined.

A. Stainless Steel Surgical Alloy

Today stainless steel is the dominant alloy for the construction of implantable devices. This is mainly due to its early introduction and development, ease of fabrication, variety of mechanical properties, and corrosion resistance (124). In 1926 Strauss was granted a patent for stainless steel (18Cr-8Ni) containing a 2-4% molybdenum addition. It was not until 1945 that the College of Surgeons recognized and recommended the 18-8 stainless steel type 316 for orthopaedic applications (6). In an attempt to standardize and optimize the composition and metallurgical quality of the currently employed implant alloys, implant specifications have been developed within various countries. In the United States, standards have been developed by the American Society for Testing and Materials-ASTM, and in Great Britain by the British Standards Institute-BSI. The ASTM Committee F4 (3) on surgical implants has developed ASTM standards F138 and F139 for stainless steels. Table 1 gives the recommended compositions for both low and high carbon types. The ASTM Designation F138-76 also includes a metallurgical requirement for a maximum inclusion content. Lower inclusion contents can enhance corrosion resistance as well as mechanical behavior (eg. fatigue) (124).

Stainless steels are produced in four main classes: ferritic, martensitic, austenitic, and precipation-hardenable. The 316L (low

Table 1

ASTM Specifications for 316 Stainless Steel Alloy

Element	Low Carbon Steel (Wt.%)	High Carbon Steel (Wt.%)
Carbon (Max)	0.030	0.08
Manganese (Max)	2.00	2.00
Phosphorous (Max)	0.025	0.025
Sulfur (Max)	0.010	0.010
Silicon (Max)	0.75	0.75
Chromium	17.00 - 20.00	17.00 - 20.00
Nickel	12.00 - 14.00	12.00 - 14.00
Molybdenum	2.00 - 4.00	2.00 - 4.00
Iron	Balance	Balance

carbon) stainless steel recommended for surgical applications is an austenitic steel. The austenitic structure is desired primarily due to its improved corrosion resistance. To maintain a fully austenitic structure at room temperature proper alloying is essential. While chromium is added for enhanced corrosion resistance, chromium is a ferrite stabilizer. Nickel, at concentrations <8%, added to the iron-chromiom system will enlarge the austenitic field such that the formation of the ferritic phase is suppressed. Other elements such as manganese and nitrogen are also added to aid in the formation of a stable austenitic structure. Molybdenum added to the alloy enhances the corrosion resistance of the

material due to its stabilizing influence on the oxide or passive layer. (The passive film theory of corrosion protection will be discussed further in the next section.) While molybdenum increases corrosion resistance, at high concentrations it can lead to the formation of a brittle sigma phase. It also is a ferrite stabilizer. To counter the ferritic effect of molybdenum, higher concentrations of nickel must be added to stablize the austenitic structure (120).

Carbon is a strong austenitic former, being 30 times more effective than nickel on a weight basis. In addition, it is a major solid solution strengthening agent. However, minimal carbon contents are highly desirable since carbon precipitates chromium carbides in the temperature range of 450 to 900°C, thereby decreasing corrosion resistance (124).

Therefore, the most desirable composition of the 316 stainless steel for surgical implants would be one with a reasonably high nickel content (11% to 12%), a very low carbon content (preferably less than 0.03%), a chromium concentration as high as possible, and molybdenum in sufficient quantities to confer adequate corrosion resistance but not too high to risk ferrite and sigma phase formations (120).

1. Corrosion Characteristics of Stainless Steel

The corrosion resistance exhibited by the surgical 316L stainless steel alloy is in part due to the formation of a complex oxide film on the alloy surface thus protecting the material from body

fluids. The ability of the passive film to confer corrosion resistance is basically determined by the following film parameters: (1) compositon, (2) structure, and (3) thickness. These parameters can be influenced by the composition of the bulk alloy, the kinetics of film formation, surface conditions of the alloy, and the corrosive medium in which the film forms.

Alloying is important in conferring a stable austenitic structure for the stainless steel and alloying is just as critical in obtaining good corrosion resistance. To describe the influence of the various alloying elements on the corrosion resistance, it is useful to refer to Figure 1. This is an idealized representation of an anodic polarization curve for an active-passive metal. An increase in corrosion resistance for a metal will result due to one or more of the following: (1) a reduction in i_p, the critical anodic current density required for passivation, (2) a reduction in i_{ps}, the passive current density, and (3) an increase in the potential range of the passive region through a more negative E_p, the primary passivation potential, a more negative E_{ps}, the potential of complete passivity and a more positive E_b, the potential for passive film breakdown. The degree of passivity can be increased by the addition of such elements as nickel, molybdenum, silicon, and chromium.

As the chromium content in the steel is increased, both the primary passivation potential, E_p, and the potential of complete passivity, E_{ps}, will be shifted in the electronegative direction, while the breakdown potential, E_b, will be shifted in the electropositive direction, thus increasing the range of the passive

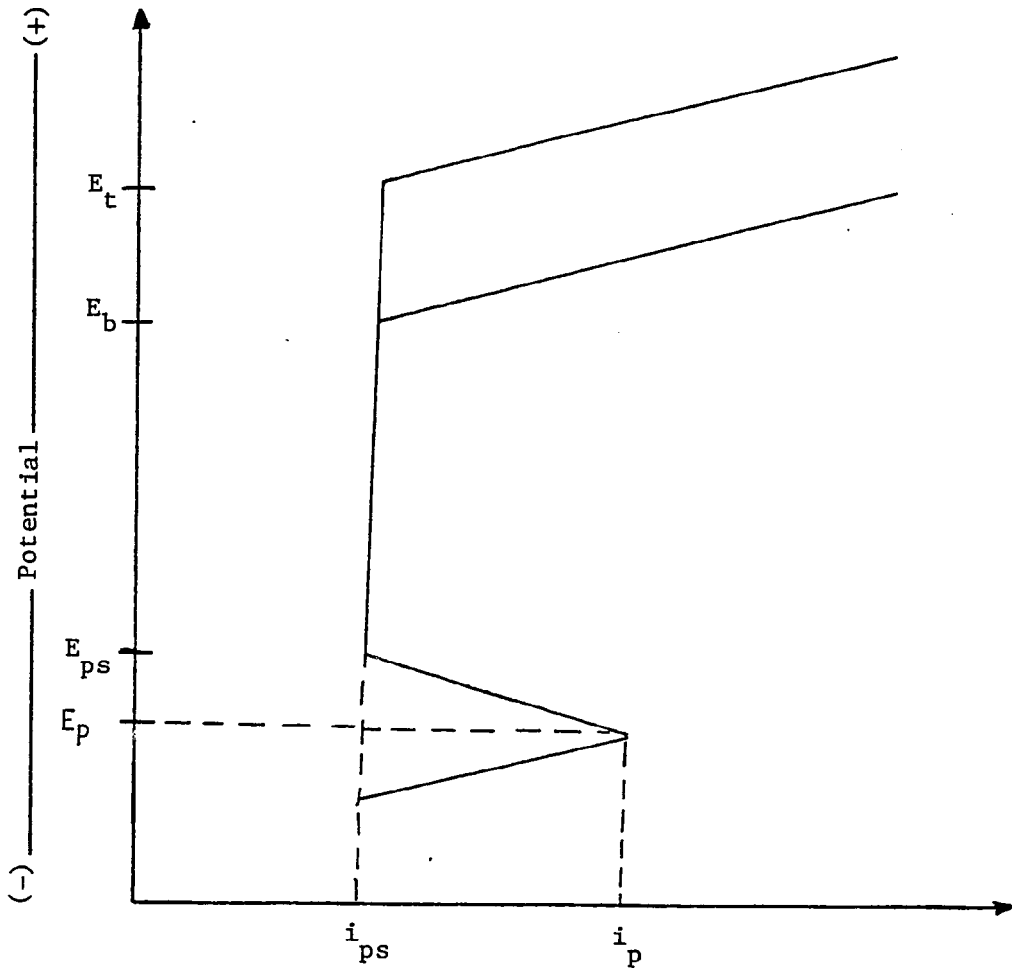

Figure 1: Idealized Anodic Polarization Curve

region. Also, there will be a decrease in the critical anodic current density, i_p, and the passive current density, i_{ps}. Addition of nickel also decreases i_p and i_{ps}, and E_b is shifted in the electropositive direction. Molybdedum will reduce i_p and shift E_{ps} in the electronegative direction. Molybdenum also increases the resistance to pitting and crevice corrosion with as little as 0.5% having a significant effect on raising pitting potentials, E_b. Small additions of silicon will improve passive properties by decreasing i_{ps} and shifting E_{ps} in the electronegative direction and E_b in the electropositive direction. Carbon in solution has only a small effect on corrosion resistance. A major problem arises when carbon precipitates as chromium carbides. Thus carbon in the alloy is minimized (124).

Proper alloying of stainless steel enhances the corrosion resistance by increasing the degree of passivity. However, implanted stainless steels are unable to resist all forms of corrosion attack that can occur in the body. Several forms of corrosion that are most often observed are: (1) pitting corrosion (2) crevice corrosion, and (3) galvanic corrosion.

Pitting corrosion is a form of extremely localized attack that results in holes in the metal. Pitting can be predicted from <u>in vitro</u> experiments by application of the protection potential theory (21,115). Figure 2 is a schematic representation of a cyclic anodic polarization curve. By reversing the potential scan at a potential greater than the breakdown potential, E_b, a hysteresis loop may be observed resulting in the repassivation curve crossing the passive region at a potential designated as the protection

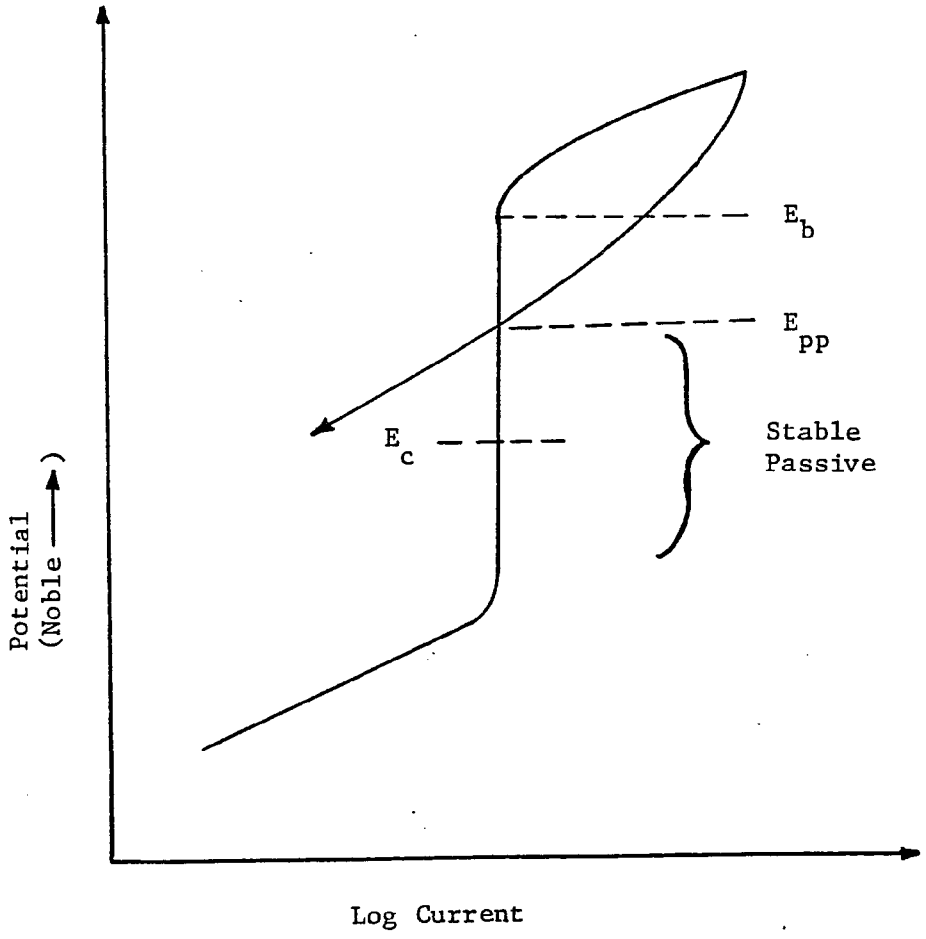

Figure 2: Cyclic Anodic Polarization Curve

potential, E_{pp}. According to the protection potential theory, if the corrosion potential for the alloy is greater than the protection potential but less than the breakdown potential, the alloy is susceptible to pitting corrosion. Figure 3 shows a cyclic anodic polarization curve for the 316L stainless steel alloy. Griffin's (46) results demonstrated a large hysteresis indicating that the alloy is susceptible to pitting corrosion. Surface analyses after generation of the polarization curve revealed significant pitting corrosion attack. Syrett and Wing (104) utilizing cyclic anodic polarization curves also showed that the 316L stainless steel demonstrated significant hysteresis loops, concluding that the alloy was susceptible to pitting corrosion. They confirmed this result with long-term immersion tests. Mueller and Greener (83) conducted polarization curves in Ringer's solution and noted that a pitting type of corrosion was observed on the stainless steel alloy.

For pitting corrosion to occur, the material must form its own pit. For active passive materials such as stainless steel alloys, this may occur through the partial disruption of the passive film and/or surface irregularities. Once the pit has been formed, the propagation of the pit continues in an autocatalytic fashion. The basic mechanism of pitting corrosion has been extensively described by Fontana and Greene (42). Crevice corrosion differs from pitting corrosion in that a crevice already exists and the material does not have to form the crevice. Due to the geometry of certain implanted devices, a crevice is provided. A material that is susceptible to pitting corrosion will also be susceptible to crevice corrosion.

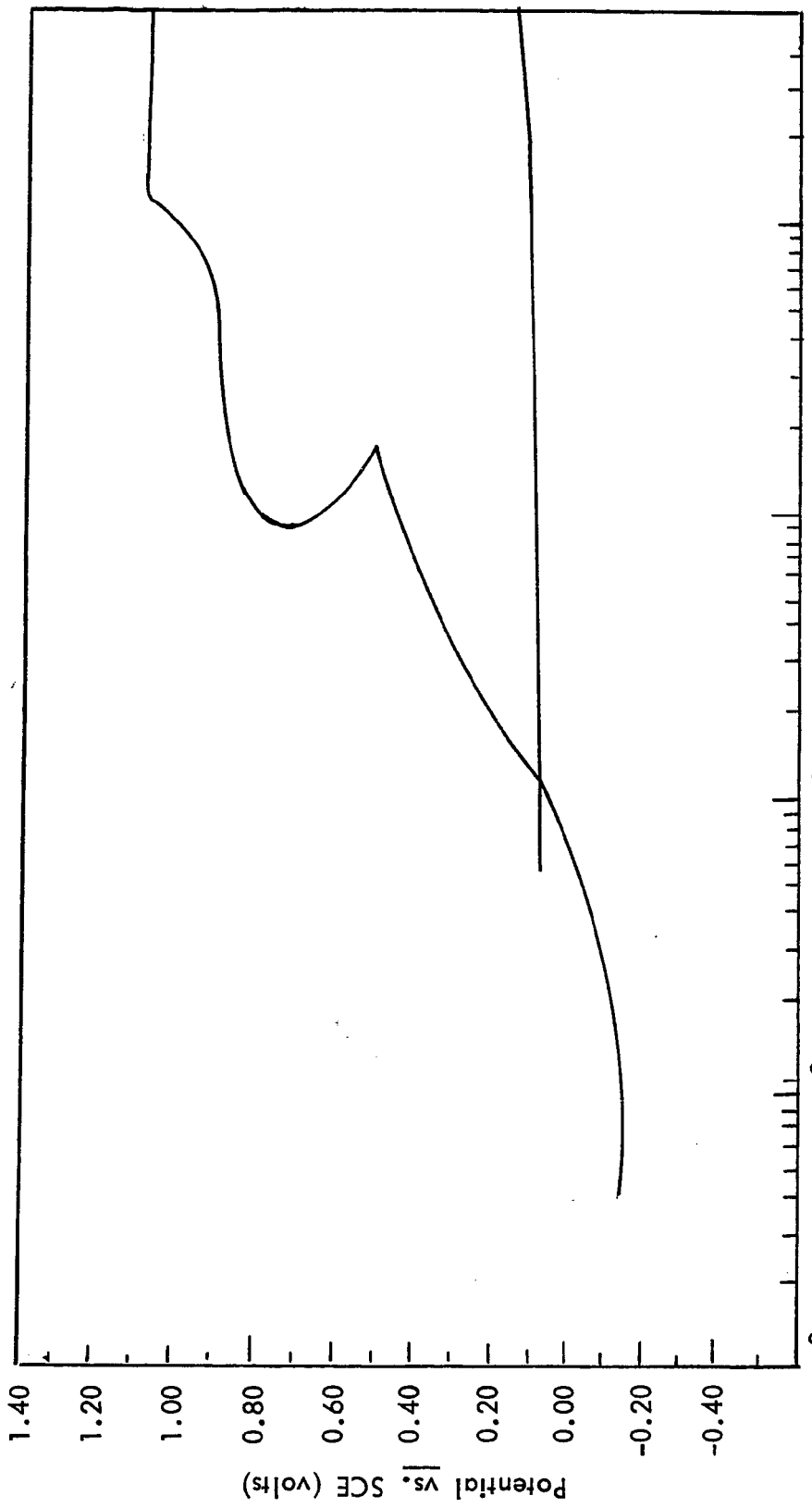

Figure 3: 316L SS Anodic Polarization Curve for Passivated-Aerated Condition (46)

Stainless steel is used for the fabrication of many multicomponent devices such as bone plates and screws. The crevices produced at interfaces are most conducive to crevice corrosion attack. Crevice corrosion observed at the gap between the screw and the plate is most often seen on the plate and within the hole near the longitudinal surfaces. Occasionally, crevice attack will be noted on the portions of the screw opposite these areas (13). Crevice corrosion has been investigated by: in vitro electrochemical analyses (73), implantation of crevice samples in animal models (44), and by surface analyses of retrieved prostheses. Cahoon and Paxton (22) metallurgically examined 17 orthopaedic implants which had been in service for approximately 1 year. Crevice corrosion was observed in the screw holes of all but one of the stainless steel implants examined, including those which had performed satisfactorily. One of the implants, a type 316L V-Moore plate, failed due to severe corrosion in three of the four countersunk screw holes.

Colangelo and Greene (27) examined Type 316 stainless steel orthopaedic devices. Of the retrieved devices, corrosion was exhibited in about 56% of the 53 devices. This was comprised of corrosion on 10% of the 30 single component devices and 91% of the 23 multicomponent devices. The latter corrosion generally occurred on contacting metal surfaces forming crevices. Therefore crevice corrosion appeared as the major form of attack and occurred in 42% of all possible sites. The frequency and severity of this attack increased with the duration of implantation. Two months were sufficient for the corrosion attack to become visible.

Metallurgical analyses of removed orthopaedic implants were also performed by Weinstein, Amstutz, Pauon, and Franceschini (112). Of 28 multicomponent stainless steel devices examined (316, 316L, 317), 27 exhibited crevice corrosion on contacting surfaces. Fretting was noted as a contributor in the crevice corrosion attack observed at the interfaces. Other investigators have suggested that fretting of the two opposing surfaces can increase the corrosion observed (24,25,62). Dr. H. H. Uhleg has stated: "The austenitic alloys containing molybdenum (types 316, 316L and 317) are the most resistant of all to seawater, but pits eventually develop within a period of one to two and a half years" (Ref. 113, p.85). Therefore in using stainless steel, one should recognize that the possibility of crevice and/or pitting corrosion is ever present and may or may not occur depending on the specific conditions (113).

The third form of corrosion, galvanic corrosion, will arise when two metals having different corrosion potentials are in contact in an electrolyte. This creates an electron flow between the two metals. When galvanic corrosion occurs, the corrosion rate of the more electronegative metal (anode) will generally be increased whereas the corrosion rate for the more electropositive metal will be decreased. The classical view of galvanic coupling of alloys for orthopaedic devices is that coupling should be avoided. Gruen and Amstutz (48) reported on a case of a failed Vitallium® (cobalt base alloy) Urist hip socket with a Type 316

®Trade name, Howmedica Inc., Rutherford, New Jersey

stainless steel femoral head component. This device had been in service for 32 months. Extensive metallic debris and corrosion products were observed within the joint. The metallurgical observations of the alloys included severe wear over areas of the femoral head and large pits in the socket. The abrasive wear on the Vitallium® was less as compared to the stainless steel. It was concluded that severe abrasive wear, fretting, and galvanic corrosion were all causes of failure and that a Vitallium/stainless steel combination should not be used as an articulating interface in the body. It should be noted that this conclusion is a result of both wear and galvanic corrosion effects.

Rostoker, Pretzel, and Galante (93) investigated the crevice and galvanic corrosion behaviors of various implant alloy couples immersed in a 1% NaCl solution maintained at 37C. The corrosion couple was formed by contacting the alloy to itself or with any one of nine dissimilar alloys and/or graphite. Alloys included in the study were Type 316L stainless steel, cast Co-Cr-Mo, wrought Co-Cr-W-Ni, Ti-6Al-4V, and Multiphase MP35N (Co-Ni-Cr-Mo). Coupling Type 316L stainless steel to itself produced pitting for the crevice configuration in as little as five days, and multiple pitting and staining were reported after 10 days. Noncoupled tested specimens of 316L required at least 50 days to demonstrate effects similar to the 10 day crevice configuration results. Coupling the stainless steel to the other alloys or graphite did not appear to accelerate the corrosion of the steel; multiple pits and staining were again observed after 10 days. The authors

concluded that the crevice corrosion of the steel was not accelerated by galvanic coupling. This conclusion was contradicted by Griffin and Buchanan (47) who reported that 316L stainless steel should not be coupled with Co-Cr-Mo, Ti-6Al-4V alloys and/or graphite from in vitro electrochemical corrosion analyses.

The three forms of corrosion, pitting, crevice and galvanic, have been studied by many investigators. Other forms of corrosion--uniform, intergranular (67,95), corrosion fatigue (22,45), and stress corrosion cracking (41,128)-have also been observed on 316L stainless steel alloys. Whether a slow release of ionic constituents occurs or whether an accelerated corrosion with an increased quantity of released ions occurs, the concern of an adverse tissue reaction due to the accumulation of ionic constitutents needs to be investigated more extensively. This, and related subjects dealing with possible implant failure due to corrosion products produced by higher corrosion rates, will be discussed in the next section.

2. Tissue Response to Stainless Steel

Tissue response to implant materials has historically been investigated by histological analyses of tissue adjacent to the implants. Considerable information has been obtained from tissue obtained from implanting materials in animal models and also from tissue adjacent to retrieved prostheses from human subjects. The interpretation of histological studies in assessing tissue compatibility of implant materials remains a problematic area. This results from the fact that the structure and morphology of the tissue adjacent to a metallic implant are influenced by many

factors: implant site, alloy composition, surface treatment, implant design, mechanical considerations, and the patient's history (124). Other avenues for investigating tissue responses to implant materials involve *in vitro* cell and tissue culture analyses. Investigations of this type can remove many of the variables associated with animal models such as endocrine and immune responses. These investigations then allow the investigator to study responses to known concentrations of individual corrosion products at the cellular level (9). It is the intent of this section to review *in vivo* and *in vitro* investigations of localized tissue responses to the 316L stainless steel alloys as well as systemic responses to the alloy.

a. Localized Tissue Response

The 316L surgical stainless steel alloy is susceptible to several forms of accelerated corrosion - pitting, crevice and galvanic forms. Also there can occur the slow passage of metallic ions into the environment from the parent alloy in the passive state (64). The fate of these constituents in the tissue adjacent to the implant is important to the question of biocompatibility.

Investigations of Ferguson, Laing, and Hodge (41) and Laing, Ferguson, and Hodge (68) were some of the earliest studies concerned with the tissue reaction to metallic implants. In their studies, cylindrical metallic specimens were implanted in the back muscles of New Zealand rabbits. The specimens were removed at various time intervals with blocks of muscle surrounding the implant. The quantity of ionic constituents in the adjacent tissue

was obtained by spectrochemical analyses. The ionic constituents released after a period of four to six months from AISI 316 stainless steel implant specimens are shown in Table 2. The control represents normal muscle (40).

Table 2

Ionic Constituents Released From AISI 316 Stainless Steel Alloy

Elemental Component	316SS (ppm)	Control (ppm)
Iron	76.8±45.7	37.9±34.6
Nickel	40.5±41.2	8.0±9.3
Chromium	76.0±55.7	3.7±4.9
Molybdenum	8.4±9.2	1.8±3.2

The results shown in Table 2 reveal significant quantities of elemental constituents of the stainless steel alloy in the surrounding tissue. The clinical significance of these quantities of ionic constituents is not yet known. Laing et al. (68) analyzed the pseudo-membrane formed around the 316L stainless steel alloy and reported that the membrane thickness was from 0.002 to 0.03 mm which in their opinion was a satisfactory response.

Williams (117) reported that products of corrosion have frequently been observed in the surrounding tissues. Sometimes these products were found in fibrous tissue, being either extra-cellular or contained within the fibroblasts. Pigmentation of tissues surrounding metal implants has been observed both clinically and histologically. With those ions remaining locally in the tissues, it is possible that various complexes are formed. The tissue

pigmentation which persists after implantation indicates that some ions do remain in the vicinity of the implant for long periods of time (117).

Escalas, Galante, Rostoker, and Coogan (38) implanted 316L stainless steel in solid (3/16 inch diameter x 0.091 inch height) and powder (8-10 μm) forms in the paravertebral muscle fibers of New Zealand albino rabbits. After six months the specimens were retrieved with the surrounding tissues. The 316L solid specimens evoked a tissue response that was graded to be moderate by the authors. The 316L powders elicited a more significant response, noting an increased cellular response of macrophages, eosinophils, and giant cells. The results of this study are similar to the findings of other investigators which have observed more significant tissue responses with powders than with the solid forms (120).

Wagner, Shabaik, Schorman, and Amsutz (110) investigated the biocompatibility of the 316L stainless steel alloy by implanting metallic debris into the knees of adult female New Zealand rabbits. X-ray diffraction analyses revealed that the stainless steel debris consisted primarily of the face-centered cubic (FCC) alloy with small amounts of body-centered cubic (BCC) alloy and Fe_3O_4. The size of the particles ranged from 0.1 to 10 μm with 75% of all particles <2μm in diameter. Particulates in the amounts of 0.5 mg and 20 mg were injected into the rabbit knees and were studied in varying time intervals up to five weeks. Approximately 40% of the debris was contained within macrophages. Metal debris was never seen in the polymorphonuclear leukocytes by light microscopy. Less

then 10% of the debris was located in the superficial layers of the synovium.

Animal investigations on the tissue response elicited by stainless steel alloys range from reports of mild (14) to extensive (32). A mild reaction may be considered as the formation of a thin cellular fibrous tissue capsule around the implant material. A severe reaction may be considered one involving a thickened capsule with extensive cellular reaction involving macrophages and foreign body giant cells to tissue necrosis. Both fibrocytes and macrophages have been shown to contain elemental constituents intracellularly causing the tissue to have a pigmented appearance. This is sometimes referred to as "metallosis". Clearly the importance of any reaction to an implanted metal is not so much the extent of tissue changes but the clinical significance.

As with the animal studies, pigmented tissues surrounding implanted stainless steel implants in human subjects have also been observed. Emnéus (36) believed these pigmented tissues occurred due to corrosion of the implant material. However, he also felt that there was no consistent relation between the amount of pigmentation and the inflammatory response. In Gruen and Amstutuz's (48) examination of a failed Vitallum®/stainless steel total hip replacement, they observed blackish pigmented tissue containing stainless steel wear debris and corrosion products. Histological examination revealed histiocytes, scattered multinucleated giant cells, and dense hyaline fibrosis.

Significant evidence exists indicating that metallic debris remains in tissue adjacent to implant materials from both animal

and human tissue analyses. An important study to conduct in retrieved tissue would be the identification of the corrosion products. This type of study should involve more than spectrochemical analyses for elemental constituents as done previously by Ferguson et al. (41) in their animal investigation. The types of precipitates deposited should be analyzed with considerable attention given to the valence state of the corrosion products. Cahoon and Paxton (22) examined tissue from retrieved stainless steel orthopaedic components. He found that the main corrosion products were $FeCO_2$ and β-FeOOH. He also found α-FeOOH, Fe_3O_4, and Fe_2O_3.

A more extensive study was conducted by Williams and Meachim (125). They found three types of foreign materials. Type I deposits were fragments of material resulting from wear processes. The smaller particles were found mainly in macrophages and the larger particles were surrounded by multinucleated cells. The authors reported no granulomatous reaction and the fibrous tissue was remarkably healthy in terms of the quantity of foreign material present. Type II deposits were sometimes greenish in color and these deposits evoked the greatest tissue response. Tissue containing significant quantities of Type II deposits frequently consisted of relatively acellular collagen or was necrotic. Analyses revealed Type II deposits to be a chromium compound with significant concentrations of sulfur, phosphorous, and iron. Type III deposits, yellowish brown, contained iron oxides, α-FeOOH and γ-FeOOH. The formation of these hemosiderin-like particles was proposed as an iron detoxication mechanism. However, in some

cases, pathological changes were seen which indicated a local tissue iron overload or iron toxicity. Although Type II and III deposits were frequently found together, the Type II, chromium compound, was considered to be more cytotoxic. Studies like the previous one are important to truly understanding tissue reactions to implant materials. By analyzing the composition of the corrosion products causing the toxic response as done by Williams and Meachim, significant improvements in tissue biocompatibility may be accomplished.

Cell cultures have been utilized by several investigators for investigating toxic responses to implant materials. Pappas and Cohen (86) and Mital and Cohen (82) utilized a human cell line derived from a nasal carcinoma-(KB)-and a cell line derived from a mouse leukemia (P1534) for analyzing the cytotoxicity of powders of 316 stainless steel and cobalt base (Vitallium®) alloys. The results of their experiments showed that the stainless steel alloy was less toxic to the cell cultures than the cobalt-base alloy. However, both alloys exhibited toxic effects, especially at the higher concentrations. Cytological studies of the cultures revealed no significant morphological alterations except for collections of brown granules in the cytoplasm. The authors were unable, from this study, to obtain a dose-response relationship.

Campbell, Meirowsky, and Hyde (23) studied the cytotoxicity of metals by observing the altered growth rate of pure fibroblast cultures obtained from hearts of chick embryos. Metal discs, 1.5 mm in diameter and 0.25 mm thick, of different metals including stainless steel were fabricated and exposed to the fibroblast

cultures. The cell cultures showed that stainless steel as well as Vitallium® were nontoxic. The culture analyses also showed that copper and vanadium were extremely toxic, i.e., the cells would not grow in the presence of these elements.

Mears (79) utilized cell cultures to study the uptake of corrosion products at the cellular level. Rat dermal fibroblasts were cultured on a stainless steel mesh. Iron, chromium and nickel radiation was detected in the cells by electron-probe micro-analyses. The iron intensity relative to the nickel and chromium intensities in the cell was about one-half the intensity that was expected for a stainless steel alloy of the following composition: 18% chromium, 8% nickel, 3% molybdenum and the remainder iron. The 18-8 stainless steel alloy will contain minute amounts of copper. Interestingly, under a static probe, a copper intensity up to 2% per cubic micron was observed in the cells exposed to stainless steel.

These in vitro cell culture experiments show that the corrosion products from stainless steel alloys can have a toxic effect on cultured fibroblasts. This has been shown to occur by the inhibition of cellular growth and the uptake of the corrosion products into the fibroblasts. This area of in vitro testing for biocompatibility should be utilized more extensively to examine what is happening at the cellular level that ultimately affects the localized tissue response to implant materials.

b. Systemic Tissue Response

It is evident from the previous sections that, as a result of corrosion, ionic constituents are released to the surrounding tissues. Pigmented tissues indicate that corrosion products accumulate. The fate of ionic constituents can be multiple. Depending on the oxidation state, the ion may bind to *in vivo* enzymes, plasma membranes, or form insoluble reaction products such as metal hydroxides. In a study of 38 patients with histologically diagnosed "metallosis," Lux and Zeisler found mean concentrations of iron, chromium, and molybdenum at a stainless steel-tissue interface with concentrations significantly higher than the control tissues. These concentrations declined logarithmically with distance from the implant, reaching normal levels at distances greater than 4 cm from the implant. Nickel, which formed 12% of the implant alloy, was not detected in the surrounding tissue (13). Nickel was presumably absent due to the high solubility of its corrosion products. The systemic fate of nickel is of critical importance since a significant percent of the population may be nickel sensitive. This will be discussed in greater detail later in this section.

Smith and Black have grouped potential systemic effects arising from metallic implants into four categories. These are: metabolic effects, immunologic effects, carcinogenic effects, and bacteriologic effects. The first three of these effects will be reviewed in some detail in this section (13).

The fate of metallic ions released by embedded implants of commonly used alloys was investigated by Ferguson, Akahoshi, Laing,

and Hodge (40) in rabbits. Spectrochemical analyses were done on the liver, spleen and lung at time intervals of six weeks and six months. For the 316 stainless steel, the spleen showed a tendency to retain nickel at sixteen weeks. An elevation of molybdenum in the liver, spleen and kidney was also evident. Accumulations of iron and chromium in the various organs were not significant. This early study demonstrated that ionic constituents of surgical implants were transported to remote organs and that the possibility of metallic ion accumulation existed. Underwood (108) considered diet-induced alterations in trace element concentrations and concluded that excessive accumulations could alter metabolic function. Thus the continued release of ionic constitutents from prostheses by corrosion and wear phenomena could also result in altered metabolic functions.

Considering the 316L stainless steel alloy, the major elemental constituents are iron, chromium, nickel, molybdenum and manganese. All of the elements are considered essential in the human diet for normal structure and function (124). To assess systemic biocompatibility of an implant alloy, the effects of these elements on normal metabolic pathways should be investigated.

Iron is essential to all higher forms of life. Studies in dogs have shown that 60-70% of the body iron is found in hemoglobin and myoglobin; 20% of the body iron is held in storage in a labile form in the liver, spleen, and other tissues and can be utilized for the regeneration of hemoglobin in case of blood loss; and 10-20% is firmly fixed in tissues (28).

Excessive iron overloads have been linked with a variety of pathological conditions, cirrhosis of the liver, bronzing of the skin, diabetes mellitis, and abnormalities of the endocrine glands (29). Weinberg (111) has expressed the belief that even small additions of iron may increase the transferrin saturation of the blood causing the individual to be more susceptible to infection. For iron storage disease to occur, an accumulation of 20-60 g of body iron would be required. According to Winter (127), a stainless steel implant containing 65% iron would have to degrade 2-6 mg of the alloy per day for 40 years. It is unlikely that any implant wears and corrodes to this extent. However, Winter has observed dying cells, acellular collagen, and tissue necrosis around type II and type III deposits in some tissue specimens. This suggested that localized tissue iron overload or iron toxicity could occur around some extensively corroded stainless steel implants. This could also mean that localized accumulations of iron in remote organs could cause iron overload resulting in altered cell metabolism.

Chromium levels in the blood normally range from 1.0 to 5.5μg/100g. The oxidation states of chromium range from Cr^{-2} to Cr^{+6} with the trivalent and hexavalent states being the greatest health hazard. Trivalent chromium has been linked with a high incidence of lung cancer in the respiratory tract. The mechanism of chromium toxicity is not entirely known; however, it has been suggested that the _in vivo_ reduction from hexavalent to trivalent states may be important. The hexavalent chromium is able to pass the plasma membrane freely and the reduction takes place in the

mitochondria. The reduction process requires three electrons which must be derived from electron-rich molecules. This could inhibit a number of metabolic processes for which these electrons are useful (124).

To analyze the organs that retain chromium, Hopkins (59) injected $Cr^{51(III)}$ intravenously into rats at levels of 0.01 and 0.1 μg Cr/100g body weight and its distribution was studied at time intervals from one-fourth hour to four days. After four days, the heart, pancreas, lung and brain retained 10-31% of their initial radioactivity while the spleen, kidney, testis, and epididymis retained from 104% to 200%. The spleen and kidney continued to concentrate Cr^{51} over the four-day period while the peak retention in the testis and epididymis was at four and eight hours.

Owen, Meachim, and Williams (85) have analyzed the chromium content in hair by neutron activation analysis of samples from 62 patients following the implantation of a Charnley hip. The Charnley hip contains stainless steel against polyethylene and the range of implantation times ranged from three to five years. "Fifty-one control subjects were also analyzed. Of the 51 control subjects, 50 showed less than 2 ppm chromium in the hair, one showed 2-5 ppm, none showed more than 5 ppm" (Ref. 85, p. 91). Fifty-nine of the 62 patients showed less than 2 ppm chromium in hair, three showed 2-5 ppm, none showed more than 5 ppm." They concluded from their study that a concern should exist over the systemic accumulation of chromium from prostheses since the risk of systemic toxic effects are still unknown.

Nickel is at a normal level at approximately 10 mg in the average adult human and the normal blood level is 1.0 to 40.0 ug/100g. Exposure to nickel, such as from parenteral administration, results in a high kidney level and raised concentration in the pituitary gland, lung, spleen, and skin (124). The most well documented systemic effects of nickel are hypersensitivity reactions and the carcinogenesis of nickel and nickel compounds. Both of these effects will be discussed in more detail in the later part of this section.

Molybdenum is a normal constituent of blood and has its highest concentration in the liver at one to three ppm. It is also found at levels of 0.05 to 0.10 ppm in mammalian muscle and other tissue. Molybdenum is considered to have a low degree of toxicity, however, some problems have been associated with the element. Symptoms of acute molybdenum toxicity include diarrhea, coma and cardiac failure. High levels of molybdenum can inhibit certain enzymes as cytochrome oxidase, glutaminase, choline esterase, and sulfide oxidase. High levels of molybdenum can also interfere with calcium and phosphorus metabolism and induce osteoporosis (124).

Manganese is at a level of 12 to 20 mg in a 70 kg man, and the normal blood level is 7.0 to 28.0 ug/100g. The higher concentrations of manganese occur in the pituitary gland, liver, kidney, and bones. Accumulations have been shown to occur in the hair. As with chromium, the valence state of manganese is important in evaluating its toxicity. For manganese, the divalent form is considered more toxic than the trivalent form. Long-term exposure

to pollution containing manganese has been shown to cause detrimental effects on the central nervous system (28).

The immunologic effect of metals is not completely known. However, more study is being given to this area of metal interaction. According to Black (13) the small size of the ionic constituents and the simplicity of their structure argue against their direct activation of either humoral or cell-mediated responses. It is thought that the ionic constituents bind with organic molecules such as albumin to form complexes called haptens. These complexes possess antigenic qualities. Besides acting as antigens through hapten formation, alloying elements of 316L stainless steel, chromium and nickel, have been shown to suppress antibody production (13).

One aspect of the effect of metals on the immune response is the formation of a skin dermatitis. Cramers and Lucht (30) reported on the necessary removal of stainless steel bone plates and screws used for tibial fracture fixation. Three patients with stainless steel devices developed a local dermatitis at three to four months after the implantation. Two of the patients had a positive patch test for chromium and cobalt and one patient had a positive test for nickel. After the implants were removed, the dermatitis disappeared.

Pegum (87) reported a case in which a 41-year-old woman had received a Wainwright stainless steel plate (8-12% nickel, 17-20% chromium, 2% manganese, 2.5-3.5% molybdenum, remainder iron) at the age of 12. Twenty-nine years after implantation, a dermatitis developed on various parts of the skin and sterile suppuration

developed around the implant. The device was removed and consequently the suppuration and dermatitis resolved. Patch tests to nickel and chromates were positive.

There are a number of reports on patients having stainless steel implants removed due to the patient being sensitized to one or more of the stainless steel alloying elements. Sensitization is often confirmed by administering the skin patch test. Of the alloying elements of 316L stainless steel, chromium (33,34,35,43, 57,106) and nickel (7,33-35,43,57,81,88,94,106) are most often positive. It would be advantageous to be able to test patients for sensitivity prior to implantation since an unnecessary surgery could be avoided. The problem with the patch test is that it is an in vivo test and it exposes the patients to solutions of the metal. Black (13) has reported on Wahlberg's investigations of metallic solutions used for patch testing. Wahlberg believes that the test solutions contain a percent of the metal greater than the threshold amount and may cause hypersensitivity to occur. In vitro testing is being investigated. Brown, Mayor, and Merrit (16) are currently using the MIF (migration inhibition factor) test and Henstenn-Petersen (55) is analyzing the lymphocyte sensitivity test for predicting patient sensitivity. Unfortunately both of these in vitro tests are still in the experimental stages.

The role of metals as carcinogenic agents is another area that is being more extensively investigated. McDougall (77) reported the first account of a malignant growth at the site of metallic plate and screws used for the fixation of a humeral fracture. Analyses of the stainless steel plate and screws revealed that the

plate's composition was 74% iron, 18% chromium, 6% nickel and the composition of the screws was 88 percent iron, 12% chromium and a trace of carbon. There was a potential difference of 80 millivolts between the plates and screws. The implants were blackened and corroded. Both the humerus and the soft tissues were discolored, and a dark serous exudate was present around the area. The malignant tissue was classified as a sarcoma of the Ewing type. Approximately 14 months after discovering the tumor, there was clinical evidence of metastasis, and six weeks later the patient died.

Harrison, McLain, Hohn, Wilson, Chalmers, and MacGowan (50) reported on two dogs in which osteosarcomas arose in association with stainless steel implants. One neoplasm occurred in the distal humerus of a 12-year-old Doberman pinscher which had been implanted with a stainless steel intramedullary pin 11 years previously. Surface examination of the pin revealed corrosion. The second neoplasm arose in the proximal tibia of a 12-year-old Irish wolfhound which had been implanted with a plate and screw assembly made of the 316L stainless steel alloy. This implant had no signs of corrosion. Infection had not occurred in either animal.

While the chemical composition of the foreign material is of importance in the induction of tumors, it has been suggested that the form of the implant and the fibrous tissue capsule which surrounds it are the principal factors influencing the production of foreign body tumors. Stinson (100) has shown that in rats, malignant tumors were produced in the fibrous capsule formed around discs of stainless steels. Other studies on the carcinogenic

effects of implant materials have shown malignant tumors to be produced in experimental animals by exposure to elemental nickel (52,60,61,101), Cr (101), and Fe (101), all elemental constituents of the 316L surgical stainless steel.

3. Summary-Stainless Steel

The 316L stainless steel surgical alloy can be very corrosion resistant under body conditions; however, pitting, crevice and galvanic forms of corrosion are all well documented. The adjacent tissue responses elicited by the stainless steel alloy are varied. Where some stainless steel implants have been shown to have a minimum response at 26 years (71), severe tissue responses with a cellular response and even necrotic tissue have been noted at much shorter time intervals. The systemic effect of these corrosion products is still unknown as is the true clinical significance of the accumulation of these products either locally or systemically.

B. Cobalt-Chromium-Molybdenum Surgical Alloy

In the early 1930's, Erdle and Prung of the Austenal Laboratories patented an alloy called Vitallium®. The original specification required 30% chromium, 7% tungsten, and 0.5% carbon in the cobalt. Tungsten was replaced by 5% molybdenum in a succeeding patent. Cobalt-base alloys were introduced to dentistry as an alternative to gold alloys due to the increasing expense of gold. In 1937, Smith-Peterson began using Vitallium® for the fabrication of his hip arthroplasty caps and about the same time Venable and Stuck also began experiments with Vitallium® to determine corrosion resistance and tissue response to the alloy based on results obtained from internal fixation plates (124). Since the 1930's, the cobalt-chromium-molybdenum surgical alloy has been used extensively in dental and orthopaedic applications. There have been modifications on the composition and structure of the alloy during this time and current requirments for the alloy are listed in ASTM F75-76 specifications (2).

Cobalt, the major element of the alloy, displays an allotropic transformation at 417C, existing in a close-packed hexagonal form below this temperature and as a FCC form from 417C to the melting point at 1495C. The addition of chromium, a body centered cubic structure, does not result in an extensive solid solution with cobalt. The solid solubility of chromium in the FCC cobalt reaches a maximum at 41 atomic percent chromium at 1310C. Therefore in the region of 70-75% cobalt and 25% to 30% chromium, a cobalt-chromium solid solution is formed. A 5% addition of molybdenum to the Co-Cr

binary system will result in a stable face centered cubic alpha phase at room temperature. The molybdenum addition also reduces the grain size produced on casting and increases the strength accordingly. These casting alloys also contain a small amount of carbon, <0.37 percent. Thus, complex chromium-molybdenum carbides tend to be precipitated interdendritically on cooling, as shown in Figure 4. Carbides, being a second phase, improve the strength and wear resistance of the alloy. However, should the carbides form a continuous network, then excessive brittleness may result (6,119,124).

1. Corrosion Characteristics of Co-Cr-Mo

Cobalt is not regarded as a corrosion resistant material. However, alloying with chromium and molybdenum produces a corrosion resistant material. This corrosion resistance is the result of the formation of a complex chromium-oxide film on the alloy surface (118). Mueller and Greener (83) conducted anodic polarization curves in Ringer's solution for the three major surgical alloys. Pure titanium remained passive at all potential values studied. Cast Vitallium® demonstrated a passive and/or oxide film breakdown potential of 700 mv. The reason for this observed breakdown was not due to a pitting type of attack but to the dissolution or breaking away of a brown corrosion layer. The 316L stainless steel demonstrated a breakdown potential approximately 100 mv more active than the cast Vitallium®. The distance between the breakdown

Figure 4: Microstructure of Cast Co-Cr-Mo (100X).

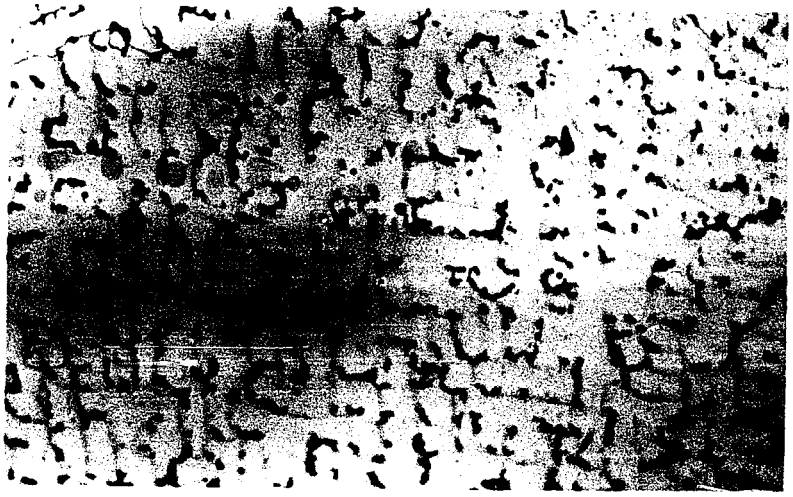

potential and the resting potential is often a means of determining the stability of the oxide film. A large distance indicates the passive film should be stable resulting in low corrosion rates. On the other hand, a narrow or small gap indicates the alloy's oxide film may breakdown resulting in increased corrosion rates. The distance for the cast Co-Cr-Mo (Vitallium®) alloy is greater than for the 316L stainless steel but is smaller than for the titanium alloy. Therefore, film breakdown is a possibility for the Co-Cr-Mo alloy under certain in vivo conditions (50).

Sometimes the wrought alloy is required. Süry and Semlitsch (102) have investigated the corrosion properties of wrought Co-Ni-Mo-Ti and air-cast Co-Cr-Mo alloys. Accelerated corrosion tests in chloride-containing solutions were conducted for each of the alloys. They observed that the wrought alloy had a greater tendency to passivate as compared with the cast alloy, resulting in a lower corrosion rate. The wrought alloy also demonstrated a higher resistance to fatigue cracking and was more resistant to selective corrosion phenomena such as stress corrosion cracking.

The susceptibility of cast Co-Cr-Mo to pitting and/or crevice corrosion has been investigated by application of the protection potential theory to anodic polarization curves. Cahoon, Bandyopadhya, and Tennese (21) conducted anodic polarization cures for 316L stainless steel and cast Co-Cr-Mo alloys in Ringer's solution. The stainless steel alloy demonstrated a large hysteresis, indicating the alloy to be susceptible to pitting and/or crevice corrosion, whereas the cast Co-Cr-Mo displayed a

small hysteresis loop. The authors concluded that the Co-Cr-Mo alloy should be resistant to crevice corrosion.

Lucas, Buchanan, and Lemons (76) conducted static anodic polarization curves with samples of the cast Co-Cr-Mo alloy. Alloy surfaces were either passivated (ASTM F86) or nonpassivated before the experiments. Hysteresis behavior was demonstrated only when the alloy was pre-passivated. The authors concluded that the observed hysteresis behavior was due to a passive film disruption at high potentials and a repassivation upon reversing the potential and not a result of a pitting corrosion process. Nonwear areas on cobalt femoral head components were examined and no areas uniquely identified as pitting corrosion were observed. Levine and Staehle (73) also conducted anodic polarization curves for cobalt-base alloys and suggested that the cobalt base alloys were the best available materials for resistance to localized attack.

Galante and Rostoker (44) implanted four Vitallium® specimens in the back muscles of rabbits. The specimens were made of thin metal sheets of 0.10-0.15 inch thickness bent to form a loop. After a 12-month period the samples were retrieved for examination. One of the cobalt specimens revealed single pits on the surface.

Cohen and Wulff (26) reported the failure of a Thorton plate and Smith-Petersen nail. The composition of the plate was a Co-Cr-W-Ni wrought alloy; all the screws were of cast Vitallium®. The clinical failure resulted from crevice corrosion at the plate and screw interface. Similarly Rose, Schiller, and Radin (91) investigated the failure of a Vitallium® nail-plate device (wrought plate and cast screws). Utilizing the scanning electron microscope

to examine the surfaces, they found microscopic cracks nucleated by corrosion pits in the nail-plate contact area. They concluded that the pits were probably due to electrochemical action aggravated by the dissimilar metal contact, stress concentration, and crevice corrosion effect of the nail-plate contact area.

Some of the previous studies raised the question of placing dissimilar metals in contact. Rose, Schiller, and Radin's findings in the previous study indicated that combinations of cast and wrought Vitallium® should not be placed in direct contact.

There are applications that would benefit from coupling of two metals for a prosthetic device. For example, there is the desire to apply a carbon coating to Co-Cr-Mo alloys for subperiosteal dental implants. Buchanan, Lemons, Griffin, Thompson, and Lucas (18) reported that carbon coupling to Co-Cr-Mo would not result in accelerated corrosion for either material.

There currently exists a total hip replacement combining a cobalt femoral head component and a Ti-6Al-4V femoral stem component. Lucas, Buchanan, and Lemons (75) investigated the coupling of these alloys using electrochemical theory. Low corrosion rates, 0.02 $\mu A/cm^2$, were predicted and they concluded that coupling of these alloys would not result in an accelerated corrosion occurring for either of these alloys. Furthermore they examined the Co/Ti interfaces of four hip implants with varying implantation times and found no evidence of accelerated corrosion. Griffin and Buchanan (47) have advised against coupling cobalt and 316L stainless steel since an accelerated corrosion could occur for the stainless steel alloy.

2. Tissue Response to Co-Cr-Mo

a. Localized Tissue Response

Accelerated corrosion of the cobalt-base alloys in the forms of pitting, crevice and galvanic corrosion was predicted to occur with less frequency than for stainless steel alloys. However, the release of ionic constituents to the surrounding tissue still occurs by diffusion of ions through the protective passive film on the alloy surface. By implanting Vitallium® specimens in the back muscles of rabbits, Ferguson et al. (41) measured the quantities of ions released to adjacent tissue. At 16 weeks, mean concentrations of 67, 76.7, and 11.5 ppm for chromium, cobalt, and molybdenum, respectively, were measured. The control values for these elements were 3.7(Cr), 2.9(Co), and 1.8(Mo) ppm. Laing et al. (68) measured the pseudo-membrane formed around the cast Co-Cr-Mo specimens and reported thicknesses of 0.001 to 0.03 mm. In a ranking system of Groups I to IV, the cast cobalt alloys were ranked in Group I and II which was considered to be a minimal response.

Laing (67) microscopically examined tissue adjacent to over 100 retrieved cobalt alloy prostheses. He reported that the tissue around the implants was generally free of excessive fibrous tissue and the cellular response to the cobalt alloy implants was slightly less than that around stainless steel implants. Small black particles were seen in phagocytes near the Co-Cr-Mo implants and spectrochemical analyses of adjacent tissue revealed the presence of cobalt, chromium and molybdenum ions. Emnéus, Stenram, and

Baecklund (37) utilized x-ray-spectrographic analyses and also demonstrated the presence of cobalt in tissues surrounding cobalt-base implants.

Co-Cr-Mo is often used for the construction of prostheses with articulating surfaces. Winter (127) examined the fibrous capsule around a Co-Cr-Mo knee prosthesis which had been in vivo 16 months. X-ray fluorescence spectroscopy demonstrated the presence of cobalt, chromium, molybdenum, and nickel in amounts approximating the chemical composition specified for the cast cobalt base surgical alloy. Carbide particles $Cr_{23}C_6$, Cr_7C_3 and Co_2C were found in the tissue as well as an intense macrophage reaction to numerous minute particles. The particles within the macrophages were not identified. However, the unusual shaped nuclei suggested that the material ingested by the phagocytes was cytotoxic.

Willert (116) examined tissue samples around joint replacements of Co-Cr-Mo/Co-Cr-Mo and Co-Cr-Mo/polymer articulating surfaces. The quantity of metallic wear particles was small but did cause a histocytic foreign-body reaction. Small particles were usually phagocytosed by mononuclear histocytes whereas foreign-body giant cells accumulated around the larger particles. Willert also reported that some of the particles were removed from the joint space via perivascular lymphatic vessels, thus alluding to a possibility of a systemic accumulation in perivascular lymphatic spaces.

Overall, the dental and orthopaedic applications served by the Co-Cr-Mo surgical alloy result in minimal tissue response. Due to the good performance of the alloy, few detailed in vivo studies of

the tissue response of the cobalt-chromium-molybdenum alloys exist. This is probably indicative of the alloy's overall good biocompatibility. However, there exists a few in vitro cell culture studies that attempt to quantitate responses elicited by the alloy. Some of these studies have been discussed in previous sections. Campbell et al. (23) found that fibroblast cultures grew well in the presence of stainless steel and Vitallium® discs. However, Pappas and Cohen (86) and Mital and Cohen (81) observed a significantly more toxic effect when fibroblastic cells were exposed to varying concentrations of Co-Cr-Mo powders than when exposed to the same concentrations of 316 stainless steel powders. This result concerned the authors since clinically Vitallium® generally elicits a less toxic response than stainless steel. One explanation given was the Vitallium® powders were obtained by milling and this caused the metal to be in a high-energy work-hardened state. Clinically Vitallium® is cast which results in a low-energy state. However, stainless steel for clinical applications is work-hardened during the fabrication processes. They believed that the stainless steel powder used in the experiment had been work-hardened to an even greater degree than clinical experiments. When annealed specimens of each of the powders were used, minimum reactivity with the cell cultures was demonstrated.

Daniel, Dingle, Webb, and Heath (31) investigated the effect of cobalt concentrations on the morphology and metabolism of rat fibroblasts in vitro. They found that cobalt chloride added to a monolayer culture of rat fibroblasts in concentration of 5 μg/ml (5 ppm Co^{+2}) killed almost all the cells within 48-hours. If the

surviving cells were grown and subjected to further intermittent exposure of cobalt chloride, a cell line was produced that would tolerate a 48-hour exposure to 7.5 μg Co^{+2}/ml. After some months, the cobalt-tolerant cells showed cytological and metabolic differences from control cells cultured for the same length of time without added cobalt chloride. The cytological changes included a wide variation in cell size and shape. The investigators studied metabolic changes such as oxygen uptake and lactic acid production on the cobalt-tolerant and non-tolerant cell lines. Both cell lines reduced the rate of oxygen uptake and increased production of lactic acid, an indication of increased rates of aeorbic and anaerobic glycolysis. This study suggested that one primary action of cobalt is on the respiratory mechanism of the cell.

Bearden (9) exposed fibroblast cell cultures to cobalt solutions within a concentration range of 7.5 to 30 μg/ml. The growth rates for the fibroblasts exposed to cobalt was less than for the fibroblasts exposed only to the growth medium (Eagle's Minimum Essential Medium with 10% fetal calf serum). The ultrastructures of the cells exposed to cobalt versus the controls were examined with transmission electron microscopy. Several interesting features were noted. The nuclear membranes were found to be more electron dense than the controls with heavily stained material along the membrane. The plasma membrane was often faint and appeared to be completely breached in areas. Cellular organelles were disorganized and some contained filamentous material. Bearden compared the observed cellular features resulting from exposure to cobalt to a sequence of ultrastructural stages described by Trump,

Valigorsky, Dees, Mergner, Kim, Jones, Pendergrass, Garbos, and Cowley (107). The sequence represented irreversible events beginning with a normal resting cell (Stage I) and ending in cellular death (Stage IV) (97).

Rae (90) investigated the effects of particulate metals on murine macrophages in vitro by cytological examination and enzyme assays. Lactic dehydrogenase (LDH), if released into the medium, indicated cellular membrane damage. Decreased levels of glucose-6-phosphate dehydrogenase (G6PD) indicated a low phagocytic capacity of the cells. When the cell cultures were exposed to particulate metals of cobalt, nickel, and the cobalt-chromium alloy (obtained from hip joint simulators), a release of LDH was observed indicating cellular damage. The activity of G6PD was found to be lower when the cells were exposed to these materials. Chromium and molybdenum were well tolerated by the macrophages and had no effect in the distribution and activity of either enzyme. Baumhammers, Langkamp, Matta, and Kilbury (8) examined gingival epithelial cells grown in cell culture on surfaces of Vitallium®, glass, tooth enamel, titanium, and vitrous carbon. Utilizing SEM, they found that the cells grew and adapted well to each of these surfaces.

b. Systemic Tissue Response

As with the stainless steel surgical alloy, corrosion of the cobalt base alloys also results in the release of ionic constituents to the surrounding tissues. Due to the dynamic condition surrounding the implant, in vivo excretion processes are always in competition with the corrosion processes, trying to

attain an equilibrium state. The excretion processes are causing the removal of ionic constituents in some form to possibly remote organs, blood circulation and/or elimination in urine or feces.

Spectrochemical analyses were done on the liver, kidney, lung and spleen at six and 16 weeks after implanting metal specimens in the back muscles of rabbits. In these studies, Ferguson et al. (40) found that cobalt was elevated in the kidney, spleen, and lung in some animals. Elevations of molybdenum were noted in the liver and kidney. Again systemic accumulations were observed and the effect of these accumulations on normal metabolism is of concern.

The major constituents of Vitallium® are cobalt, chromium and molybdenum. In the previous section, overloads of chromium and molybdenum were linked to several pathological conditions. Due to the critical nature of the valence state for chromium, metabolic pathways could definitely be altered. The remaining element, cobalt, will be examined in this section.

Cobalt is an essential trace element with an average body content ranging from 0.7 to 49 mg. The normal function of cobalt is confined to its role in the metabolism of vitamin B_{12}. In general, cobalt is not considered to be a toxic metal.

Low levels of cobalt injected into rats have been shown to produce anemia, a condition not proven in humans. In contrast, cobalt has been shown to have an erythropoietic effect. Erythropoietic production in the kidney is stimulated during respiratory alkalosis that results from raised cobalt levels (124).

Cobalt toxicity due to increased dietary intake was demonstrated in beer drinkers from Quebec. Cobalt was absorbed in the

heart muscles leading in some cases to cardiomyopathy. Studies in laboratory rats have also shown that when pure cobalt devices have been implanted, accumulations of cobalt have been found in the heart muscle. Cobalt, like most transition metals, can exhibit a range of toxic effects arising from the complexes they can form. This is especially true with enzymes where histidine, serine, and cysteine are all potential ligands. There exists a definite possibility of altered metabolism due to increased levels of cobalt in the body.

The question of hypersensitivity to the surgical Co-Cr-Mo alloy is important to address. Cobalt-chromium alloys are likely offenders in this respect since cobalt and the chromates are common sensitizers. Halpin (49) reported a case in which fractures of the radius and ulna were fixed with Vitallium® plates and screws. Seven years after surgery a painful swelling appeared over the extensor aspect of the forearm and after eight years a sarcoma was expected. A histological examination of the removed tissue revealed no evidence of neoplasia. The specimen was composed of skeletal muscle showing a massive fibrotic reaction. The periphery of the lesion contained fibroblasts and inflammatory cells, including lymphocytes, mast cells, plasma cells and eosinophils. After removal of the fixation device, the swelling disappeared and the patient had function of the arm and hand. Standard patch testing revealed the patient was sensitive to cobalt.

There exists considerable debate over the use of cobalt-to-cobalt alloy bearing surfaces. It is postulated by some to be a contributing factor to metal hypersensitivity and possible

prosthetic loosening. Deutman, Mulder, Brian, and Nater (33) reviewed 15 patients with failed McKee-Farrar prostheses. They found that two of the patients were metal-sensitive. Benson, Goodwin, and Brostoff (12), found a high incidence of unexpected metal allergy in patients who had received a metal-to-metal (Co-Cr-Mo/Co-Cr-Mo) McKee hip prosthesis. Of the 32 patients having a McKee hip prostheses, one was sensitive to nickel alone, two to nickel and cobalt in combination, three to cobalt alone, and three to chromium alone. In contrast, the incidence of metal sensitivity in those with a Charnley prosthesis (metal-to-plastic) was no higher than in the control group. Prosthetic loosening in the former group was observed only for patients sensitive to chromium. This occurred for two of the three patients sensitive to chromium.

Evans, Freeman, Miller, and Vernon-Roberts (39) conducted patch tests on 14 patients with loose cobalt-chromium on cobalt-chromium joint replacements. Nine were metal-sensitive to either chromium, nickel, or both. Twenty-four patients with normally functioning securely fixed McKee-Farrar prostheses were negative to all the sensitivity tests. They concluded that after total joint replacement, bone necrosis and subsequent loosening of the prostheses may be due to the development of sensitivity to the metals used. Since the incidence in metal sensitivity increased with the use of metal-on-metal articulating surfaces, they preferred the metal-polymer articulating surfaces. Jones, Lucas, O'Driscoli, Price, and Wibberley (64) examined seven patients with McKee hip arthroplasties which became unsatisfactory after periods

varying from nine months to four years. Six of the patients were cobalt-positive but negative to nickel and chromium. The patients all experienced pain, and radiological features included acetabular fracture, bone resorption, loosening and dislocation of the prostheses. Atomic absorption analyses revealed increased cobalt concentrations in the urine, adjacent bone, and the joint fluid.

Brown, Lockshin, Smith, and Bullough (15) also explored the possibility that wear products of cobalt-chromium articulating surfaces might lead to sensitivity to metal wear products and in turn to loosening of a component of the prostheses. They conducted patch tests for sensitivity to cobalt, nickel, and chromium on 20 patients with sterile, loose McKee-Farrar hip replacements. All tests were negative in all patients. In five patients they also conducted the lymphokine assays for migration inhibition factor and blastogenic factor. Only one assay was positive. Their findings did not support the thesis that hypersensitivity to metal was a cause of component loosening after McKee-Farrar total hips.

There now exists considerable data demonstrating that a percentage of the population is metal sensitive. Vitallium®, containing cobalt and chromium, has two elemental constituents that often result in positive patch tests. A question that needs to be answered is whether an implant alloy can sensitize a person or can the implant only cause a hypersensitivity reaction in a person already sensitized. Obviously, more research needs to be conducted in this area.

Another area of systemic biocompatibility concerns the carcinogenic effect cobalt-chromium-molybdenum alloys may have. Swanson,

Freeman, and Heath (105) injected particulate debris from a Co-Cr-Mo hip simulator into thigh muscles of 40 rats. After a 25 month period, 22 tumors were observed. Heath discovered earlier that cobalt particles in the size range of 3.5 to 17 microns injected into rats were carcinogenic. Later work by Heath revealed that chromium debris injected into rats did not cause tumor formation. It was concluded that cobalt was responsible for the carcinogenic effects of the Co-Cr-Mo debris used in their experiment. However, it has been shown that chromates can be carcinogenic. Thus, the interaction of the released chromium from Co-Cr-Mo implants cannot be disregarded.

Oppenheimer, Oppenheimer, Danishefsky, and Stout (84) implanted samples of Vitallium® into 25 rats with two implantations per rat. After a latent period of 453 days, five malignant tumors had been formed. Of the tumors produced, all were fibrosarcomas except for one osteogenic sarcoma. Heath, Freeman, and Swanson (53) produced malignant sarcomas by implanting samples of Co-Cr-Mo particulate debris into the skeletal muscle of two-month-old female rats. Seven rats were injected and 14 tumors formed. The tissue examined revealed sarcomas which varied in type from cellular tumors with some fiber formation and appearance of giant cells to an osteofibrosarcoma. The neoplasms contained large clumps of a granular material together with some crystalline needles of various sizes.

The findings of the previous investigations demonstrate that tumors as a result of Co-Cr-Mo implanted alloys could be a reality in humans. This is by no means a foregone conclusion, but it is a

hazard to be investigated most carefully. For example, it is known that nickel is carcinogenic for laboratory animals and also presents carcinogenic hazards for humans. The same is true for cobalt. Metallic chromium presents no carcinogenic hazard for rats or humans, however, chromates are carcinogenic for both. Thus the corrosion and wear products of the cobalt-chromium-molybdenum alloy could be a possible carcinogenic hazard.

In summary, the cobalt-chromium-molybdenum alloy exhibits good corrosion resistance. The alloy appears to be well tolerated by the adjacent tissues. However, due to the release of cobalt and chromium alloying elements the possibility of hypersensitivity and carcinogenic effects is of real concern.

C. Titanium-6Aluminum-4Vanadium Surgical Alloy

Enthusiasm developed for surgical applications of titanium in the 1940's. In 1945 at the American College of Surgeons meeting, the following declaration was made by Leventhal, "The ideal metal for use in the fixation of fractures . . . would be a metal having the physiologically inert characteristics of Vitallium® and the mechanical and physical characteristics of the S-Mo metal" (Ref. 72, p. 473). In 1950, Leventhal reported on some experiments in which titanium was implanted into the soft tissue and bone of rabbits. Good tolerance was noted and it was also claimed that the metal possessed adequate mechanical properties. Williams (124) reported on a study by Clarke and Hickman, conducted in 1953, which showed titanium to have excellent corrosion resistance as a result of electrochemical investigations. It was not until the 1960's that the material was tested in humans for orthopaedic applications. Emnéus, Stenram, and Baecklund (37) studied a series of 110 Moore prostheses. One group of devices was constructed of titanium and another group was constructed of Vitallium®. No differences were found between the groups and no signs of chemical irritation were noted whenever a titanium prosthesis was removed. One observation was made concerning tissue discoloration. The authors, however, did not report any adverse affects associated with the tissue discoloration. Through the 1960's and 1970's, pure titanium and titanium alloys have been introduced into numerous areas. Presently, titanium is used in oral surgery - endosseous blades, mandibular reconstruction; orthopaedics - total joint replacement,

fracture plates; cardiovascular surgery - prosthetic heart valves, pacemaker encapsulation; and neurological surgery - cranial reconstruction. Of course these are only a few of the metal's applications. However, it does demonstrate that the physical and chemical properties of titanium offer a wide variety of uses (124).

Commercially pure titanium is essentially a very dilute titanium-oxygen alloy (122). The British Standard Specification contains a specification for a maximum of 0.5% oxygen. At these low oxygen concentrations, all the oxygen is in solution and the structure is a single phase. Titanium exists in two allotropic forms; at room temperature, α-titanium or the close-packed hexagonal structure is stable and at temperatures greater than 992.5C the β-titanium or the body-centered cubic form is stable.

Alloying can control the stability of the α and β phases. Elements that form interstitial solid solutions with titanium tend to stabilize the α-phase. Oxygen, nitrogen, carbon, and aluminum are all α-stabilizers. Certain transition elements such as molybdenum, niobium, tantalum and vanadium are all β-stabilizers. The predominant titanium alloy used for implant purposes is the Ti-6Al-4V ternary alloy. The transition element vanadium in the titanium-aluminum system tends to counteract the strong alpha (α) stabilizing effect of aluminum, such that both the α and β phases are stable at room temperature. The phase distribution and morphology of the alloy will be determined by its exact composition and thermal history. Figure 5 shows the microstructure of an equiaxed alpha and beta structure. An alloy demonstrating this microstructure has the desired mechanical properties, strength and

Figure 5: Microstructure of Equiaxed Alpha and Beta Phases in Ti-6Al-4V (200X).

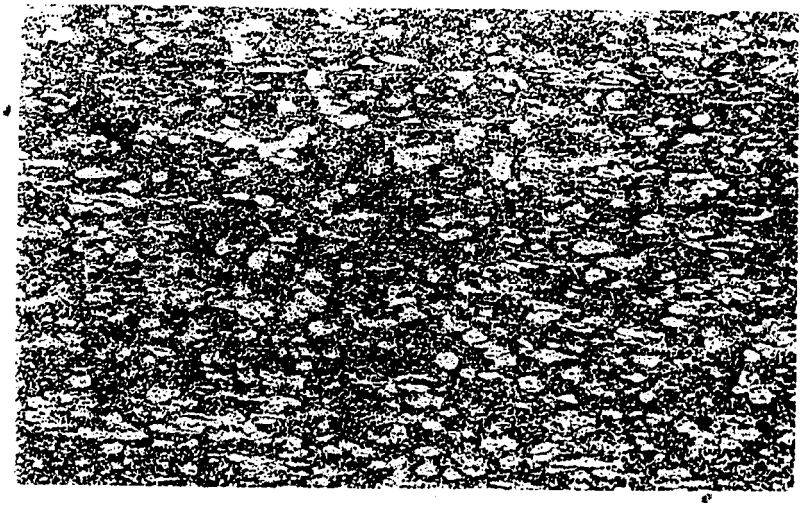

ductility for surgical applications. This microstructure can be obtained by aging the alloy at 530C. An alloy that is heavily worked above 900C will have a microstructure of transformed beta (Figure 6). This material has a low ductility and should be annealed (6,70,122)).

1. Corrosion Characteristics of Ti-6Al-4V

Titanium is a highly reactive metal. Paradoxically, it is this reactivity which makes the metal so resistant to attack by aqueous environments. Pourbaix diagrams of potential versus pH are useful for determining if a metal will exist in a passive state, i.e., form a stable oxide film, or corrode. In the pH range of body fluids, the titanium metal forms a titanium dioxide film that protects it from further oxidation. The extent to which titanium passivates is almost unique.

Electrochemical corrosion analyses have demonstrated the excellent corrosion resistance of both the titanium metal and the Ti-6Al-4V alloy. Figure 7 is a schematic representation of two anodic polarization curves. Curve B is typical of a material whose passive film is subject to disruption at a breakdown potential, E_b. Upon disruption of the passive film, increased corrosion rates result. On the other hand, curve A represents a material whose passive film remains stable over a range of potentials and the current remains low. The lower the value of E_b, the more susceptible the material is to passive film disruption. As discussed earlier, the relationship between the breakdown potential and the

Figure 6: Microstructure of Transformed Beta Phase - Ti-6Al-4V Alloy (200X).

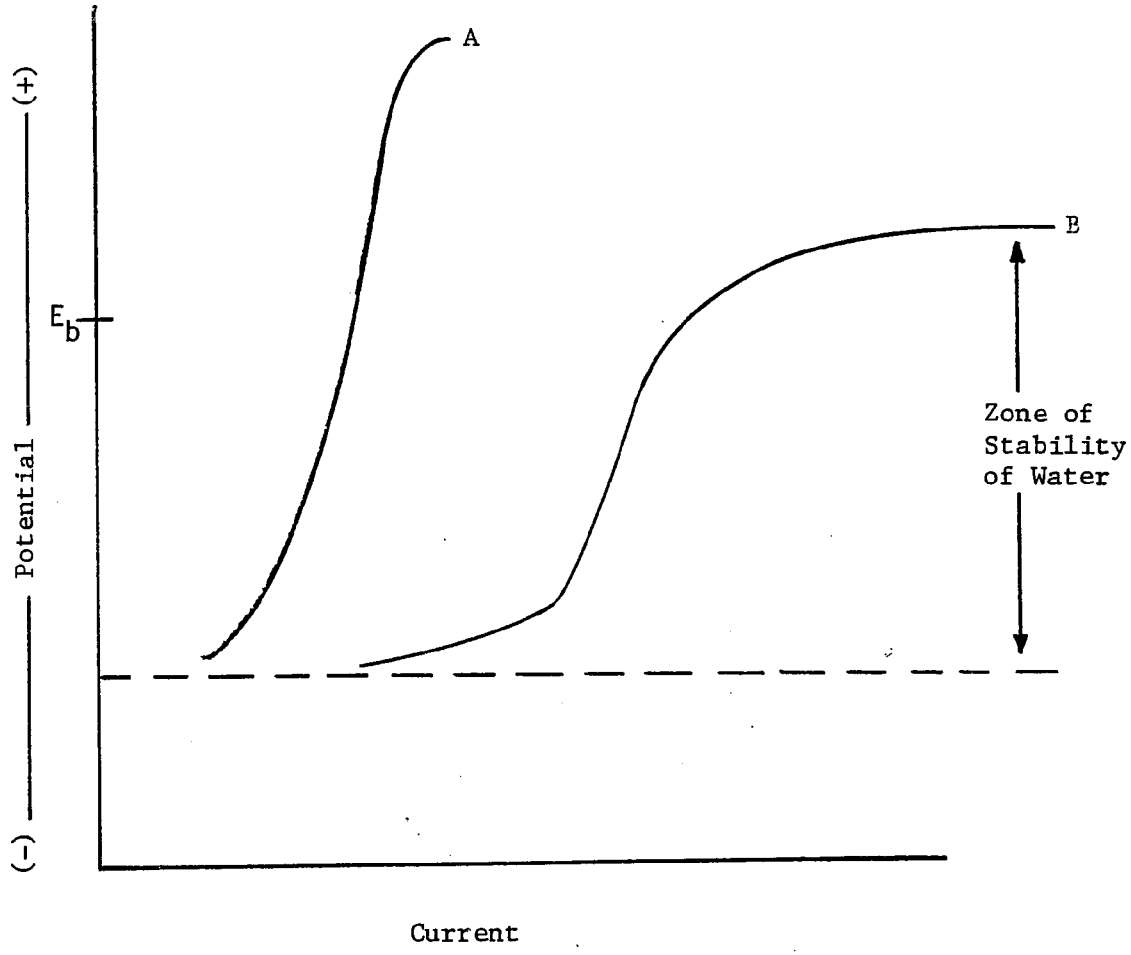

Figure 7: Two Anodic Polarization Curves

rest potential may be significant in analyzing a material's corrosion characteristics. Hoar and Mears (58) reported data on this relationship. Table 3 shows the results from his investigation.

Table 3

Rest Potentials Versus Breakdown Potentials for Surgical Alloys

Material	Resting Potential 480 Hr. in deaerated 0.17M NaCl (volts vs S.H.E.)	Breakdown Potential in deaerated 0.17M NaCl (volts vs S.H.E.)
304 Stainless Steel	0.20	0.20
316 Stainless Steel	0.3-0.5	0.4-0.48
Cast Co-Cr-Mo	0.5	0.87
Titanium	0.37	9
Titanium Alloy	0.23	25
Tantulum	0.36	24

This table shows that the stainless steel alloy will be susceptible to film breakdown since the rest and breakdown potentials are almost the same. The breakdown potential is significantly higher than the resting potential for the cobalt alloy. However, the breakdown potential is less than the oxygen reduction potential of 1.0 volt thus indicating that the alloy may be susceptible to corrosion if the potential rises high enough. Titanium and the titanium alloy demonstrate breakdown potentials much higher than either the resting potential or the oxygen-reduction potential, again demonstrating the excellent corrosion resistance of the titanium alloy.

Solar, Pollack, and Korostoff (98) investigated the passive film behavior of commercially pure titanium, Ti-6Al-4V and nitrided Ti-6Al-4V by utilizing anodic polarization and pulse potentiostatic capacitance techniques in Ringer's solution at 37C. In all tests, the alloys demonstrated passivity over the entire experimental range of potentials. This potential range exceeded the oxygen-reduction reversible electrode potentials. The materials did not exhibit a breakdown potential. They concluded that under static conditions, titanium and Ti-6Al-4V should withstand exposure to physiological chloride solutions at body temperature indefinitely.

Cornet, Muster, and Jaeger (29), utilizing in vitro polarization experiments in Ringer's and a modified Earle's electrolyte, showed that the Ti-6Al-4V alloy had a breakdown potential of +850 mV vs S.C.E., cast Co-Cr-Mo, 200-400 mV vs S.C.E., and 316L stainless steel, 0 to 200 mV vs S.C.E.. Again the titanium showed superior corrosion resistance.

Titanium and its alloys are reported to be immune from pitting corrosion attack under conditions encountered in the body (122). Also, due to the wide range of stability of titanium oxides, even under deaerated conditions as would exist in a crevice condition, this form of corrosion does not occur. This is definitely an advantage titanium possesses over the stainless steel alloys which are especially susceptible to pitting and crevice corrosion.

In vitro experiments have shown titanium to have a higher resting potential than other implant alloys. Therefore, coupling titanium to another alloy should not accelerate corrosion of titanium in the couple. However, the other alloy in the couple may

or may not experience an increased corrosion rate. It has been shown that titanium may be coupled to Co-Cr-Mo (74) and graphite (47) without an accelerated corrosion occurring. However, it has been strongly recommended that titanium not be coupled to stainless steel since the corrosion rate of the stainless steel alloy was predicted to be increased (47).

Fretting corrosion occurs when two surfaces are in rubbing contact in corrosive environments. The oxide film formed by titanium was shown in the static in vitro corrosion experiment to render the material passive over a wide range of potentials. Under wear conditions, it has been reported that the oxide film is not sufficiently stable, thus galling and seizing of titanium or the titanium alloy bearing systems may be a significant problem. A number of surface treatments have been proposed to improve the tribological properties of the material. One method is by anodizing the surface resulting in an enhancement of the oxide layer. Other methods involve the diffusion of interstitial ions into the surface layers, flame spraying of metals and/or metal oxides such as molybdenum, and lastly electroplating of other metals on the surface.

In recent years, some studies have been published showing that titanium when articulated with polytheylene can give in vivo wear rates equivalent to stainless steel and cobalt-chromium alloys. This is contradictory to earlier experiments and theoretical predictions. However, there now exists more effort to improve the stability of the oxide film thus making titanium acceptable for bearing surfaces.

2. Tissue Response to Ti-6Al-4V

The previous section has shown that under static conditions titanium and titanium alloys exhibit excellent corrosion resistance due to the formation of a stable oxide film. There still remains controversy over the use of titanium as a bearing surface. While good corrosion resistance has been predicted for titanium, tissue discoloration is often observed in tissues adjacent to the implant. It is the intent of this section to examine the localized tissue response as well as the systemic responses to the Ti-6Al-4V alloy.

a. Localized Tissue Response

In 1951, Leventhal (72) reported that implanting titanium into subcutaneous tissue of rabbits and also into the femora of rats produced no adverse tissue reactions. Also in the 1950's, Beder and Gilbert (10) and Beder, Stevenson and Jones (11) investigated the tissue response to titanium in dogs. In the earlier study, titanium disks, 0.25 inch diameter by 0.013 inch thickness, were implanted into the rectus abdominus muscles of dogs. Removal of the disks revealed that a fibrous capsule had formed in each case. There was no evidence of leukocytic infiltration but a fibroblastic response was present. It was therefore concluded that the titanium was well tolerated by living tissues of dogs. In the latter study, a titanium bone plate and screw assembly were used for fixation of a fractured femur. The plate remained in situ for 120 days and was checked at intervals radiographically. The fractured femur demonstrated a gradual increase in callus formation. There was no

evidence of osteolytic activity around the bolts or nuts, in or on the bone, and no tissue reaction in the soft tissue portions.

Albrektsson, Branemark, Hansson, and Lindstrom (1) investigated titanium screws which had been inserted into the mandibular, maxillar, tibial, temporal and iliac bones without the use of cements. The objective of their study was to obtain osseointegration, i.e., a direct contact between the living bone and the implant. Direct bone-implant bonding has been demonstrated utilizing ceramic materials for the implant materials (66). Alberktsson et al. believed that bonding could occur between bone and the ceramic oxide layer of TiO, TiO_2, Ti_2O_3 and Ti_3O_4 on a titanium implant. Utilizing scanning electron microscopy, they demonstrated a close topographical relation between the implant and bone. Collagenous filaments from the bone were seen adhering to the actual surface of the implant. The mechanism of anchorage of the collagen appeared to be of the same type as for the attachment of Sharpey's fibers to bone. Jaw implants had to penetrate the gingiva to function as a support for a dental bridge. The skin penetration caused no adverse soft tissue effects. Also no toxic reactions were observed in the cells hindering the implant. The overall conclusion of the study was that osseointegration could be established utilizing titanium implants with no adverse tissue response.

Titanium clips were implanted in rabbit brains by H. von Holst, Collins, and Steiner (109). After six months the brain specimens were sectioned and stained for light microscopy. The

examination revealed neither tissue reaction nor pigmentation around the titanium implant.

The previously sited studies demonstrated that titanium implants in a variety of applications are well tolerated by the surrounding tissue. However, one common observation in a number of studies involving titanium implants is the dark brown-black particles in the adjacent tissues. Williams (121,123) and Meachim and Williams (78) observed pigmented tissue around titanium implants and reported for nine of 19 implants a maximum titanium concentration of 100 ppm dried weight and for three of the nine implants, values greater than 2000 ppm. For the samples above 2000 ppm there was no obvious correlation between the titanium content of the tissue and the duration of implantation which ranged from 24 to 57 months. Ferguson et al. (41) reported concentrations of 237 ± 168 ppm from dry ash specimens around titanium implants in rabbit muscle.

To assess the possibility of a toxic response to the increased levels of titanium in the surrounding tissue, Laing et al. (68) correlated the quantity of titanium in the tissues to the thickness of the fibrous capsule surrounding the implant. While large concentrations were measured, the average pseudo-membrane thickness was 0.002 to 0.03 mm which was considered by the authors to be low. The increased titanium concentrations did not result in increased capsule thickness. Meachim and Williams (78) found no obvious correlation between membrane thickness and titanium content. In their histological investigations, they also found no correlation between the titanium content of the tissue and any of the following

features: the presence of leukocytic response, the presence of neutrophils, the presence of granulation tissue, and the amount of necrotic debris at the tissue-implant interface.

Meachim and Williams (78) analyzed the debris associated with titanium implants and found two types of particles and designated them as type A and type B particles. Type A particles gave a positive Perl's staining reaction for ferric iron, and morphologically were usually indistinguishable from haemosiderin. Type B particles appeared dark brown to black and most of these particles gave a negative Perl's staining for ferric iron. These particles usually accumulated at the zone of the fibrous capsule and were observed within the cytoplasm of the fibrocytes, unidentified perivascular cells, and macrophages. There was no correlation between the thickness of the capsule and the type B particulate material.

Emnéus et al. (37) also noted black pigments in tissue around titanium implants. They suggested that the titanium may go into solution as Ti^{+3} which later complexed with organic substances. This stabilized the trivalent titanium by forming a strong complex. They believed that the formation of a stable titanium complex explained the mild reaction often observed even in the presence of large amounts of titanium.

Determining the clinical significance of metal release from titanium implants is difficult. Many of the previous studies cited indicated that the concentration of titanium could not be correlated with tissue responses. Scales, cited by Meachim and Williams (85), has stated that he has not encountered any patient

showing an undesirable effect due to a titanium implant. Meachim and Williams reviewed the clinical, radiological, and laboratory findings of patients with titanium implants. The conclusion was that in only one case did the release of titanium into the tissue have a clinically significant effect and this conclusion was difficult to prove. In a few other cases, metal release could have been a contributory factor in the decision to remove the implant. From this and previous studies it would seem that titanium does not have a particularly harmful effect on local tissues (124).

Tissue cultures have been utilized to investigate the toxicity of titanium. As previously cited, Rae (90) studied the effects of particulate metals in cells from the peritoneum of mice by assaying lactate dehydrogenase (LDH) and glucose-6-phosphate (G6PD) enzymes. Titanium showed no effect on the cells as measured by their enzyme activities. Other tissue culture screening methods have also shown titanium to be nontoxic (8,54,63).

The other elements - aluminum and vanadium - have both been found to be toxic from cell culture studies. Sisca, Thonard, Lower, and George (96) exposed human epithelial cell lines to discs of aluminum and the results of tissue culture experiments showed a severe reaction. Vanadium was shown to be extremely toxic in cell culture experiments conducted by Campbell et al. (23). In 21 fibroblast cultures, 13 of the cultures did not grow at all and the remaining eight showed a marked inhibition of growths.

b. Systemic Tissue Response

Some of the previous studies have raised the possibility of systemic transport of elemental constituents of the Ti-6Al-4V alloy by the bloodstream, either in solution or as particles within the macrophages. The transport of the constituents theoretically can alter trace elemental concentrations, thus affecting the normal metabolic processes of cells. As with the stainless steel and cobalt base alloys, questions concerning allergic responses and carcinogenic reactions should be addressed.

Ferguson et al. (40) observed that when they implanted titanium specimens in rabbit muscles an accumulation of titanium occurred in the spleen and lung of one animal. Implanted titanium raised the titanium content in the spleen to a mean of 451.5 ppm at six weeks and subsequently declined to 13 at 16 weeks. In the lung, the mean concentration of titanium was elevated in two animals to 53.5 ppm at six weeks, while at sixteen weeks, the mean value was 8 ppm. These experimental studies demonstrated that systemic transport of titanium from an implant site does occur.

The effects of the elemental constituents - titanium, aluminum and vanadium on metabolic processes of biological systems needs to be more extensively investigated. Titanium appears to be well tolerated by the tissues even though there is no evidence that it is an essential trace element. Absorption through the gastro-intestinal tract appears to be poor while pulmonary absorption is more significant. Some evidence exists to show that titanium dioxide dust may be a mild pulmonary irritant (28).

Vanadium is generally accepted to be toxic. The toxicity increases as valency increases with pentavalent vanadium being the most toxic. Among the vanadium oxides, the pentavalent vanadium pentoxide is more soluble and more toxic than the less common trioxide or dioxide. Numerous biochemical alterations have been linked to vanadium exposure. These included depression of synthesis or increased catabolism of cystine and cysteine with an overall lowering of serum protein sulfhydryl groups. Vanadium oxides have been shown to be a respiratory irritant in rats, mice and rabbits. With the wide range of possible effects of vanadium, the valence state of the released vanadium from the alloy will be important in determining the effect the element will have (28).

Aluminum toxicity has been shown by King, Savory, and Willis (65) in patients with chronic renal failure and has been related to renal osteodystrophy and dialysis encephalopathy. Spencer, Kramer, Osis, Wiatrowski, Clemontain, and Lender (99) have shown that small amounts of fluoride in water are beneficial in preventing caries. The availability of fluoride for absorption may depend on the presence of certain materials in the intestine. Studies in animals have shown that calcium, magnesium and aluminum reduce the intestinal absorption of fluoride.

There is considerable evidence to suggest that metal sensitivity may be a very important factor in the overall biocompatibility of implants. This is especially true for the cobalt-base alloys and the stainless steel alloys where testing has revealed significant numbers of patients sensitive to nickel, chromium and cobalt elements. Elves, Wilson, Scales, and Kemp (35) patch tested

50 patients for sensitivity and found that 19 patients gave positive reactions. Of these 19, only one tested positive for vanadium and no patient tested positive for titanium. It would seem wise to use titanium implants if a patient is suspected of being sensitive to metals.

The literature contains very few studies indicating that the titanium alloy may be carcinogenic. Memoli, Woodman, Urban, and Galante (80) implanted powder and solid forms of the Ti-6A14V alloy in 26 rats. In the titanium solid implant group, five malignant neoplasms were observed, none of which involved the implant site. Of these five neoplasms, two were lymphoreticular neoplasms. Compounds of titanium, $Ti(C_2H_5)_2$, have been shown to induce sarcomas at injection sites in rats. Titanium implants have been used for implant applications only 20 years. This may be the reason for no reports of carcinomas involving implants, the latency period for development may not have been reached.

Overall, the Ti-6A1-4V alloy has the best corrosion resistance of the major implant alloys. Most of the literature indicated that the tissues adjacent to a titanium implant may be pigmented but the tissue response to the pigmentation is minimal. The titanium base alloy also appears to be the least likely of the implant alloys to cause either hypersensitivy reactions or carcinogenesis.

D. Objectives of This Investigation

The three major surgical alloys - 316L stainless steel, Co-Cr-Mo, and Ti-6Al-4V - all possess good corrosion resistance. This property is one reason for choosing the alloys for implant applications. The belief that good corrosion resistance implies that the material is inert is a misconception. These alloys when implanted will release ionic constituents to the surrounding tissue. This release of material has been observed in tissue adjacent to implanted materials in laboratory animal experiments and also in human tissue adjacent to retrieved prostheses. The biological effects of the released ionic constitutents on the normal function of cells is an area that has not been extensively investigated. In vitro tissue culture experiments have been utilized by several investigators for determining toxic effects produced by implant materials on cells. The actual quantity of corrosion products exposed to the cells as well as the effect of the elemental constituents composing the corrosion products was not controlled in the previous investigations. Therefore the effect of known concentrations of corrosion products and/or their elemental constituents is still unknown. While in vivo animal studies have reported tissue responses to implant alloys from histological examinations, they have not investigated ultrastructural cellular responses experienced by the in vivo cell and the effects these morphological changes may have on the cell's normal function.

The overall objectives of this investigation were to determine the quantities of elemental constituents released from the three major surgical alloys during corrosion processes and to examine

the biological effects of these constituents by *in vitro* cell culture and *in vivo* laboratory animal investigations. The specific aims of this investigation were the following:

1. Utilize atomic absorption analyses for determining the quantities of elemental constituents released during both accelerated corrosion processes and during the passive diffusion of ions from the implant to the surrounding tissue;
2. Utilize *in vitro* fibroblast cell cultures for examining the biological effects of released constituents on cultured cells; Investigate cell survival and morphological changes after exposing cells to corrosion product solutions and solutions of the elemental constituents comprising the corrosion products;
3. Implant alloy specimens, inject corrosion product solutions along implant interfaces in laboratory animals and examine the biological effect these corrosion products have on *in vivo* fibroblast cells; Examine fibrous capsules formed in response to the implant material with light microscopy and also with transmission electron microscopy;
4. Examine the ultrastructures of *in vitro* and *in vivo* cells after exposure to varying concentrations of stainless steel corrosion products.

CHAPTER II

MATERIALS AND METHODS

A. Materials

The surgical alloys* investigated were: (1) the iron base, (Fe-Cr-Ni) 316L stainless steel alloy (ASTM F138), (2) the cobalt base, Co-Cr-Mo surgical alloy (ASTM 75), and (3) the titanium base, Ti-6Al-4V surgical alloy (ASTM F136). The chemical compositions of these alloys are shown in Table 4.

B. Methods

The experimental methods performed in this study included:

1. Atomic absorption analyses of corrosion products,
2. In vitro cell culture analyses,
3. In vivo animal model analyses, and
4. Electron microscopic analyses of cellular ultrastructures.

These sections will be presented separately in this chapter.

*Alloys furnished by Zimmer, Inc., Warsaw, Indiana.

Table 4

Chemical Compositons of Alloys (%)

Element	316L S.S.	Co-Cr-Mo	Ti-6Al-4V
C	0.015	0.28	0.029
P	0.020	0.008	
S	0.007	0.008	
Mo	2.20	5.71	0.024
Si	0.48	0.80	0.096
Mn	1.80	0.44	0.018
Fe	Remainder	0.32	0.15
Cu	0.21		0.013
V			4.19
Al			5.97
Ni	13.76	0.11	0.058
Cr	18.4	28.4	0.22
W		0.026	
O		0.005	0.139
N		6.076	0.007
Remainder		Co	Ti

1. Atomic Absorption Analyses of Corrosion Products

The literature survey described the corrosion characteristics of the 316L stainless steel, Co-Cr-Mo, and Ti-6Al-4V surgical

alloys. A process occurs for each of the alloys where a release of ions occurs by a diffusion of constituents through the passive-oxide film to the surrounding electrolyte. The passive film remains stable, resulting in a minimal loss of material. However, under certain conditions, the passive film may be disrupted resulting in an increase or accelerated release of ions. The elemental composition of corrosion products released under passive and accelerated corrosion conditions was determined.

Cylindrically shaped samples of each of the alloys (1.0 cm in diameter and 1.5 cm in height) were mechanically and chemically cleaned. This included wet grinding with 240 and 600 grit silicon carbide paper, polishing with 1.0 μm alumina suspended in water, and degreasing by boiling in benzene for five minutes followed by thorough rinsing. To obtain corrosion product solutions for analyses, a sample of each alloy was placed in a potentiostatic polarization test system which has been described in detail in previous publications (19,105). The electrolyte was a 0.9% sodium chloride solution adjusted to pH 7.00 ± 0.05 with sodium bicarbonate and maintained at a temperature of 37 ± 1C. For an accelerated corrosion process to occur, the passive film was disrupted at a potential greater than the breakdown potential for the iron and cobalt base alloys (8). The potentials are shown in Table 5. Also shown is the time of application for generation of the corrosion product solutions and the final current attained. Three corrosion product solutions for the cobalt and stainless steel alloys were obtained and one for the titanium alloy. After application of the potentials to the alloy, precipitated complexes

Table 5

Parameters for Generating Corrosion Products Under Accelerated Conditions

Sample	Alloy	Applied Potential (Volts vs S.C.E.)	Time	Final Current
1	316LSS	+0.800V	3.0 hrs.	70.5mA
2	316LSS	+0.800V	2.5 hrs.	41.2mA
3	316LSS	+0.800V	2.0 hrs.	34.5mA
4	Co-Cr-Mo	+0.800V	26.5 hrs.	0.5mA
5	Co-Cr-Mo	+0.800V	26.0 hrs.	1.2mA
6	Co-Cr-Mo	+0.800V	10.0 hrs.	1.5mA
7	Ti-6Al-4V	1.8V	2 wks.	1.8μA

were observed in the electrolyte. The suspensions were collected, dissolved with concentrated HCl, and analyzed by atomic absorption spectrophotometry. All solutions were stored either in clean Nalgalene or glass containers.

Corrosion product solutions generated under passive conditions were also analyzed. Cylindrical samples of the three alloy systems were mechanically and chemically cleaned as previously described. After these cleaning operations, the samples were passivated according to ASTM F86 specifications. This included immersing the specimens in a 10% phosphoric acid, rinsing with distilled water, and then immersing in 40 weight percent nitric acid solution at 60C for 30 minutes. The specimens were sterilized in a steam autoclave at 121C for 30 minutes as a final step. Three samples of each alloy were passivated and placed in separate sterile tubes

containing 10 ml of a sterilized 0.9% sodium chloride solution. A control containing only a sterile saline solution was also made. These were placed in an incubator for six weeks at a temperature of 37 ± 1C. At the end of this period, the corrosion product solutions were collected and analyzed by atomic absorption spectrophotometry.

Three atomic absorption units were utilized for analyzing the corrosion product solutions. The Varian Flame Model 1000 atomic absorption unit was used when concentrations of the element in the corrosion product solution were expected to be large, such as Fe, Ni or Cr for the stainless steel alloy and Co or Cr for the Co-Cr-Mo alloy under accelerated conditions. When elemental concentrations were expected to be small and a greater sensitivity was required, either a Varian Model 1200 atomic absorption unit with a Model 63 carbon rod atomizer and ASJ53 automatic sample dispenser or a Perkin Elmer Model 2380 unit with a HGA 500 programmer and AS40 automatic sampler was used. This was necessary for Mo, Mn, Ti, Al, and V determinations in corrosion product solutions generated during accelerated conditions and for all the elemental determinations of corrosion products generated under passive conditions. The Varian flame atomic absorption unit is sensitive down to 25 ppm and the graphite furnaces units are sensitive down to 10 ppb.

Parameters necessary for all atomic absorption analyses of corrosion product solutions are shown in Appendix A. The atomic absorption instruments were calibrated for each element prior to testing. This was done to insure optimization of all

the instrument's parameters. Calibration standard concentrations and absorption readings are given in Appendix B, Parts I-V, for each of the elements. A linear regression analysis was applied to the calibration data and the correlation factor, r, is given for each series of standards.

2. In Vitro Cell Culture Analyses

To investigate tissue responses to corrosion products, human gingival fibroblasts (HGF) primary cell cultures were used. The cells were grown in 75 cm^3 Falcon tissue culture flasks in a 5% continuous flow CO_2 incubator at 37C. Growth medium for the cells was Waymouth's Medium - MB 752/1 (Gibco Laboratories) with 10% calf serum addition, referred to as Waymouth's Complete Medium. The exact formula for the growth medium is provided in Appendix C. The fibroblast cells were grown in flasks until a confluent monolayer was obtained. At this time the cells were split into other flasks or added to 96-well tissue culture plates. The procedure for splitting cells is given in Appendix D.

Mixtures of synthetic corrosion product solutions based on the chemical composition of the alloy were made with atomic absorption standards*. For example, the chemical composition of the 316L stainless steel alloy is 64% Fe, 18.5% Cr, 13.5% Ni, 2.2% Mo, and

---

*Fisher and Banco atomic absorption standards were used.

1.8% Mn. Based on this chemical composition, a 200 ppm synthetic corrosion product solution containing Fe, Ni, Cr, Mo and Mn was made from atomic absorption standards. Serial dilutions of the corrosion product solution were made with Waymouth's complete medium resulting in a concentration range of 100 ppm to 0.375 ppm for the cell culture analyses. Since the major elements of the 316L stainless steel alloy are Fe, Cr, and Ni, solutions of these individual elements were also made with the atomic absorption standards in the same concentration range as had been done for the synthetic corrosion product solutions.

For the culture analyses, a flask of HGF was trypsinized and resuspended in Waymouth's complete medium (Appendix C). A 0.2 ml cell suspension alliquot was added to each well of a 96-well plate. Four 96-well plates were made on Day 0. The number of cells per 0.2 ml solution varied. However, it was the intent to add low numbers of cells on Day 0 to facilitate counting procedures. By Day 3, the cells had attached to the bottom of the tissue culture plate and had a healthy appearance. On Day 3, the growth medium was removed from the cells. The concentrations of synthetic stainless steel corrosion products as well as the concentrations of individual elements, Fe, Ni and Cr, were added to the wells of the tissue culture plates. A set of controls containing only Waymouth's complete medium was also added. A typical arrangement for the controls, corrosion product solutions, and elemental solutions to the 96-well tissue culture plate is shown in Figure 8. Three wells were made for each of the concentrations and also for the Waymouth controls.

Figure 8: Tissue Culture Plate.

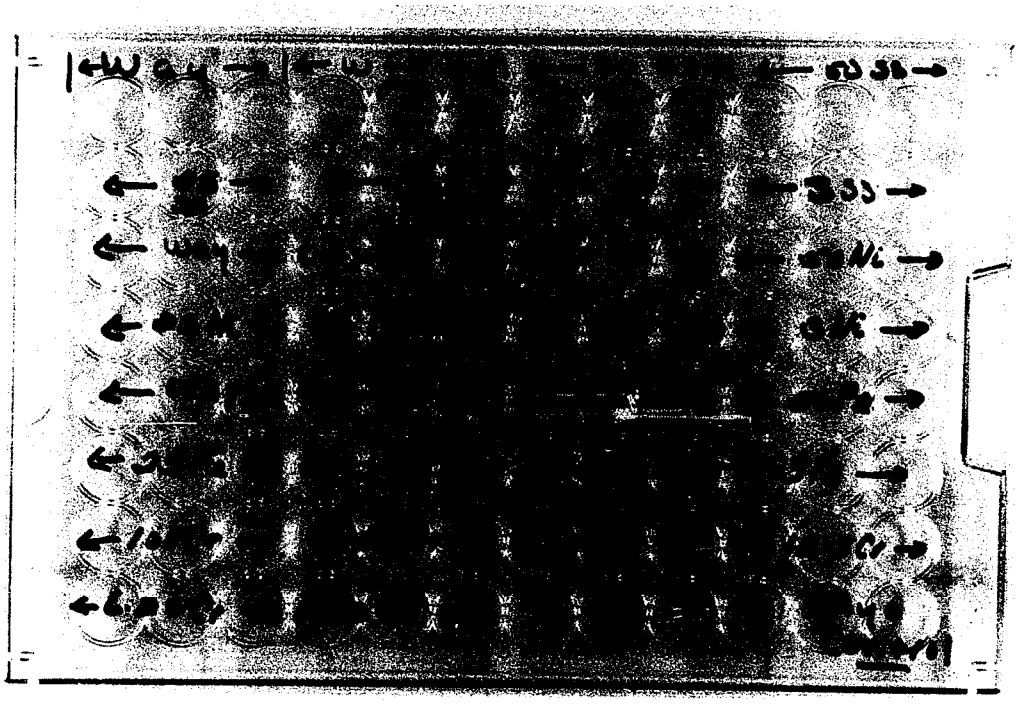

The same procedure was followed for the Co-Cr-Mo and Ti-6Al-4V alloys. For the Co-Cr-Mo surgical alloy, the percent of Co, Cr and Mo are 66%, 28.42% and 5.79%, respectively. Therefore a 200 ppm synthetic corrosion product solution of Co, Cr and Mo was made from atomic absorption standards. Serial dilutions with Waymouth's complete medium were made resulting in a concentration range of 100 ppm to 0.375 ppm for the cell cultures. Solutions of the same concentrations were also made of the individual Co, Cr, and Mo elements. These solutions were added to the 96-well tissue culture plates in the same manner as had been done for the stainless steel alloy. For the Ti-6Al-4V alloy, the chemical composition is 90% Ti, 6% Al and 4% V. Based on this chemical composition, a 200 ppm synthetic corrosion product solution was made as well as solutions of the individual elements Ti, Al and V in the same concentrations used for the previous alloys.

The corrosion product solutions and the individual element solutions were added on Day 3 to the monolayer of cultured fibroblasts. Four plates were made for each alloy so that the cells could be examined on the next four consecutive days. Thus on Day 4, the HGF cells were examined and photographed (Kodak Panatomic-X black and white negative film) at 50X magnification with a Nikon phase contrast camera system. The cells were dehydrated and fixed with methanol, stained with a 0.1% toluidene blue solution, and photographed (Panatomic-X Kodak Film) at 20X magnification for counting purposes. This procedure was repeated on Days 5, 6, and 7. Cells in each well were counted on Days 3-7. Counting the cells was facilitated by projecting the film onto a screen. The

counts were made by separating the screen into regions depending upon the density of cells and all cells were counted. This procedure was followed for each of the alloys and graphs of average cell numbers versus time were constructed. A "Student's" t distribution with a 90% confidence level was applied to the data collected on the last day of the experiment.

3. In Vivo Animal Model Analyses

Cylindrically shaped (0.5 cm in diameter and 1 cm in height) specimens of the 316L stainless steel, Co-Cr-Mo, and Ti-6Al-4V alloys were implanted in the back muscles of New Zealand white rabbits. Prior to implantation, the alloys were mechanically and chemically cleaned, and passivated according to ASTM F86 specifications. Six specimens of the same alloy were implanted in the muscle layers of each rabbit as shown in Figure 9. Two rabbits were implanted for each alloy. The specimens remained in situ for a period of six weeks prior to the introduction of additional corrosion products. This time interval allowed the formation of an intact fibrous tissue capsule around each of the implants.

To accelerate the tissue reactions to corrosion processes, synthetic corrosion product solutions were injected with a 22-gauge needle at the implant-fibrous capsule interface at week 6 and week 7. Solutions for injections were made from atomic absorption standards as described in the previous section and based on the chemical composition of the alloy. Figure 9 shows the sites of injections for each of the alloys. Concentrations injected were

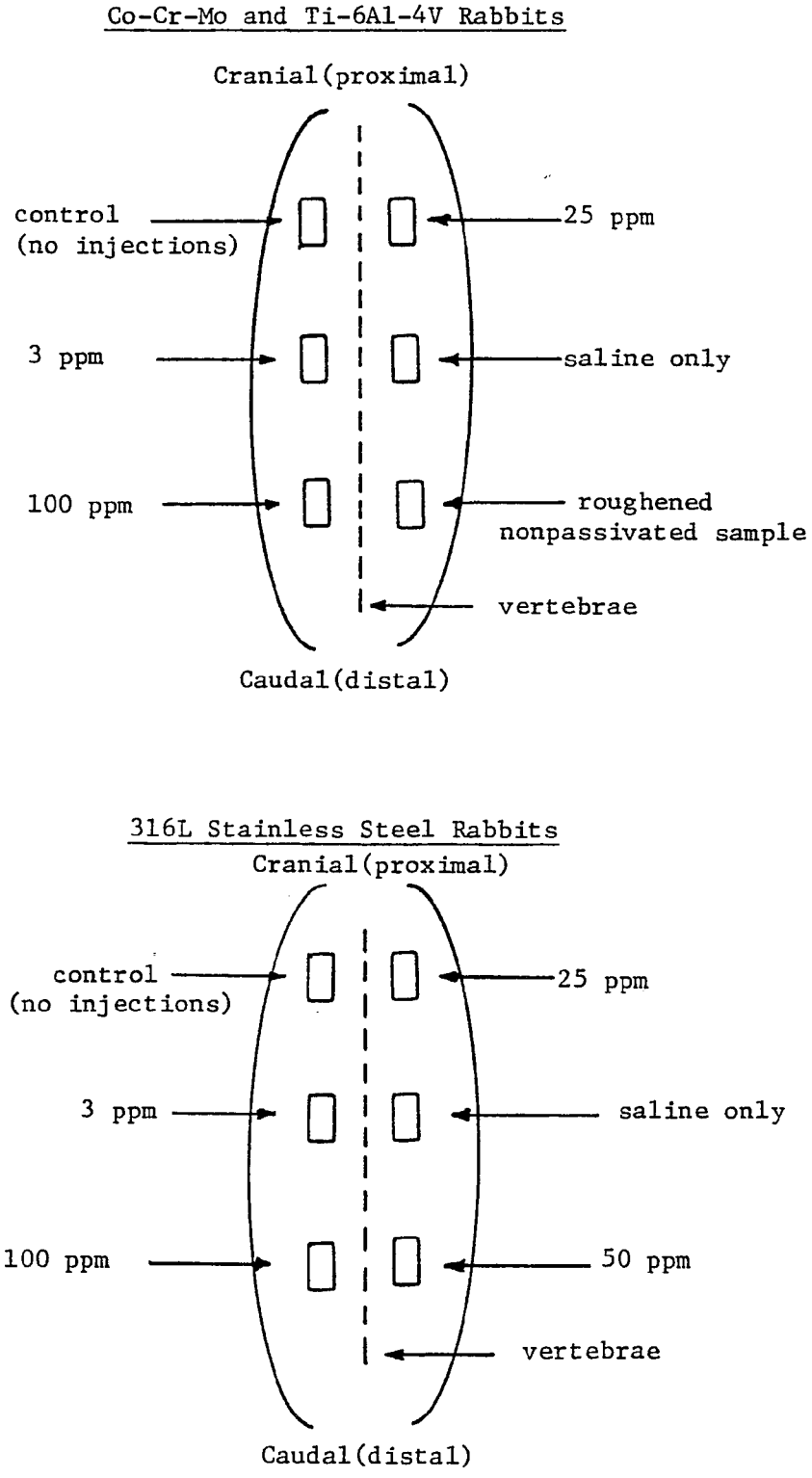

Figure 9: Schematic for the Corrosion Product Implants and Injections.

100, 25 and 3 ppm for the Co-Cr-Mo and Ti-6Al-4V alloys and 100, 50, 25 and 3 ppm for the stainless steel alloy. Instead of the 50 ppm corrosion product injection used with the stainless steel alloy, a specimen having a roughened, nonpassivated surface was used in the right distal location for the cobalt and titanium alloys. At the left proximal site, the alloy specimen did not receive an injection. This site served as a control. For the animal model, the synthetic corrosion product dilutions were made with a 0.9% sodium chloride solution instead of the Waymouth's complete medium used for the in vitro tissue culture experiments. Therefore saline was injected at the right middle site to check for any adverse tissue response to the carrier. Two injections, 1 ml each, were made at weeks 6 and 7. Thus the local concentrate exposed to the tissues was 200, 50, and 6 ppm for the cobalt and titanium alloys and 200, 100, 50, and 6 ppm for the stainless steel alloy. For the initial group of rabbits, swabs for bacterial contamination were conducted. All tests were negative.

At week 8 the implants were retrieved. The rabbits receiving the cobalt and titanium alloys were fixed by injecting a Karnovsky solution into the left ventricle of the heart (Appendix E shows the formula for the Karnovsky solution). The implant and adjacent tissue were placed in the Karnovsky solution for a five-to-six hour period and then stored in a phosphate buffer (Appendix E). The tissue was cut transversly along the middle of the implant, parafin embedded, and stained with Hematoxylin and Eosin (H & E) for light microscopy. No bacterial swabs were made due to the fixation method.

The stainless steel implants were retrieved and the tissue adjacent to the implants immediately fixed with a 2.5% gluteraldehyde solution. The tissue sections were cut into very small pieces due to the low diffusion rate of the glutaraldehyde. These tissue samples remained in the glutaraldehyde for a two-to-three hour period followed by exposure in a 0.1M cacodylate buffer at pH 7.35 for five hours to remove residual glutaraldehyde. These tissue samples were prepared for transmission electron microscopy. Other sections of tissue adjacent to the stainless steel implants were fixed with 10% buffered formalin parafin embedded, stained with H & E, and examined by standard light microscopy techniques.

Standardized photomicrographs of each transverse tissue capsule site were prepared and evaluated for cross comparison with the visual microscope images. Criteria for analyzing the tissue were the fibrous capsule thickness, the extent of phagocytic reaction, and the presence or absence of a granuloma at the implant site. A number system for scoring the individual criterion was devised. The scoring for a response was 0, 1, 2 or 3 with 3 being a severe response. For example, an extremely thick capsule, an extensive cellular response involving the capsule and adjacent muscle, or the presence of a large granuloma would each receive a score of 3 resulting in a final score of 9. Each capsule was ranked as a function of corrosion product concentration and alloy composition. Capsules having no corrosion product injections or only saline injections were also ranked.

4. Electron Microscopic Analyses of Cellular Ultrastructures

The ultrastructure of both *in vivo* and *in vitro* cells was examined utilizing transmission election microscopy (TEM). The fibrous capsules adjacent to stainless steel implants were fixed with 2.5% glutaraldehyde and prepared for TEM analyses. The procedure for dehydration and embedding of the tissues in low viscosity Spurr medium is presented in Appendix F. The capsules prepared for TEM had been exposed to two injections of synthetic stainless steel corrosion product solutions having concentrations of 100, 25 and 3 ppm each. Capsules having had no injections were also prepared for TEM and those capsules served as a control. After tissue preparation and embedding procedures, thin sections were made with an ultratome and subsequently stained with uranyl acetate and lead citrate for examination.

Cell cultures exposed to concentrations of synthetic stainless steel corrosion products were also prepared for transmission electron microscopy. Corrosion product solutions with concentrations of 100, 25 and 3 ppm were prepared with atomic absorption standards as done for the cell culture analyses. These solutions were added to a monolayer of HGF. Controls containing only Waymouth's complete medium were also added. The cells were exposed for a 24-hour period. After this time period, the cells were trypsinized and fixed with a 2.5% gluteraldehyde solution. The procedure for cell preparation and embedding in Spurr medium was identical to that used for the *in vivo* cells as recorded in Appendix F. After embedding, thin sections were made and stained with uranyl acetate

and lead citrate. All ultrastructural analyses were made with a Phillips 300 electron microscope at an accelerating voltage of 60 kV.

Ultrastructural changes as a function of synthetic stainless steel corrosion products were observed for the in vitro cultured cells and in vivo cells from the tissue capsules. Cellular alterations were recorded photographically at magnifications of 10,000X for each corrosion product concentration. Cellular organelles such as the mitochondria, plasma and nuclear membranes, and rough endoplasmic reticulum (RER) were examined. Changes in these ultrastructures were compared to a sequence of ultrastructural alterations recognized by Trump et. al. (107). These events eventually lead to cellular necrosis. The ultrastructural alterations were observed and the frequency that these events occurred were recorded for each concentration. This information was collected for both the in vitro and in vivo cells.

CHAPTER III

RESULTS AND DISCUSSION

A. Atomic Absorption Analyses of Corrosion Products

The results obtained from the atomic absorption analyses of stainless steel corrosion products generated under pitting conditions are shown in Table 6. The chemical composition of the alloy based on the five elements Fe, Ni, Cr, Mo and Mn is 65.9% Fe, 19.3% Cr, 14.4% Ni, 1.9% Mn, and 2.3% Mo. These values were compared with the results from the atomic absorption analyses. The most significant finding was that the corrosion product solution had less chromium than expected when compared to the chemical composition of the alloy. The microstructure of surgical grade stainless steel is a homogeneous solid solution austenitic structure. These results indicate that the alloy might not be truly homogeneous and that some areas could possibly have had less chromium than others. The results from the atomic absorption analyses could be explained by the corrosion process occurring preferentially at areas with lower concentrations of chromium, thus resulting in lower chromium concentrations in the electrolyte. Surface analyses of the alloy showed a pitting corrosion attack of some areas with the remaining surfaces showing little corrosion.

Table 6

Atomic Absorption Analyses of Stainless Steel Corrosion Products Generated Under Pitting Conditions

Sample	Element	ppm	Atomic Absorption Analyses of Corrosion Product Solution (%)	Average of A.A. Analyses vs Chemical Composition of the Alloy
1	Fe	57.75	69.4	
2	Fe	6.0	63.54	69.8% vs 65.9%
3	Fe	6.0	24.5	
1	Cr	9.8	11.8	
2	Cr	38.0	10.6	17.7% vs 19.3%
3	Cr	5.3	14.6	
1	Ni	12.3	14.8	
2	Ni	13.6	14.9	14.2% vs 14.4%
3	Ni	4.6	13.0	
1	Mn	1.45	1.7	
2	Mn	1.45	1.6	1.9% vs 1.9%
3	Mn	0.80	2.3	
1	Mo	1.91	2.3	
2	Mo	2.18	2.4	2.2% vs 2.3%
3	Mo	0.67	1.9	

The results from the atomic absorption analyses for Co-Cr-Mo corrosion product solutions generated under accelerated corrosion conditions are shown in Table 7. The chemical composition of the cobalt alloy based only on the Co, Cr and Mo elements is 66% Co, 28.42% Cr and 5.79% Mo. Comparing these values with the results from the atomic absoprtion analyses revealed a higher value for cobalt and a slightly lower for chromium than was expected. The Co-Cr-Mo microstructure is a solid solution of Co, Cr, and Mo with complex chromium-carbides precipitated along the interfacial grain boundaries during cooling, Figure 4. Surface analyses of the alloy after generation of the corrosion products at potentials greater than the breakdown potential revealed an etched surface for the alloy. The chromium carbides appeared raised indicating that the solid solution phase had preferentially corroded leaving the carbides. This could lead to elevated cobalt in the electrolyte. Since the carbides are compounds with chromium, lower concentrations of chromium could have been released to the electrolyte.

To generate corrosion product solutions under accelerated conditions for the Ti-6Al-4V alloy, a potential of 1.8 volts was applied for a period of two weeks. At the end of this time period, the final current was only 1.8 μamps. Analysis of the electrolyte with the Perkin Elmer graphite furnace atomic absorption unit revealed very low concentrations of 0.0099 ppm Al, 0.012 ppm V and 0 ppm Ti (Table 8). Under the static corrosion conditions of this experiment, the alloy did not experience a film breakdown which would have resulted in higher corrosion rates and greater concentrations of the elements in the electrolyte.

Table 7

Atomic Absorption Analyses of Co-Cr-Mo Corrosion Products Generated Under Accelerated Conditions

Sample	Element	ppm	Atomic Absorption Analyses of Corrosion Product Solution (%)	Average of A.A. Analyses vs Chemical Composition of the Alloy
1	Co	13.2	74.1	
2	Co	30.9	74.5	74.2% vs 66.0%
3	Co	19.9	74.0	
1	Cr	4.2	23.6	
2	Cr	9.5	22.9	11.8% vs 28.4%
3	Cr	5.9	21.9	
1	Mo	0.415	2.3	
2	Mo	1.074	2.6	3.0% vs 5.8%
3	Mo	1.11	4.1	

Table 8

Atomic Absorption Analyses of Ti-6Al-4V Corrosion Products Generated Under Accelerated and Passive Conditions

Sample	Element	ppm-range	Average ppm
"Accelerated" solution	Ti	0	0
Passive #1	Ti	0.0-0.0198	0.0055
Passive #2	Ti	0	0
Passive #3	Ti	0.0-0.0055	0.0027
Control	Ti	0	0
"Accelerated" solution	Al	0.0074-0.0124	0.0099
Passive #1	Al	0.0049-0.0521	0.0286
Passive #2	Al	0.3451-0.3724	0.3588
Passive #3	Al	0.0844-0.0869	0.0856
Control	Al	0.0025-0.0050	0.0037
"Accelerated" solution	V	0	0.0118
Passive #1	V	0	0.0104
Passive #2	V	0	0.0079
Passive #3	V	0	0.0066
Control	V	0	0.0104

Mears (79) has reported the breakdown potential for the Ti-6Al-4V alloy to be 25 volts VS S.H.E.. Running the experiment at 1.8 volts vs SCE obviously did not cause film disruption. However, conducting the experiment at 25 volts seemed unrealistic considering that body conditions would never experience such high potentials. Thus, under static *in vivo* conditions the titanium alloy should not breakdown. Further analyses under nonstatic

conditions may provide interesting correlations with *in vivo* analyses of tissue adjacent to Ti-6Al-4V implants.

The results of the atomic absorption analyses for the stainless steel corrosion products generated under passive conditions are given in Table 9. All the concentrations from these analyses were very low. Referring to the iron data in Table 9, the average concentrations of iron for the three samples were 0.1729, 0.1598 and 0.0922 ppm. The control, containing only a 0.9% saline solution, had an average iron concentration of 0.0975 ppm, a higher reading than sample 3. Small elevations in the samples were also observed for chromium, molybdenum and manganese. Nickel demonstrated the highest values, however the lower value for some of the samples was not significantly higher than the upper value for the control. For the analyses, the readings for the samples were generally higher than for the control, indicating that a diffusion of ions into the electrolyte had occurred. Since the magnitudes of the elements in the samples were only slightly higher than the control in many cases, further experiments are required before conclusions could be made.

The results from the atomic absorption analyses for the Co-Cr-Mo corrosion products generated under passive conditions are shown in Table 10. While all the results were higher than the control solutions, the values were still in a part per billion (ppb) range. As with the stainless steel passive corrosion product analyses, further analyses and experimental changes need to be made prior to forming any conclusions.

Table 9

Atomic Absorption Analyses of Stainless Steel Corrosion Products Generated Under Passive Conditions

Sample	Element	ppm-range	Average ppm
1	Fe	0.1383-0.2144	0.1729
2	Fe	0.1245-0.2075	0.1598
3	Fe	0.0899-0.945	0.0922
Control	Fe	0.0692-0.1199	0.0975
1	Ni	2.2850-2.343	2.314
2	Ni	2.407-2.582	2.494
3	Ni	2.459-2.512	2.486
Control	Ni	1.948-2.029	1.988
1	Cr	0.0386-0.0396	0.0391
2	Cr	0.0325-0.0354	0.0340
3	Cr	0.0321-0.0344	0.0335
Control	Cr	0.0222-0.0269	0.0245
1	Mo	0.0694-0.0707	0.0070
2	Mo	0.0549-0.0622	0.0585
3	Mo	0.0545-0.0642	0.0594
Control	Mo	0.0468-0.0570	0.0513
1	Mn	0.1133-0.1272	0.1203
2	Mn	0.0746-0.0746	0.0746
3	Mn	0.1051-0.1106	0.1078
Control	Mn	0.0802-0.0802	0.0802

Table 10

Atomic Absorption Analyses of Co-Cr-Mo Corrosion Products Generated Under Passive Conditions

Sample	Element	ppm range	Average ppm
1	Co	1.447-1.524	1.489
2	Co	1.514-1.628	1.571
3	Co	1.573-1.651	1.612
Control	Co	1.306-1.381	1.343
1	Cr	0.0311-0.0363	0.0314
2	Cr	0.0316-0.0335	0.0326
3	Cr	0.0344-0.0368	0.0356
Control	Cr	0.0222-0.0269	0.0245
1	Mo	0.0311-0.0524	0.0417
2	Mo	0.0541-0.0735	0.0647
3	Mo	0.0553-0.0561	0.0557
Control	Mo	0.0468-0.0570	0.0513

The results of the Ti-6Al-4V corrosion products generated under passive conditions are given in Table 8. These values are all extremely low. Vanadium was not detected at all in the three passive solutions and the values for titanium were extremely low. Aluminum showed a slight elevation. Comparing the results from the accelerated conditions with the passive conditions revealed no significant differences. The low values reported for each of the experiments indicated that both experiments were under passive conditions where ions are released under a slow diffusion process.

In summary, atomic absorption analyses of corrosion products generated under accelerated conditions for the cobalt base and stainless steel surgical alloys revealed that ionic constituents are released preferentially. For stainless steel, pitting may occur preferentially at lower chromium composition sites and for the Co-Cr-Mo alloy, corrosion may preferentially occur at the solid solution phase. The Ti-6Al-4V alloy did not experience accelerated corrosion under the static conditions employed in this experiment. The atomic absorption analyses of the passive corrosion conditions revealed slightly elevated amounts of the elements. Since these elevations were so close to the control solution of 0.9% saline, conclusions were not made pending further analyses and experimental changes. One obvious change in these experiments would be to increase the surface area of the alloy and expose the material for longer periods of time before conducting the analyses. This would increase the elemental concentrations in the electrolyte versus the control solution. Then conclusions could be possible.

B. In Vitro Cell Culture Analyses

Cell cultures utilized for biocompatibility testing of implant alloys have been previously sited (81,86,90). In general, cell cultures have been utilized in association with polymer testing much more than for alloys (5,17,56,69,89,92,114,126). The use of cell cultures for toxicity studies has been criticized in that they do not contain the humoral and neural responses that exist *in vivo*. While this is a valid criticism, cell cultures are a relatively

simple system which can allow studies of specific events in a controlled environment. For each of the alloys in this investigation, varying concentrations of synthetic corrosion product solutions and also a range of concentrations of the elements comprising the alloys were added to a human gingival fibroblast cell culture system.

Figure 10 shows the results from exposing cells to solutions of nickel. The graph, Figure 10, shows the average number of cells versus time for the tissue culture system. Statistical analyses were applied to the data for Day 7 using the "Student's" t distribution with a 90% confidence level. Error bars were constructed for the confidence interval for the control or Waymouth's solution. Maximum and minimum error bars are also shown on the data obtained from exposing the cells to metallic ion solutions. On Day 7, nickel concentrations > 25 ppm inhibited the growth rates of the fibroblasts. However, nickel concentrations $\leq$ did not inhibit the growth of the cells as compared to the cells exposed only to Waymouth's medium. While the effect of the elements on the cellular growth rates is an important parameter, alterations in the cellular morphologies are probably even more important. If the elemental constituents significantly alter cellular morphologies, normal functioning of the cell could also be significantly altered. Figures 11A-B show cells exposed only to Waymouth's compete medium. In Figure 11A there is a lower density of cells than in Figure 11B. The cells shown in these figures have the long spindle shape, typical of adhering fibroblasts in cultures. The cells shown in Figures 12A-D were exposed for three days to nickel concentrations

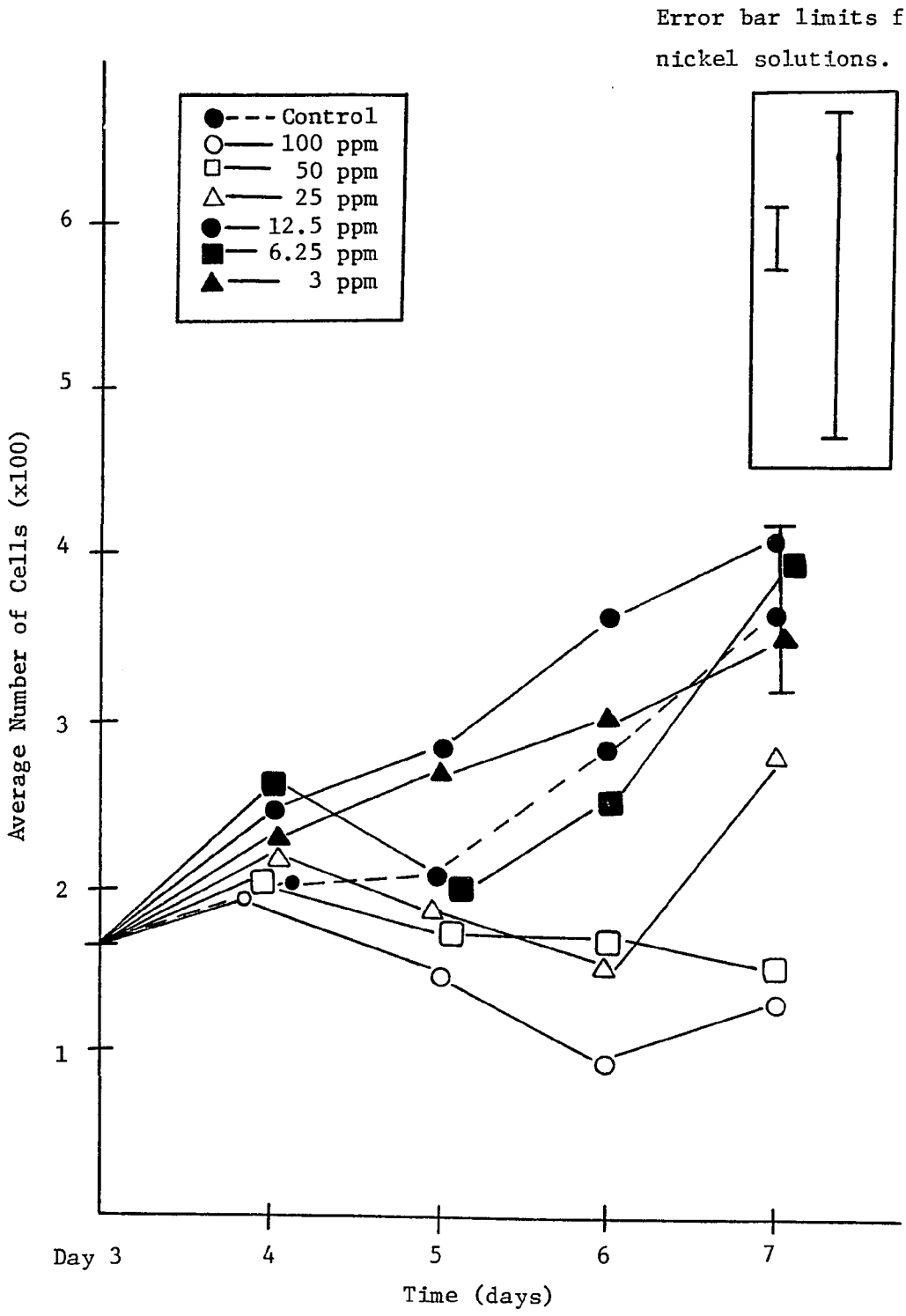

Figure 10: HGF Exposed to Nickel Solutions

Figure 11: Normal Human Gingival Fibroblasts.

A. Low density of cells (100X)

B. Increased density of cells (100X)

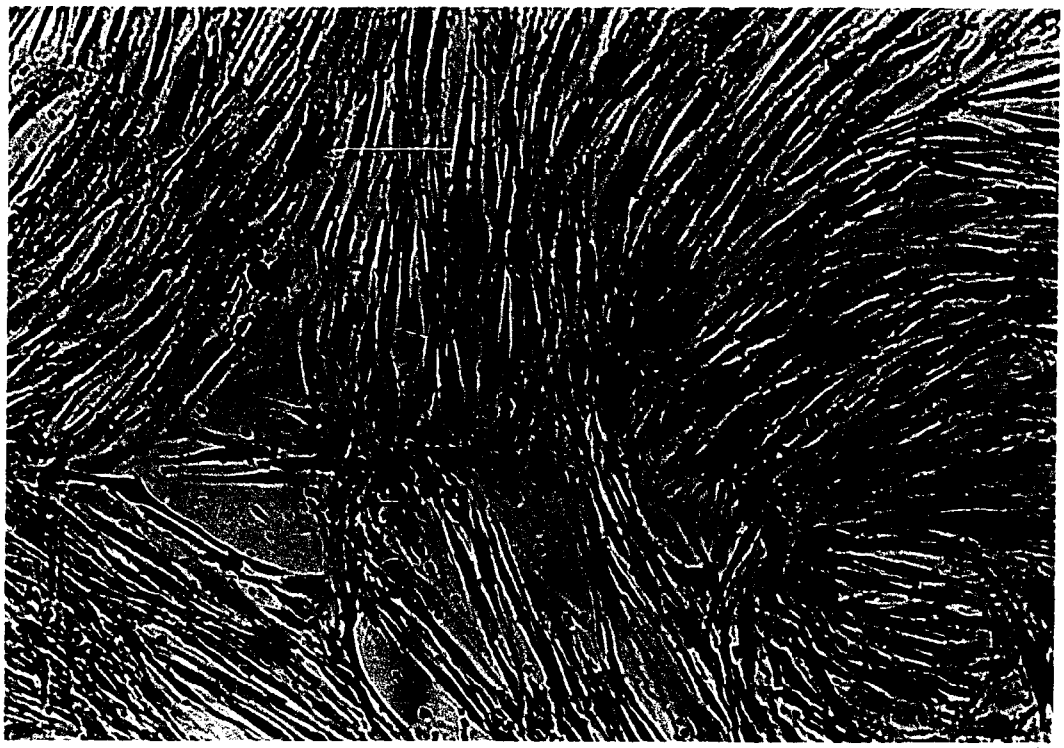

Figure 12: Human Gingival Fibroblasts Exposed to Nickel at the Following Concentrations (100X):

A. 100 ppm Ni B. 25 ppm Ni

C. 12.5 ppm Ni D. 3 ppm Ni

of 100, 25, 12.5 and 3 ppm. At 100 ppm, cellular morphologies were altered but at 12.5 ppm the morphologies were normal. Even at 25 ppm Ni, some cells show the spindle shape of the normal fibroblast. On Day 7 of the experiment, the cells still had a normal appearance at the 12.5 ppm concentration. Overall, the effect of nickel on the cells was not nearly as toxic as will be shown for some of the other elements.

Iron, at concentrations $\leq$ 12.5 were similar to the control, while at concentrations > 12.5 ppm the growth rate of the cells was inhibited on Day 7 (Figure 13). Figures 14 A-D show cells exposed for three days to concentrations of iron. Again the higher concentrations caused altered morphologies. The cells had a flattened appearance as compared to the control cells. At 12.5 ppm, the cellular morphologies were more similar to the controls and displayed a more healthy appearance. On Day 7, the cells exposed to 12.5 ppm still had normal appearances. At all concentrations shown in Figure 14, a dark staining precipitate is evident. Iron resulted in a precipitate in the cell culture system more than the other elements investigated.

Chromium inhibited the growth rates of the cells at all concentrations by Day 7 (Figure 15). On Day 5 of the analysis, the cellular morphologies resulting from exposing the cells to concentrations as low as 3 ppm showed significant alterations. Figures 16A-D show cells exposed to various concentrations of chromium on Day 6. These cellular morphologies were all significantly altered. Exposing HGF to lower concentrations, 1.5, 0.75 and 0.375 ppm chromium, Figure 17A-D, resulted in less altered cellular

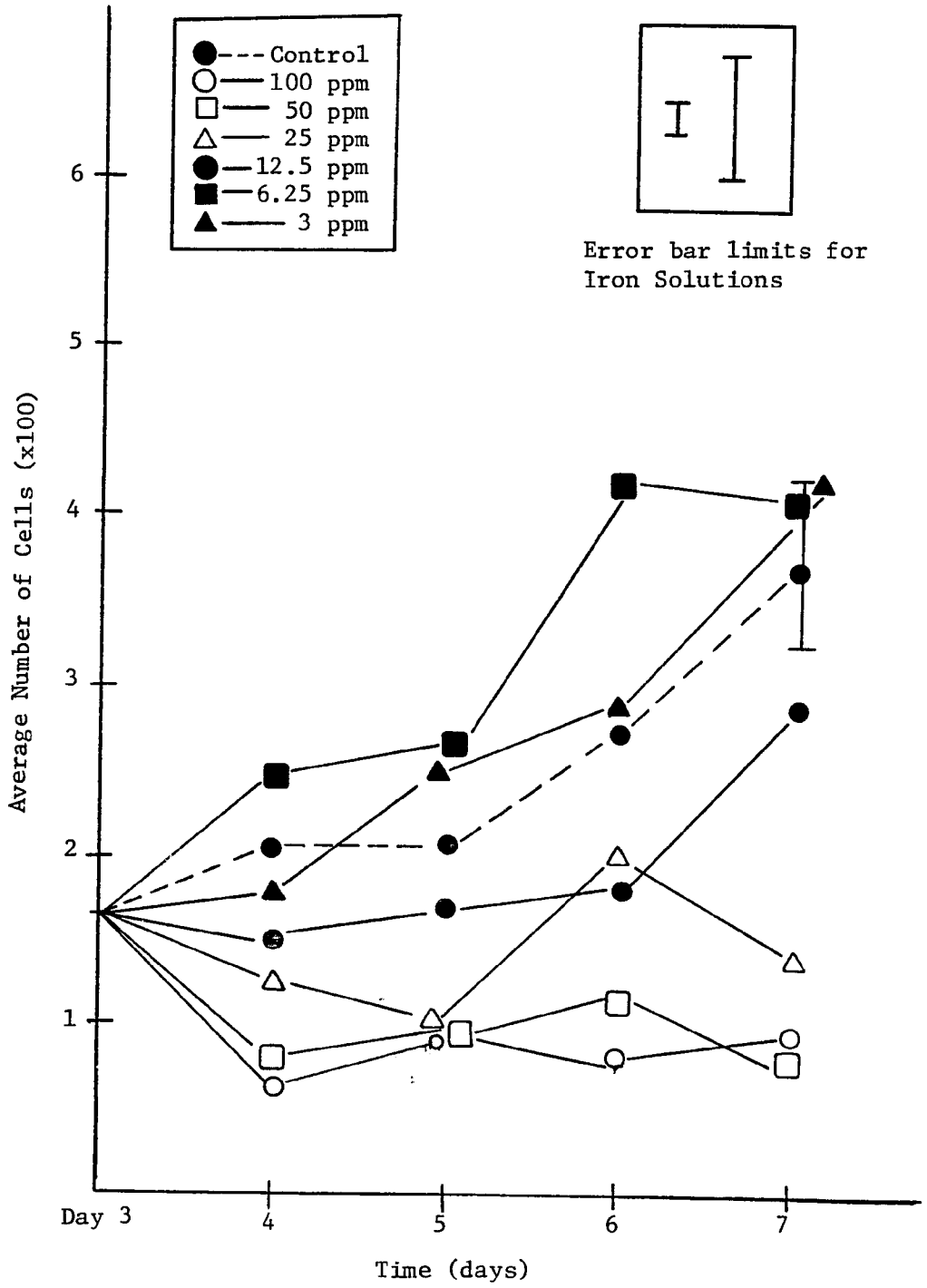

Figure 13: HGF Exposed to Iron Solutions

Figure 14: Human Gingival Fibroblasts Exposed to Iron at the Following Concentrations (100X):

A. 100 ppm Fe B. 25 ppm Fe

C. 12.5 ppm Fe D. 6.25 ppm Fe

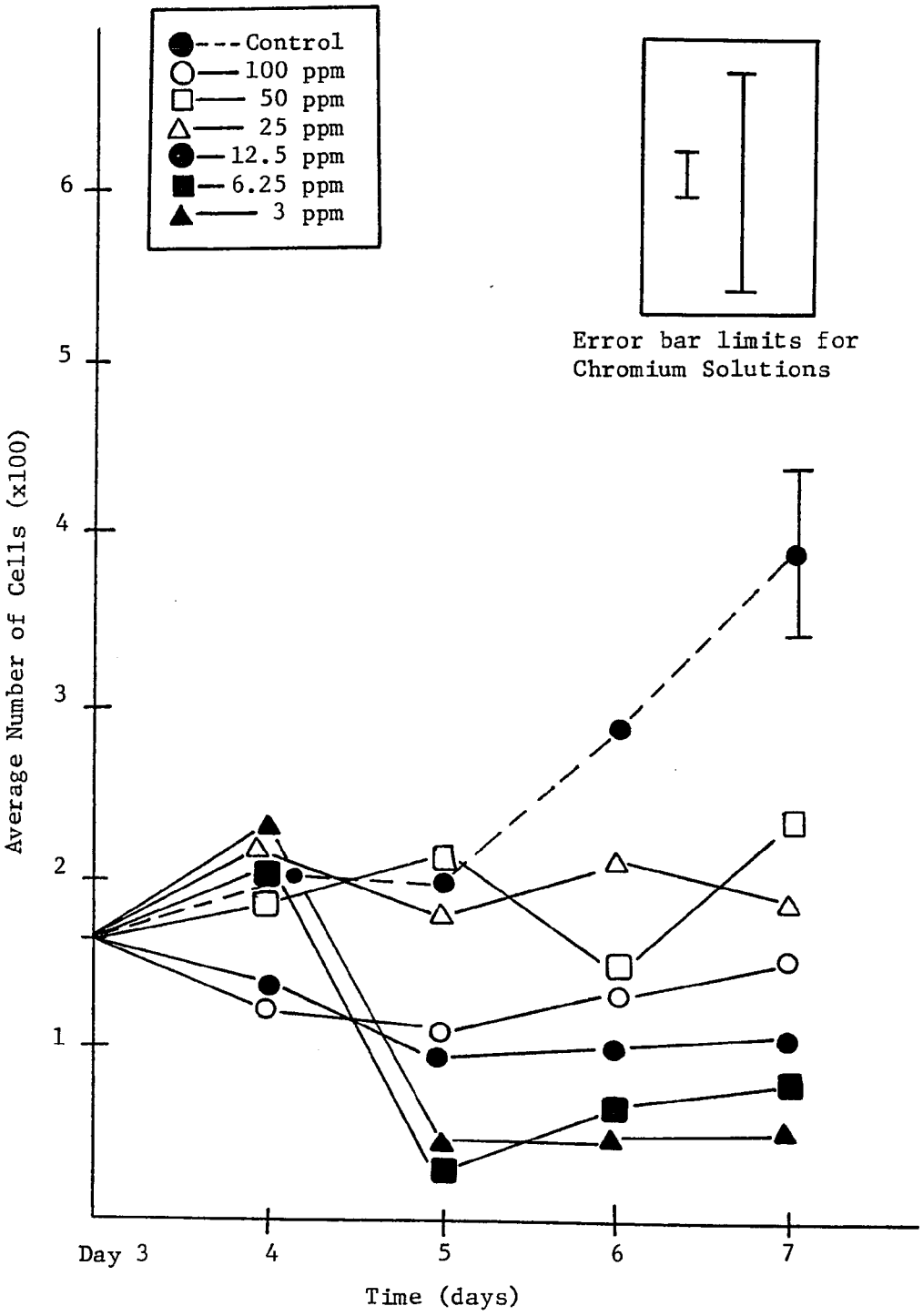

Figure 15: HGF Exposed to Chromium Solutions

Figure 16: Human Gingival Fibroblasts Exposed to Chromium at the Following Concentrations (100X):

A. 100 ppm Cr B. 25 ppm Cr

C. 12.5 ppm Cr D. 3 ppm Cr

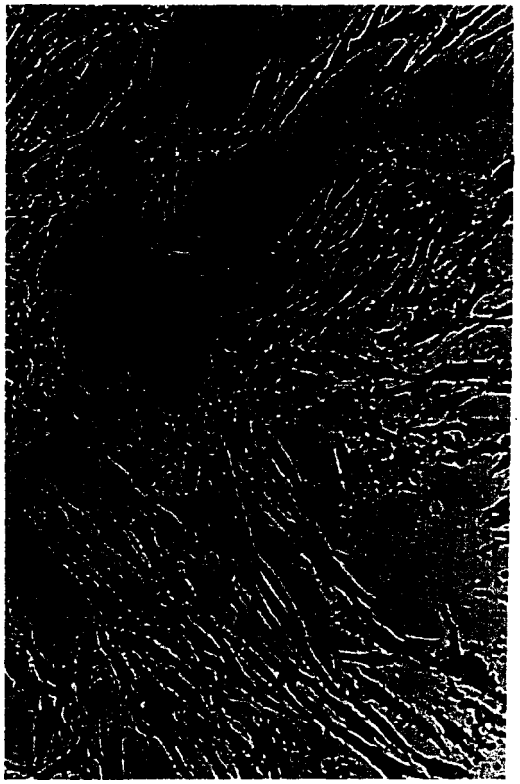

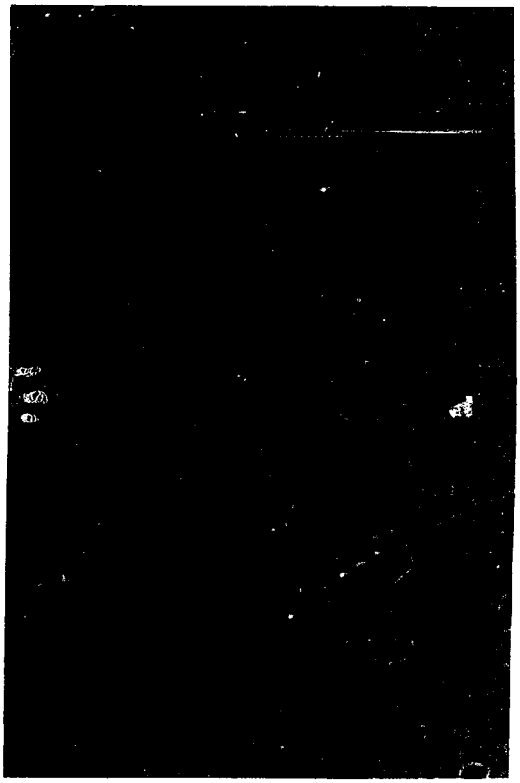

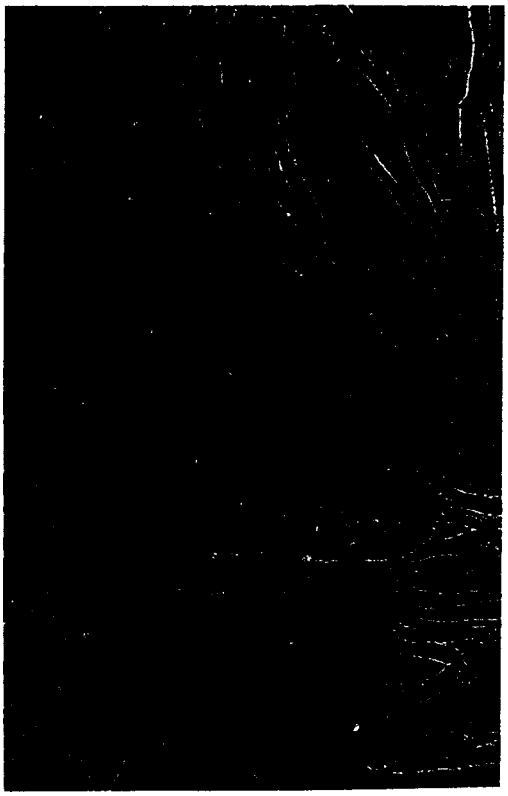

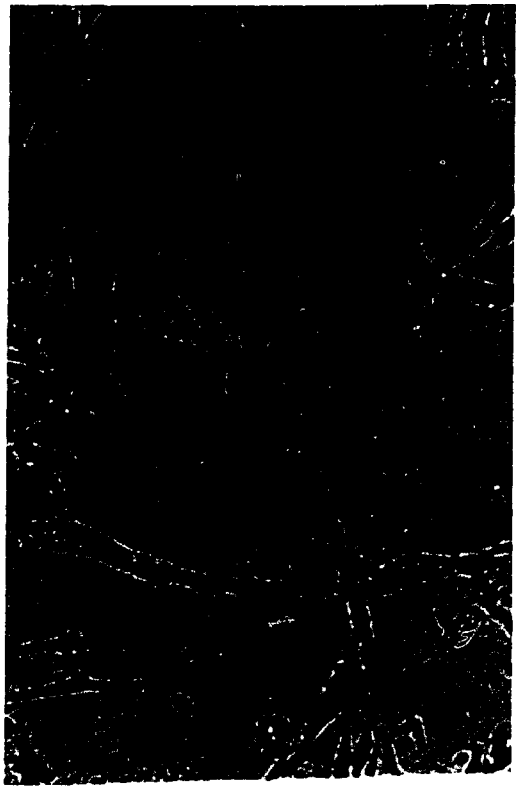

Figure 17: Human Gingival Fibroblasts Exposed to Chromium at the Following Concentrations (100X):

A. 3 ppm Cr B. 1.5 ppm Cr

C. 0.75 ppm Cr D. 0.375 ppm Cr

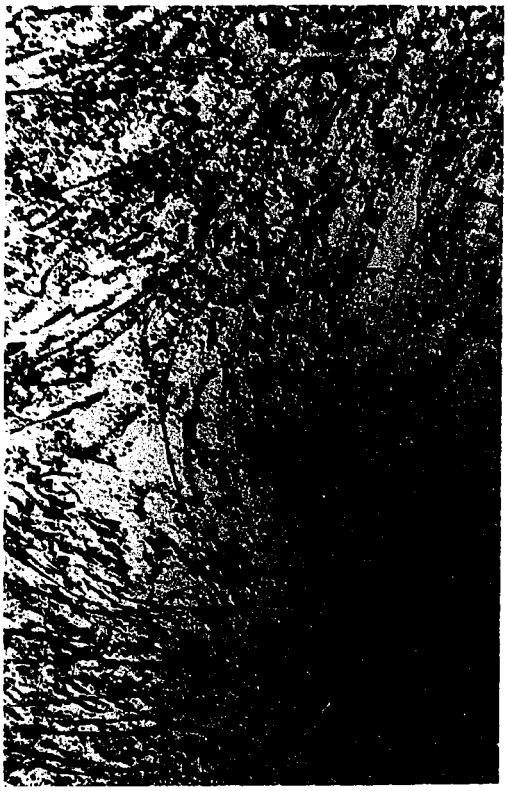

morphologies at the 0.75 and 0.375 ppm concentrations. When the chromium concentrations were lowered to 0.375 ppm, the cellular morphologies displayed a more normal appearance. The experiment shown in Figure 17A-D contained a higher density of cells prior to the addition of the chromium solutions than the experiment shown in Figure 16A-D. Thus the spindle shape of the cells (Figure 17) at chromium concentrations of 0.375 ppm was not as elongated as the normal cells shown in Figures 11A and 11B. However, the density of the cells did not appear to alter the results of the experiment. Toxic effects were produced by chromium at the 3 ppm concentration in both experiments. The effect of chromium was much more toxic to the HGF at earlier times and at much lower concentrations than either iron or nickel.

Figure 18 shows the effect of the stainless steel synthetic product solutions on the cultured fibroblasts. All the concentrations shown inhibited the growth rates of the cells by Day 7. Figures 19 and 20 display the cellular morphologies resulting from exposure to the synthetic corrosion product solutions for three days. The morphologies were significantly altered at concentrations greater than 3 ppm. It was not until the concentrations were reduced to 1.5 ppm that the cells were similar to the control. These significantly altered morphologies were observed as early as Day 5 with a 3 ppm corrosion product solution. A 3 ppm corrosion product solution represents 2 ppm Fe, 0.6 ppm Cr, and 0.42 ppm Ni. Referring to Figures 19 and 20, a 3 ppm solution exhibited toxic effects. Iron and nickel should not be causing these toxic effects at the low concentrations represented. However, chromium

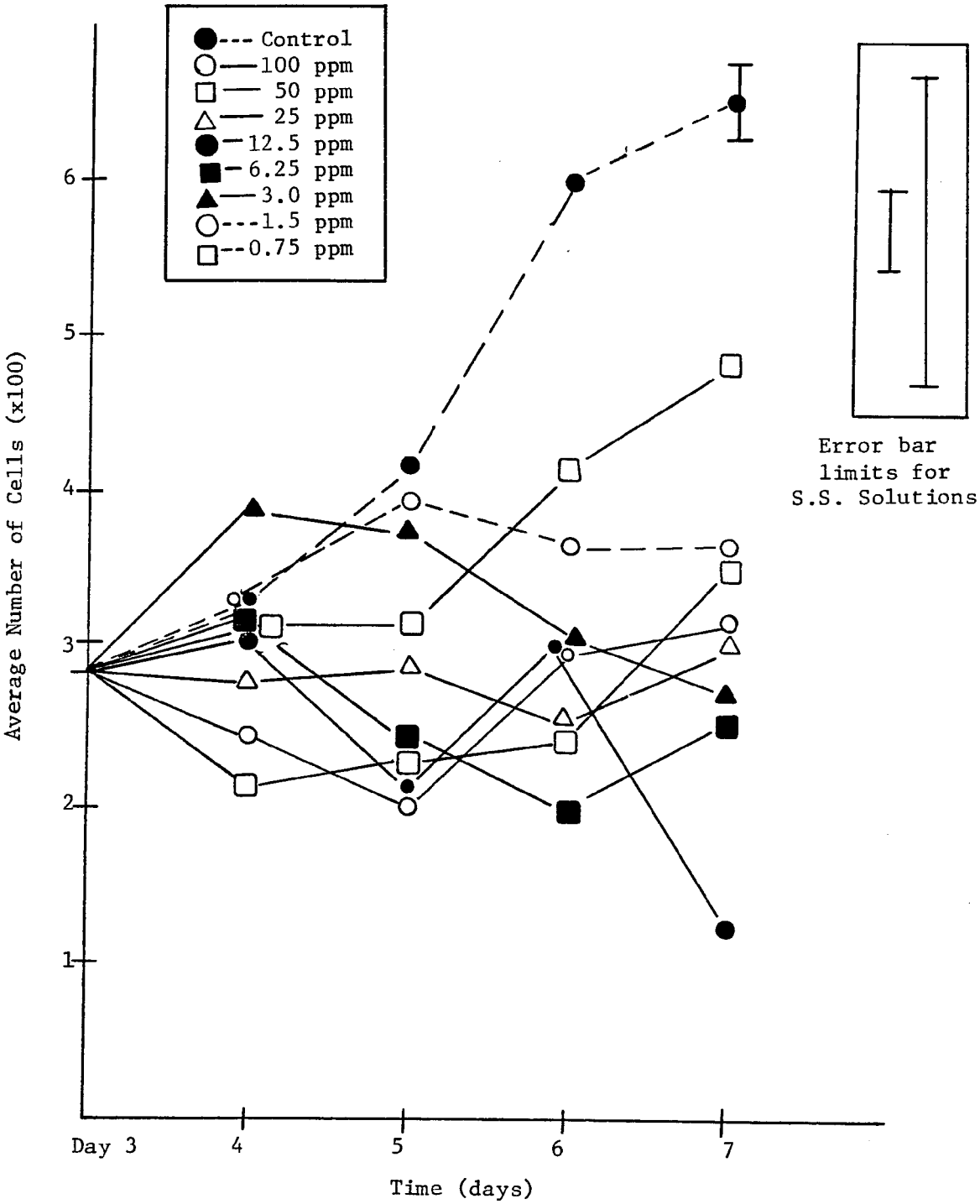

Figure 18: HGF Exposed to 316L Stainless Steel Corrosion Products

Figure 19: Human Gingival Fibroblasts Exposed to 316L Stainless Steel (S.S.) Synthetic Corrosion Products at the Following Concentrations (100X):

A. 100 ppm S.S.

B. 50 ppm S.S.

C. 25 ppm S.S.

D. 12.5 ppm S.S.

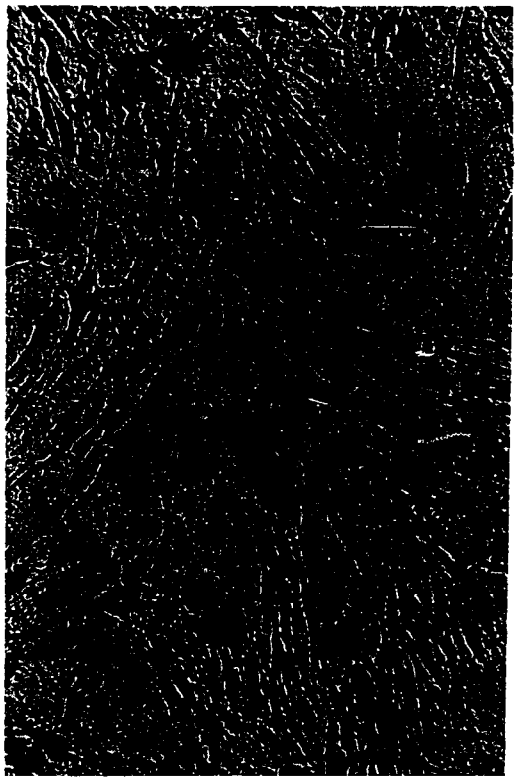

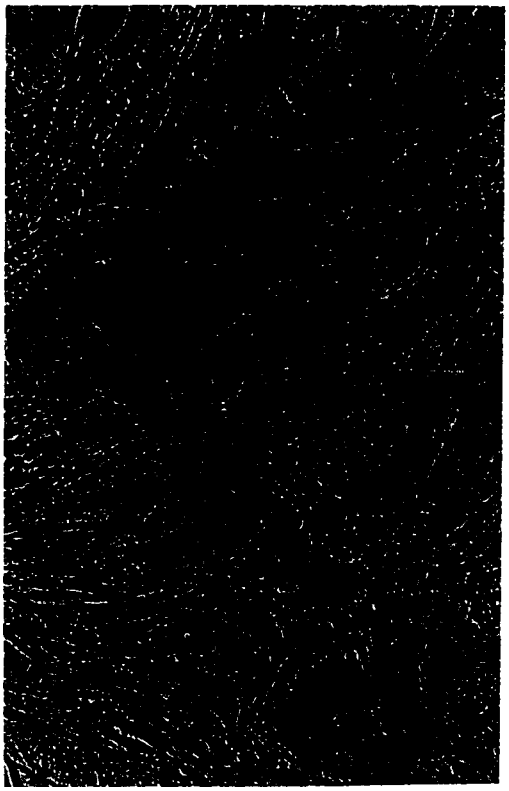

Figure 20: Human Gingival Fibroblasts Exposed to 316L Stainless Steel (S.S.) Synthetic Corrosion Products at the Following Concentrations (100X):

A. 6.25 ppm S.S. B. 3 ppm S.S.

C. 1.5 ppm S.S. D. 0.75 ppm S.S.

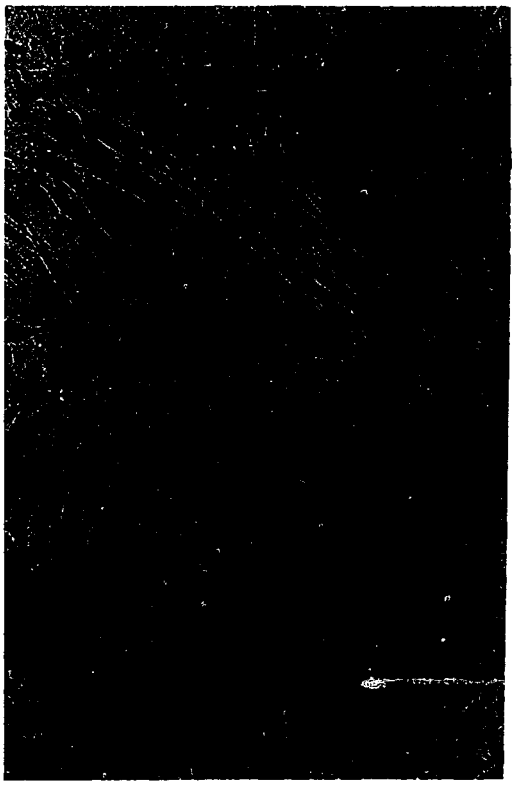

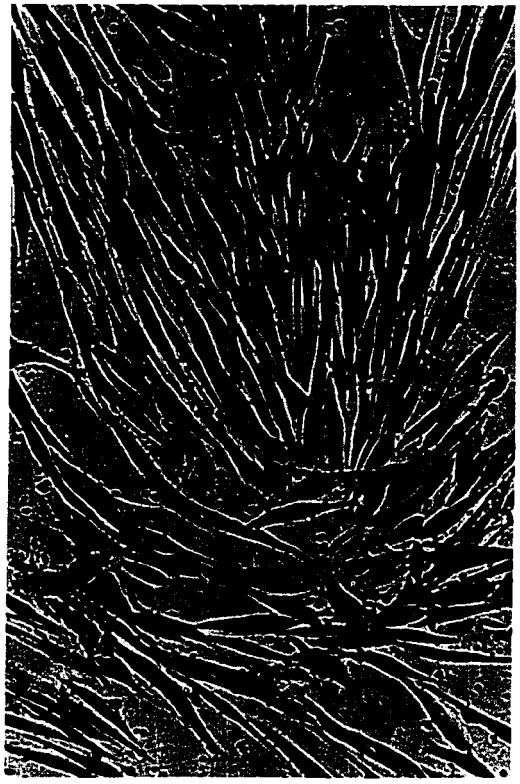

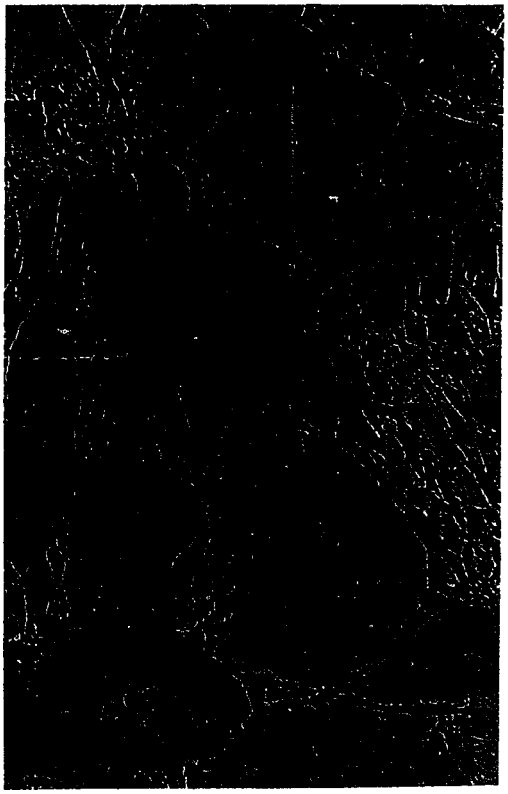

demonstrated toxic effects down to a concentration of 0.375 ppm. Thus it seems that chromium would be the most significant contributor to the toxic effects observed for a 3 ppm stainless steel solution. Cells exposed to a 1.5 ppm stainless steel solution displayed significantly improved morphologies. A 1.5 ppm synthetic corrosion product solution represents 1.0 ppm Fe, 0.3 ppm Cr, and 0.21 ppm Ni. The amount of chromium in a 1.5 ppm stainless steel solution is less than 0.375 ppm Cr noted previously as a upper limit for nontoxic effects. Cellular morphologies improved even more with a 0.75 ppm stainless steel solution. A 0.75 solution contains only 0.15 ppm Cr. It appears that the toxic effects of the corrosion product solutions result, to a large extent, from the quantity of chromium in the solution.

The effect of exposing Co-Cr-Mo synthetic corrosion product solutions and the individual elements cobalt and molybdenum on the growth rates of HGF was also investigated. For the cobalt solutions, Figure 21, growth rates of the HGF approached the control at concentrations $\leq$ 12.5 ppm on Day 7. Cellular morphologies of some cells (Figures 22A-D), appeared normal at a concentration of 25 ppm cobalt. For molybdenum, concentrations $\leq$ 50 ppm did not inhibit the growth rates of the fibroblasts, Figure 23. Examining the morphologies of cells exposed to molybdenum solutions revealed some normal shaped fibroblasts at concentrations as high as 100 ppm (Figures 24A-D). The toxic effect of molybdenum was less than that of any other element examined.

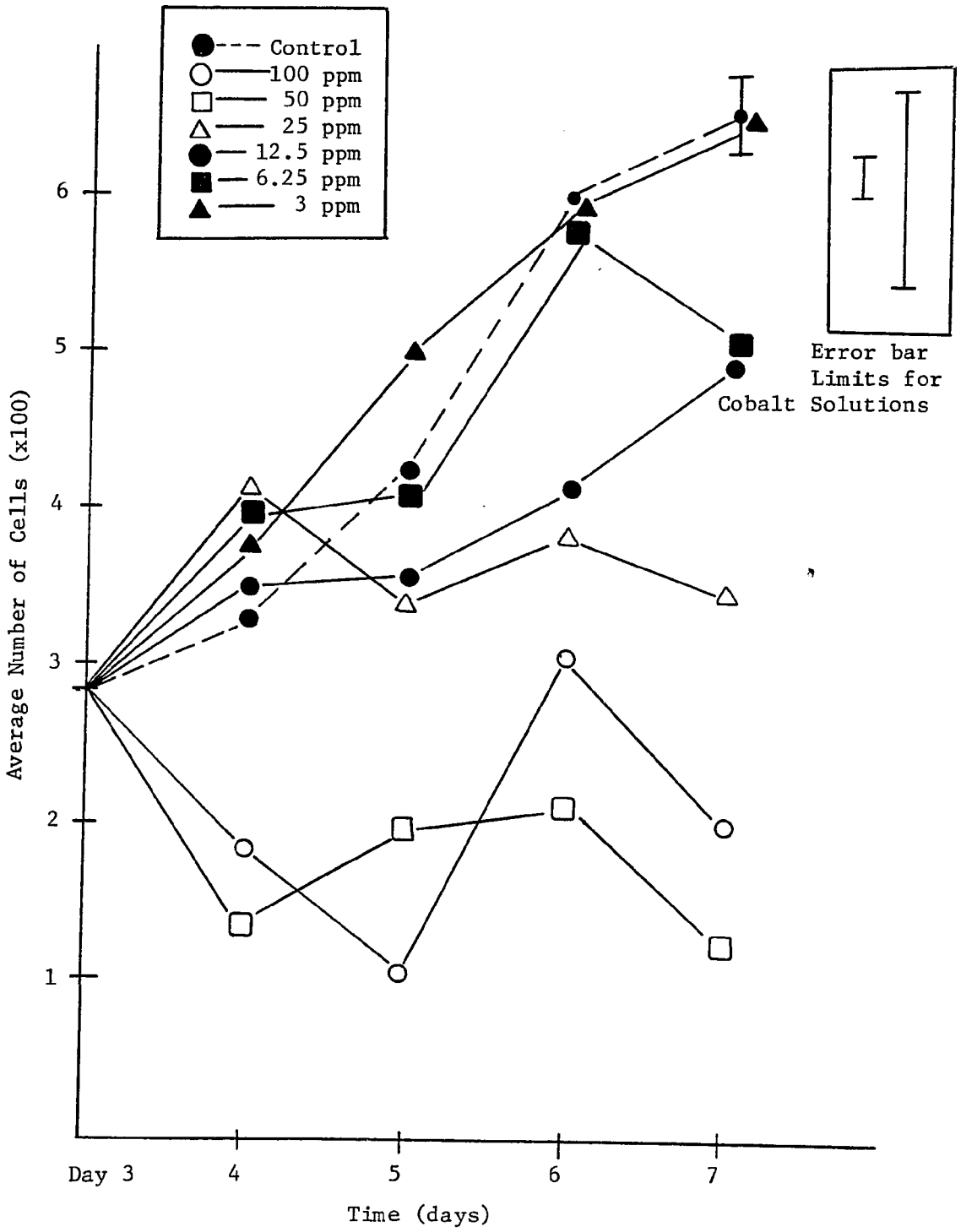

Figure 21: HGF Exposed to Cobalt Solutions

Figure 22: Human Gingival Fibroblasts Exposed to Cobalt at the Following Concentrations (100X):

A. 100 ppm Co B. 25 ppm Co

C. 12.5 ppm Co D. 3 ppm Co

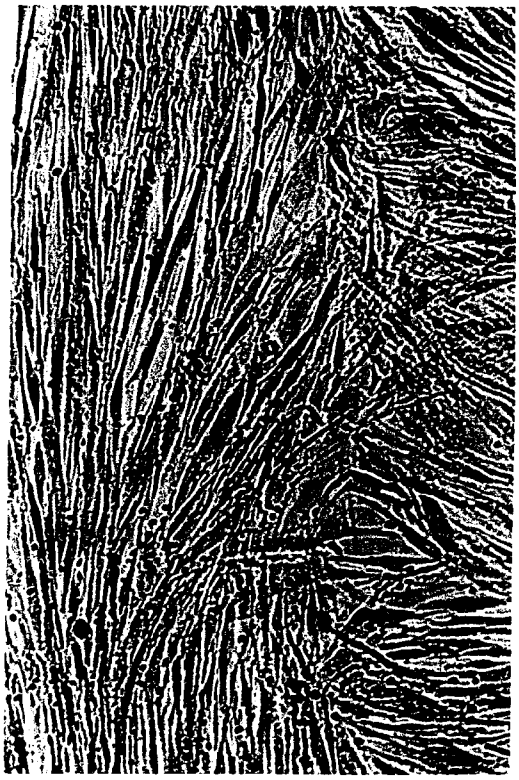

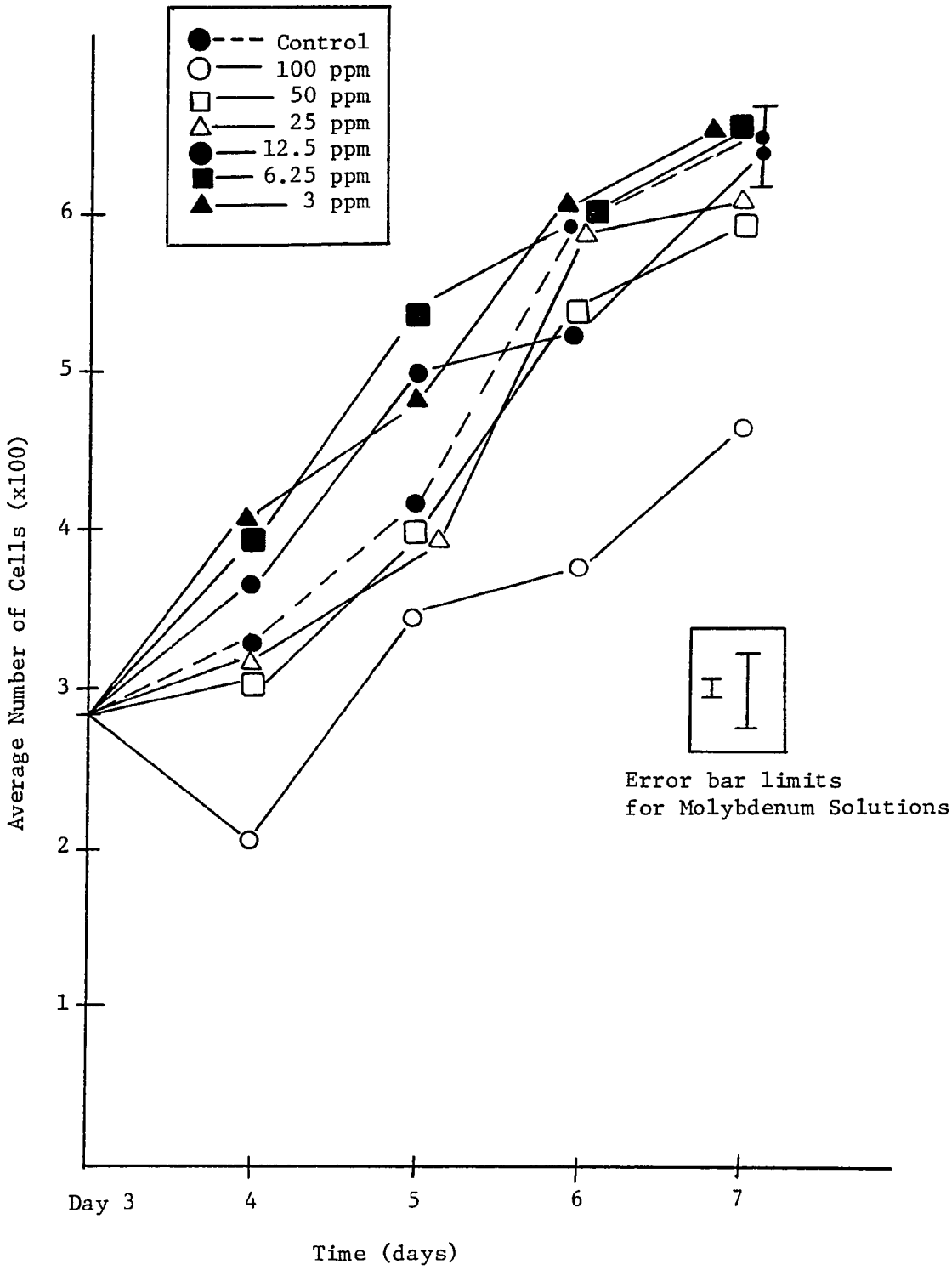

Figure 23: HGF Exposed to Molybdenum Solutions

Figure 24: Human Gingival Fibroblasts Exposed to Molybdenum at the Following Concentrations (100X):

A. 100 ppm Mo B. 25 ppm Mo

C. 12.5 ppm Mo D. 3 ppm Mo

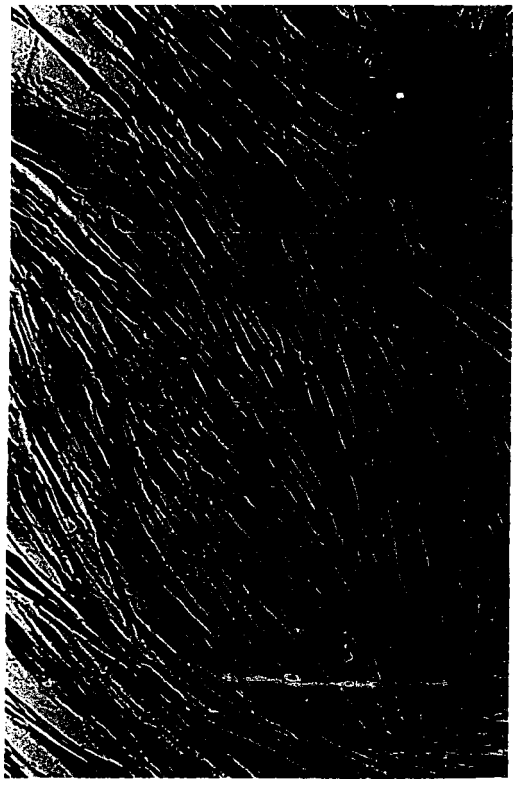

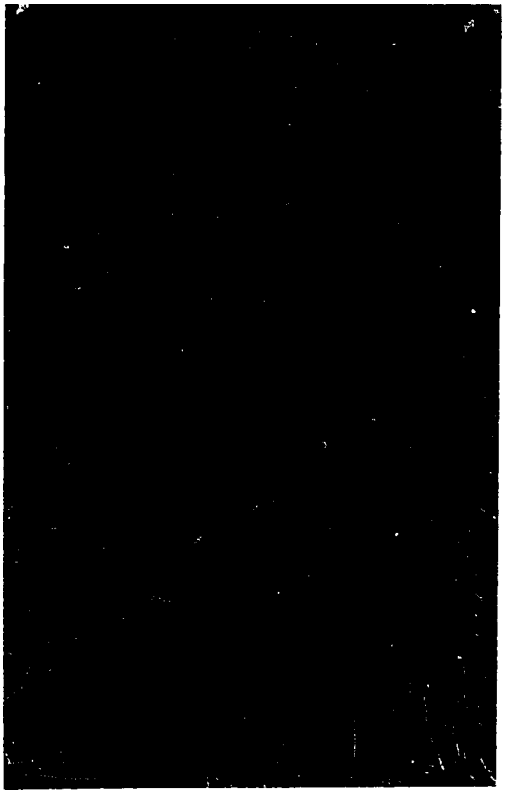

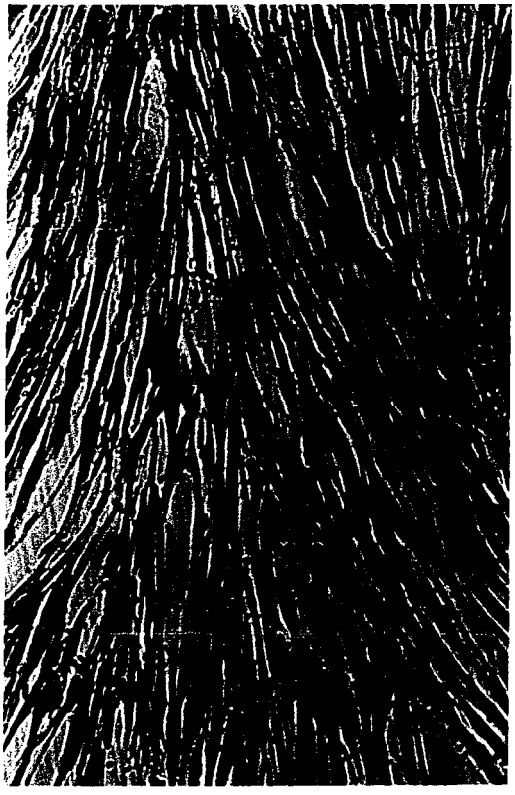

Synthetic corrosion product solutions of Co-Cr-Mo inhibited the growth rates of the HGF at all the concentrations shown in Figure 25. The morphologies shown in Figures 26A-D clearly show the detrimental effects of the Co-Cr-Mo corrosion product solutions. Decreasing the concentrations from 3 ppm to 0.75 ppm, Figures 27A-D, showed that the morphologies of the cells were more normal at a 0.75 ppm concentration, but toxic effects were clearly demonstrated at a 1.5 ppm concentration.

The cell density in the experiment shown in Figure 27 was significantly higher than in the experiment shown in Figure 26. The higher cell density caused the cells to have less room for attachment. Thus, the cells shown in Figure 27 have a more "bunched" appearance with the cells exposed to 3 ppm appearing more circular. In contrast, the cells exposed to 3 ppm Co-Cr-Mo in Figure 26 have a more elongated appearance.

A 1.5 ppm solution of Co-Cr-Mo represents 1.0 ppm Co, 0.45 ppm Cr, and 0.09 ppm Mo. Cobalt and molybdenum at such low concentrations should not individually result in these toxic effects. However, it was previously shown that chromium did not display normal morphologies until the concentration was reduced to 0.375 ppm. Thus the toxic effects displayed at 1.5 ppm Co-Cr-Mo solution would probably be a result of the chromium in the solution. At 0.75 ppm Co-Cr-Mo, the morphologies significantly improved. A 0.75 ppm Co-Cr-Mo solution represents 0.5 ppm Co, 0.223 ppm Cr, and 0.005 Mo. Thus the 0.75 ppm Co-Cr-Mo solution contains a lower amount of chromium than 0.375 ppm. Again, chromium appears to be the largest contributor to the toxic effects

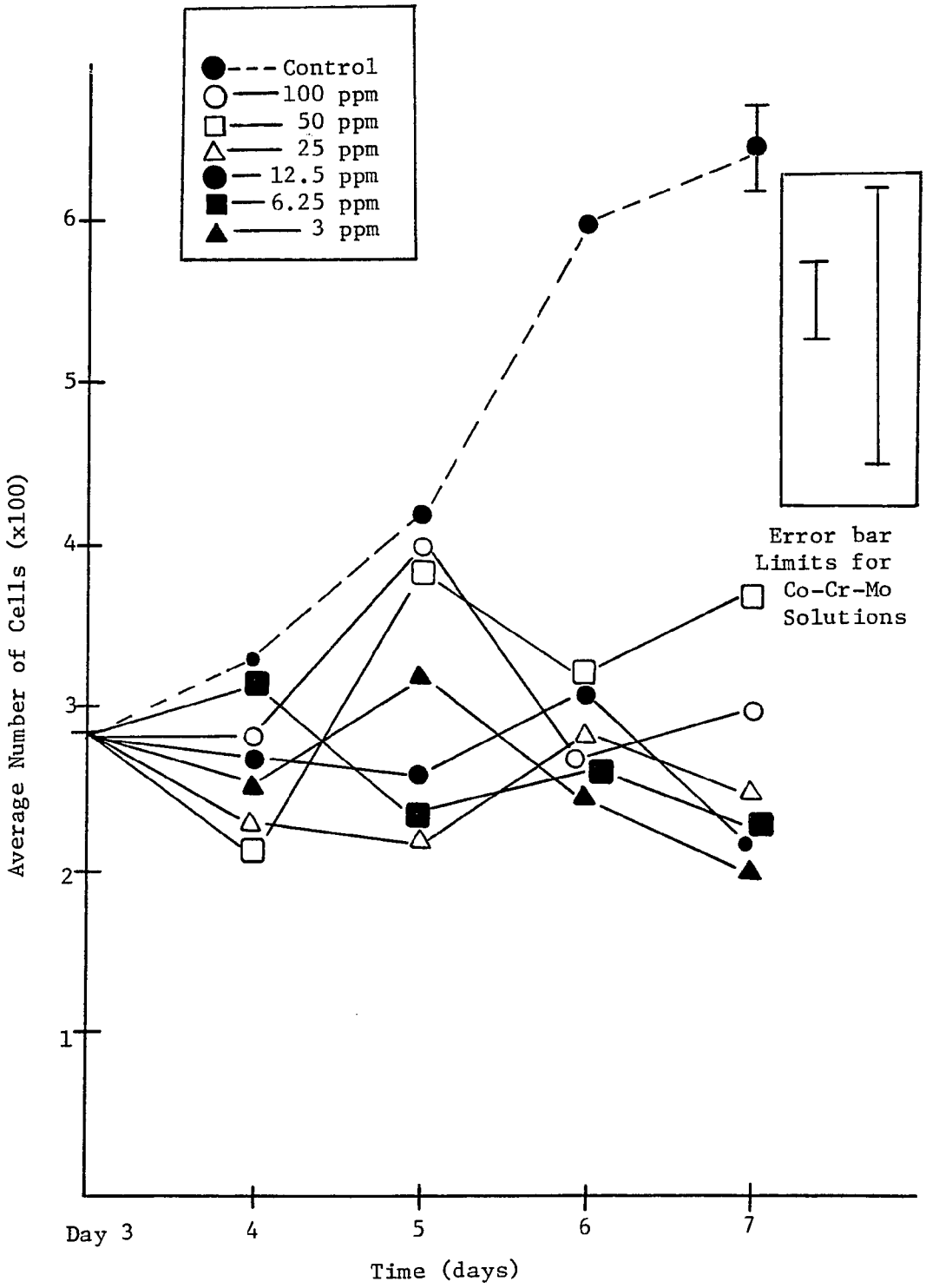

Figure 25: HGF Exposed to Co-Cr-Mo Corrosion Product Solutions

Figure 26: Human Gingival Fibroblasts Exposed to Co-Cr-Mo Synthetic Corrosion Products at the Following Concentrations (100X):

A. 100 ppm Co-Cr-Mo

B. 25 ppm Co-Cr-Mo

C. 12.5 ppm Co-Cr-Mo

D. 3 ppm Co-Cr-Mo

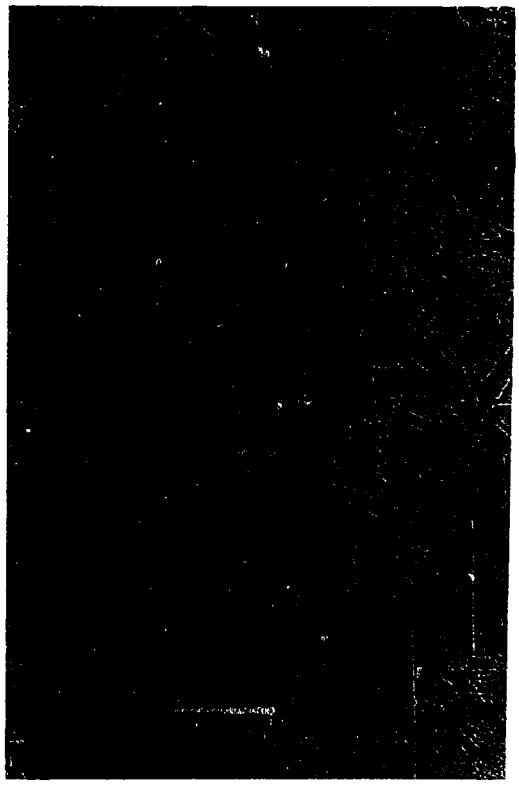

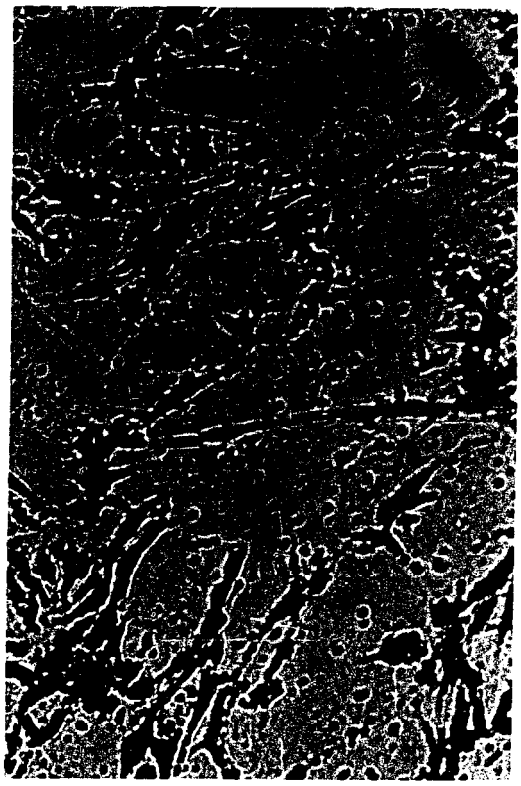

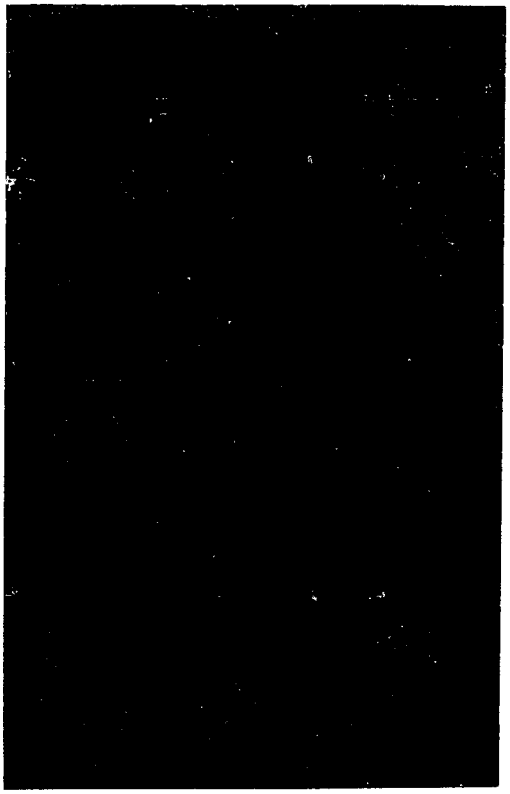

Figure 27: Human Gingival Fibroblasts Exposed to Co-Cr-Mo Synthetic Corrosion Product Solutions at the Following Concentrations (100X):

A. 3 ppm Co-Cr-Mo

B. 1.5 ppm Co-Cr-Mo

C. 0.75 ppm Co-Cr-Mo

D. 0.375 ppm Co-Cr-Mo

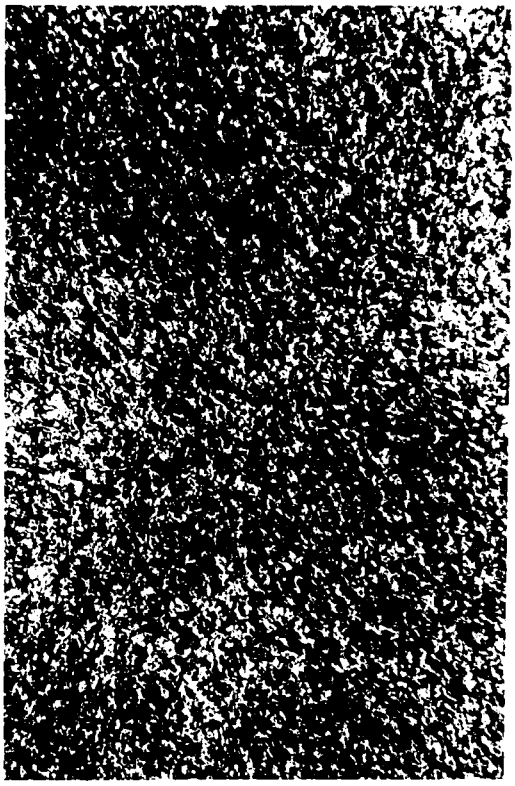

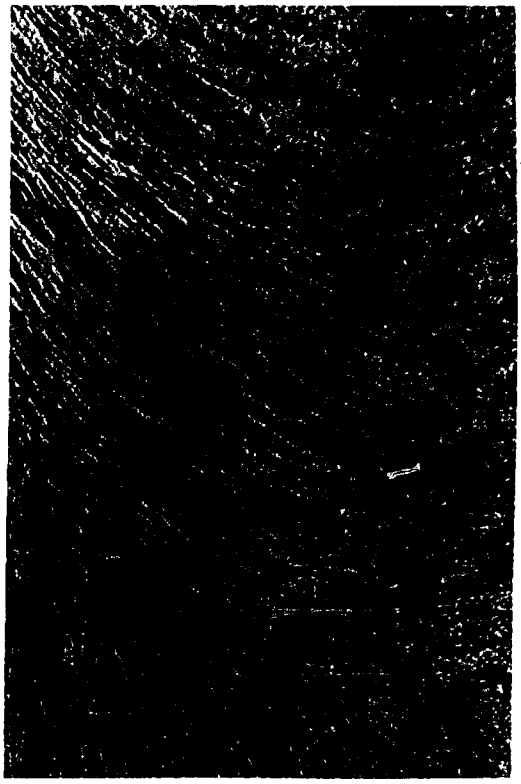

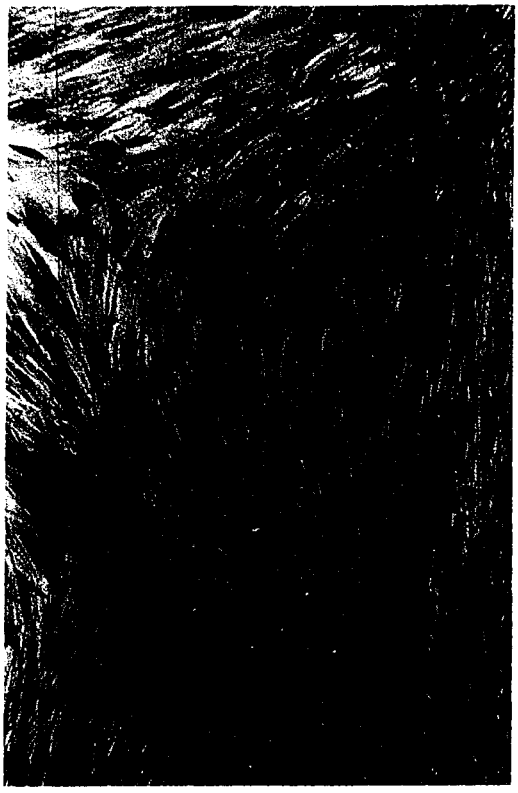

observed. The toxic effects appear to occur at chromium concentrations > 0.375 ppm.

Another interesting observation was that a lower concentration, 0.75 ppm, of the Co-Cr-Mo alloy was required before normal morphologies were found in comparison to the stainless steel, 1.5 ppm. This could be partly due to the increased chromium concentrations in the Co-Cr-Mo alloy. The tissue culture analyses conducted by Papas and Cohen (86) showed that the Co-Cr-Mo alloy powders elicited a more toxic response than did equal quantities of stainless steel powders. This result was surprising to the investigators. Maybe one reason for this result was an increased release of chromium in the cell cultures of the Co-Cr-Mo alloy. Since alloy powders were added to the culture system, the quantity of chromium available to the cells is not known.

Chromium clearly elicited toxic effects in the cell culture analyses. One significant contribution to the adverse effects observed might have been the valence state of the chromium. In Chapter I it was discussed that Cr^{+3} was not able to enter a cell membrane while Cr^{+6} was small enough to do so. If chromium entered the cell, an alteration of normal metabolism was a possibility. Determination of the valance state of chromium in this investigation could have revealed a range of valences. Chromium was in solution with Waymouth's complete medium which contained a variety of proteins, amino acids, vitamins, and salts, all of which contained possible binding sites. This complex solution was exposed to fibroblasts which also offered possible binding sites. Therefore multiple valence states could have existed. The

determination of the chromium valences would have to be done experimentally. However, to understand the effects these ionic constituents have on cells, further investigations on the element's oxidation states are critical.

The results of the Ti-6Al-4V alloy and the individual elements comprising the titanium-base alloy were investigated in the same manner as used for the stainless steel and cobalt base alloys. Titanium inhibited the growth rates of the HGF at all concentrations shown on Day 7 (Figure 28). However, concentrations < 6.25 ppm approached the control through Day 6. Examining cellular morphologies resulting from exposure to titanium solutions revealed some normal cellular morphologies at concentrations of 12.5 ppm but a greater improvement was observed with 3 ppm titanium solutions (Figures 29A-D). Exposing cells to aluminum concentrations < 25 ppm did not inhibit the growth of the cells as compared with the control on Day 7 (Figure 30). Cellular morphologies showed relatively normal conditions at concentrations of 25 ppm on Day 6, Figures 31A-D. On Day 7, concentrations $\leq$ 25 ppm still exhibited normal morphologies. Aluminum tended to cause a precipitate; this dark staining material appeared in Figure 31. Vanadium significantly inhibited growth rates of the fibroblasts at all concentrations, Figure 32. Cellular morphologies shown in Figures 33A-D displayed significant alterations. Decreasing the vanadium concentrations showed some cells with normal morphologies at 1.5 ppm, Figures 34A-D. However decreasing the vanadium concentration to 0.75 ppm resulted in normal morphologies for

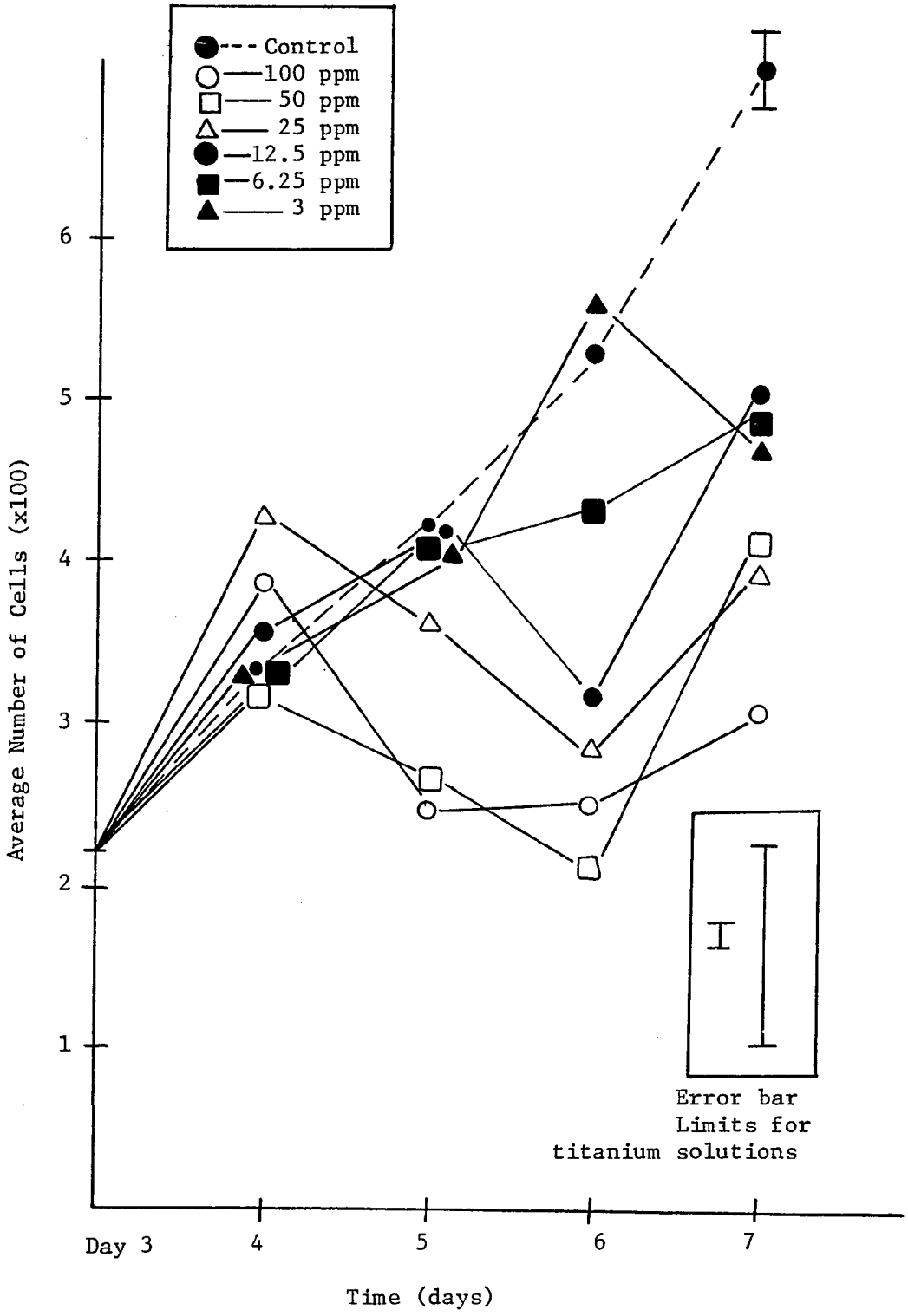

Figure 28: HGF Exposed to Titanium Solutions

Figure 29: Human Gingival Fibroblasts Exposed to Titanium at the Following Concentrations (100X):

A. 100 ppm Ti

B. 25 ppm Ti

C. 12.5 ppm Ti

D. 3 ppm Ti

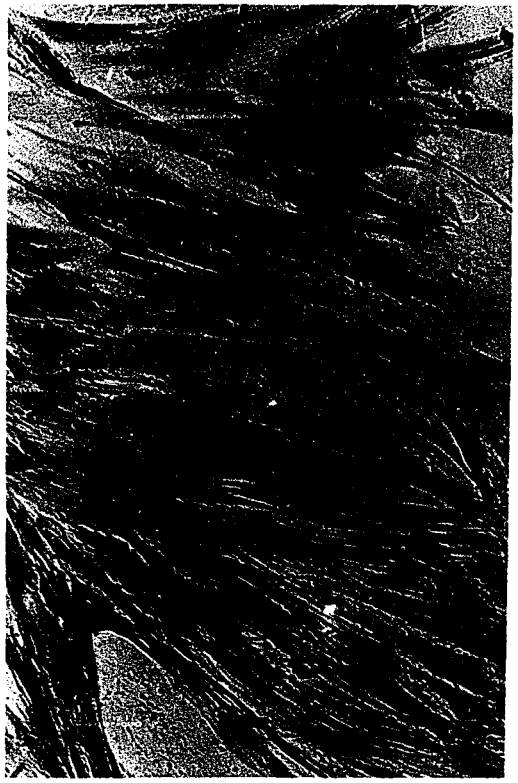

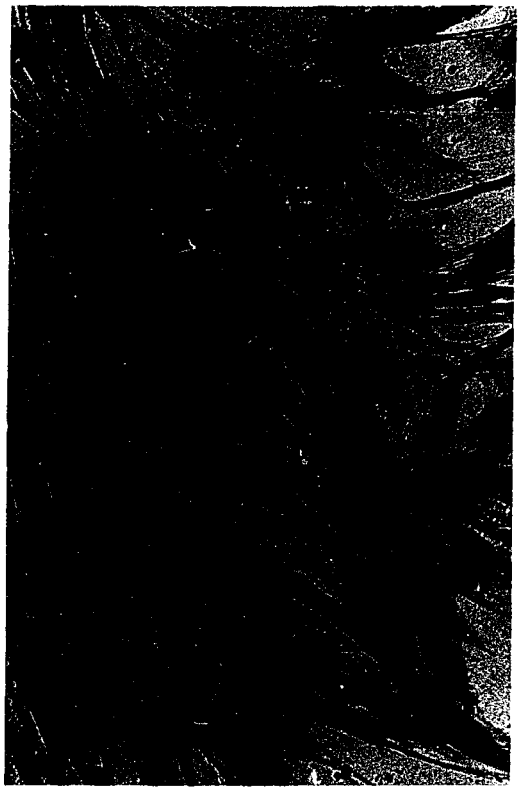

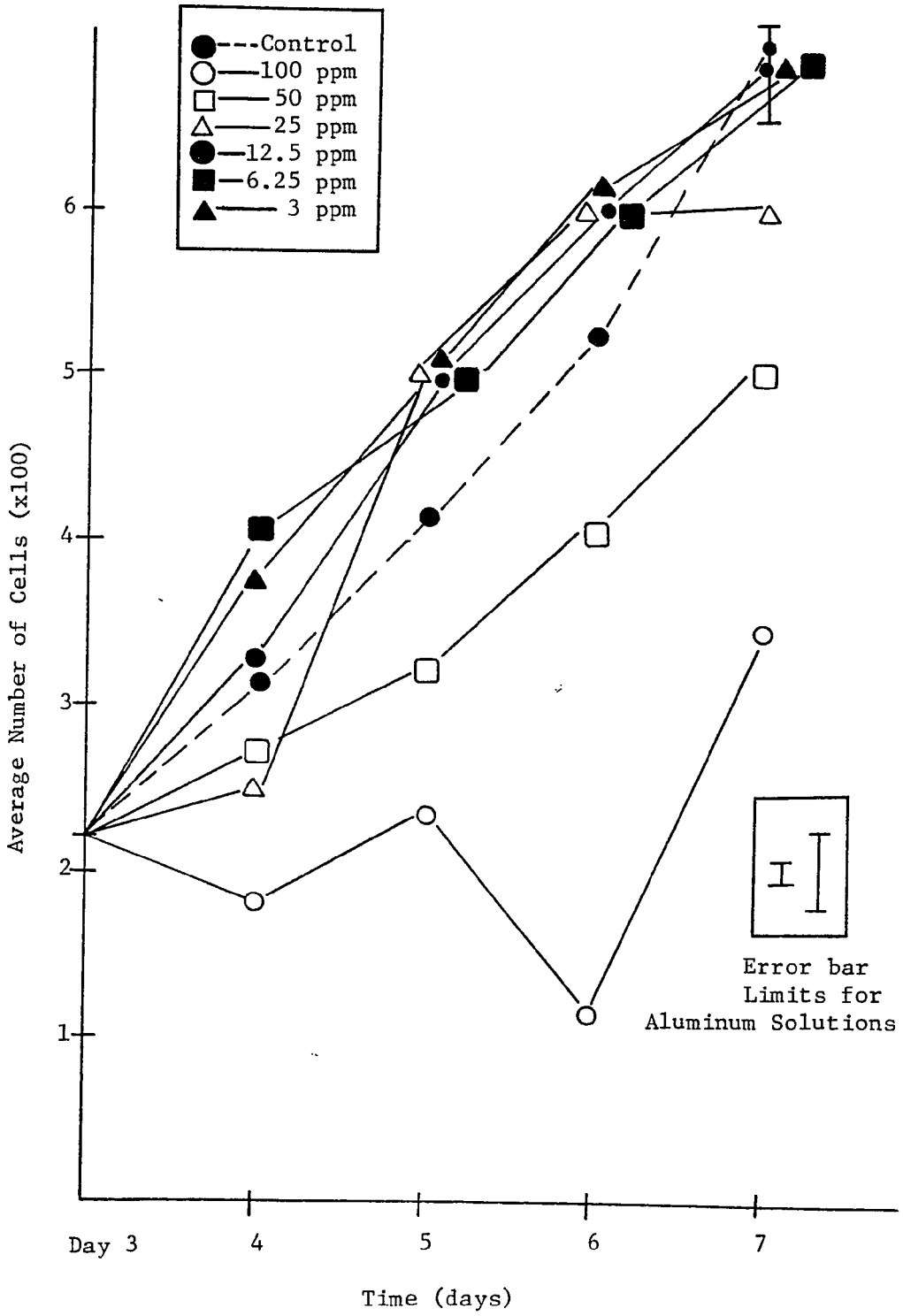

Figure 30: HGF Exposed to Aluminum Solutions

Figure 31: Human Gingival Fibroblasts Exposed to Aluminum at the Following Concentrations (100X):

A. 100 ppm Al

B. 25 ppm Al

C. 12.5 ppm Al

D. 3 ppm Al

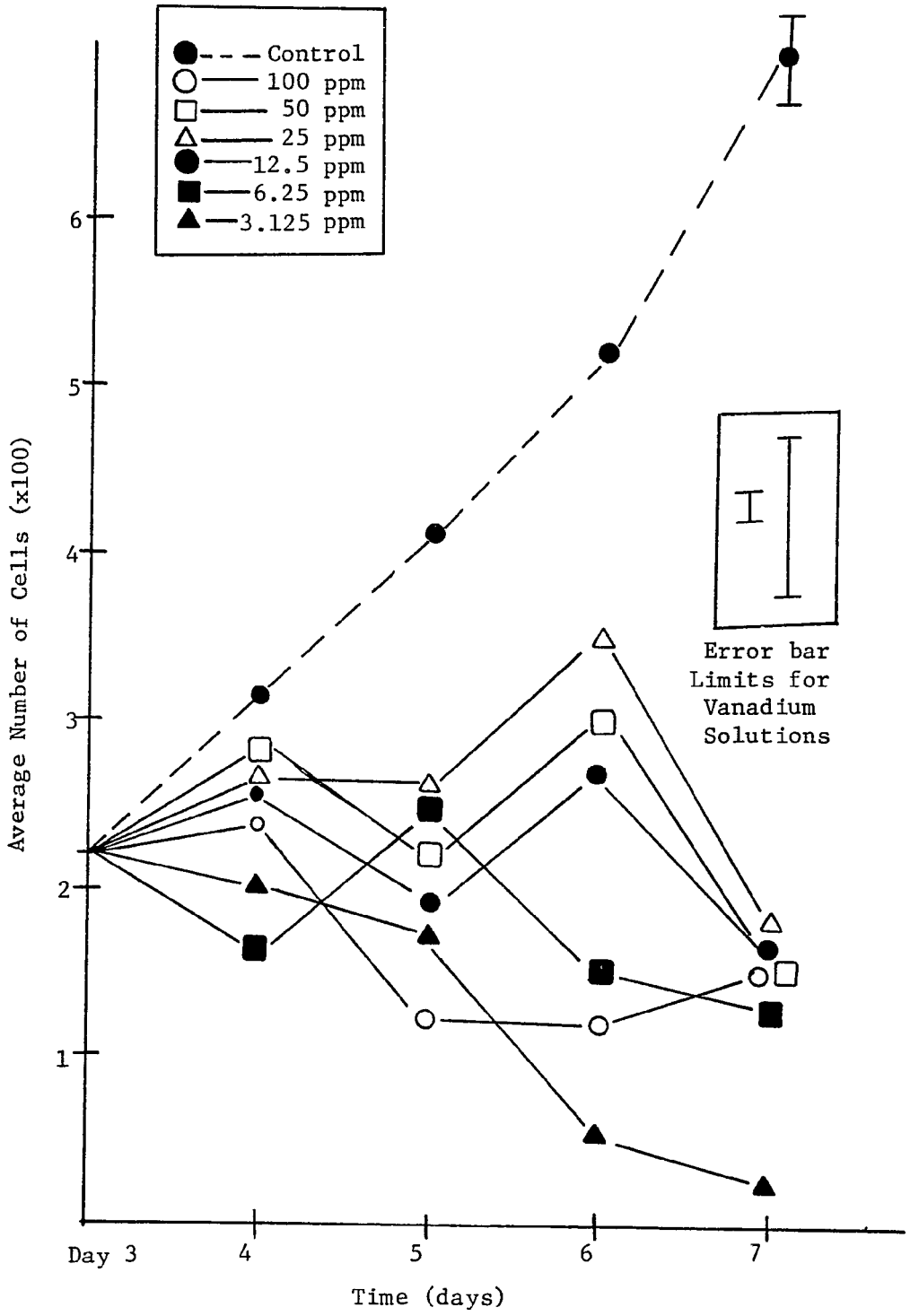

Figure 32: HGF Exposed to Vanadium Solutions

Figure 33: Human Gingival Fibroblasts Exposed to Vanadium at the Following Concentrations (100X):

A. 100 ppm V B. 25 ppm V

C. 12.5 ppm V D. 3 ppm V

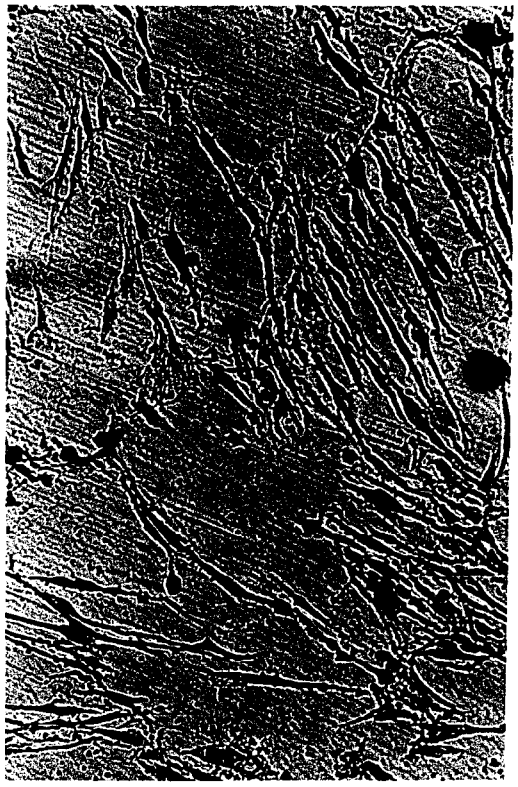

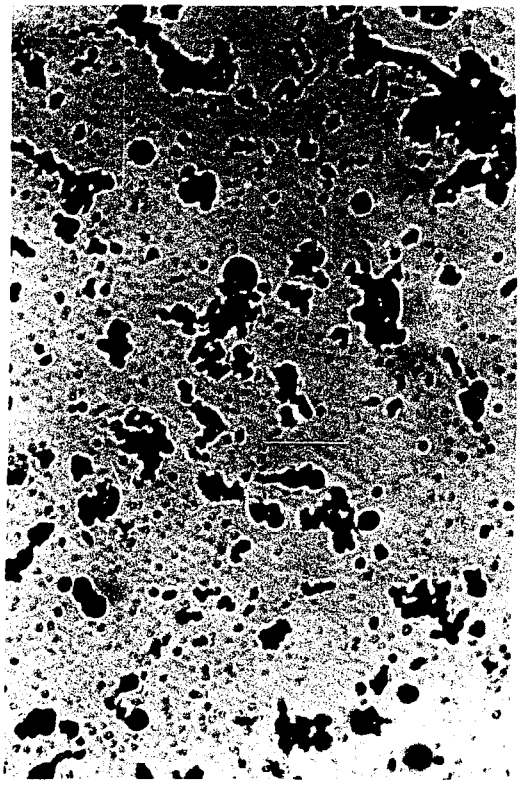

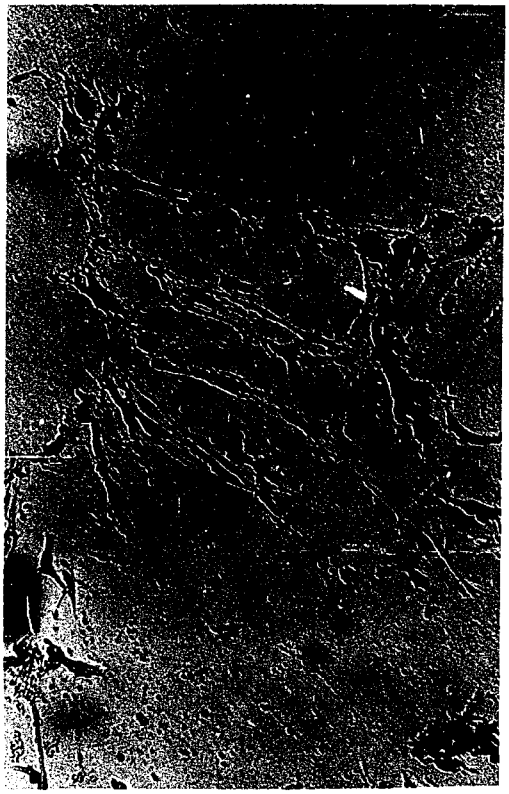

Figure 34: Human Gingival Fibroblasts Exposed to Vanadium at the Following Concentrations (100X):

A. 3 ppm V

B. 1.5 ppm V

C. 0.75 ppm V

D. 0.375 ppm V

almost all of the cells shown. The cell density in Figure 34 was higher than in Figure 33.

For the synthetic corrosion product solution of Ti-6Al-4V, depressed growth rates were observed at all concentrations shown in Figure 35. Cellular morphologies, Figure 36, resulting from exposure to Ti-6Al-4V solutions exhibited significant alterations at the elevated concentrations. The cells displayed a rounded instead of spindle shape characteristic of normal fibroblasts. Vanadium exhibited similar cellular alterations.

At a 3 ppm concentration of Ti-6Al-4V, the cellular morphologies significantly improved. However, at 6.25 ppm a toxic effect was still demonstrated. A 6.25 ppm Ti-6Al-4V solution represents 5.6 ppm Ti, 0.375 ppm Al and 0.25 ppm V. Individually, these elements should not result in a toxic effect. However, collectively a toxic effect was observed. While vanadium is the most toxic of the elements in the Ti-6Al-4V alloy, a synergistic effect may be causing the toxic effects observed when cells were exposed to Ti-6Al-4V.

To summarize the tissue culture experiments, the upper limit for nontoxic responses as judged primarily by observations of cellular morphologies was 1.5 ppm for the stainless steel alloy and 0.75 ppm for the Co-Cr-Mo alloy. These concentrations represent 0.3 ppm Cr, and 0.225 ppm Cr, respectively, for these two alloys. However, the lower limits where toxic responses were still noted were 3.0 ppm for the stainless steel alloy (contains 0.6 ppm Cr) and 1.5 ppm for the Co-Cr-Mo (contains 0.45 ppm Cr). When chromium was added to the cell cultures individually, concentrations of

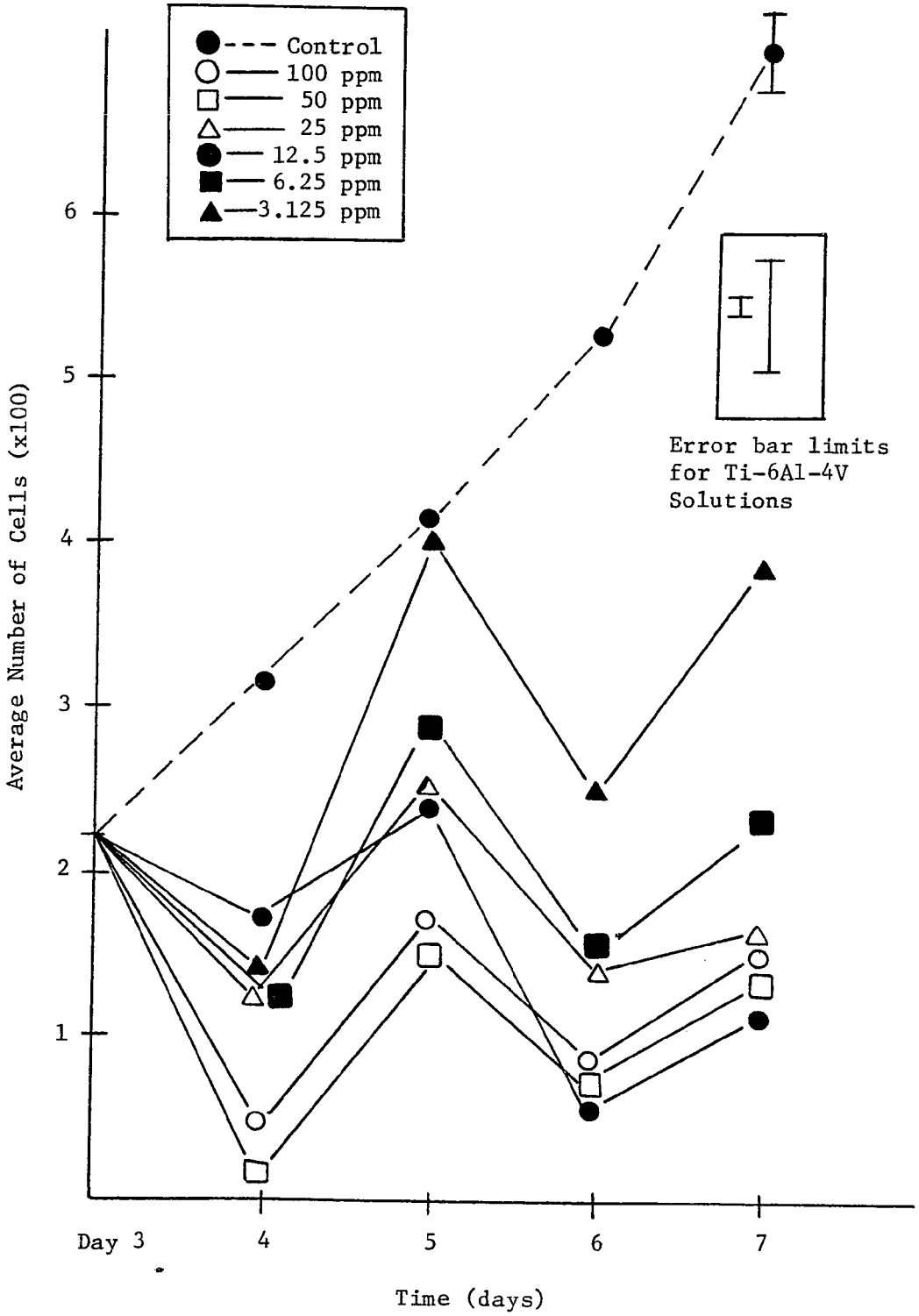

Figure 35: HGF Exposed to Ti-6Al-4V Corrosion Product Solutions

Figure 36: Human Gingival Fibroblasts Exposed to Ti-6Al-4V Synthetic Corrosion Product Solutions at the Following Concentrations (100X):

A. 100 ppm Ti-6Al-4V

B. 25 ppm Ti-6Al-4V

C. 12.5 ppm Ti-6Al-4V

D. 3 ppm Ti-6Al-4V

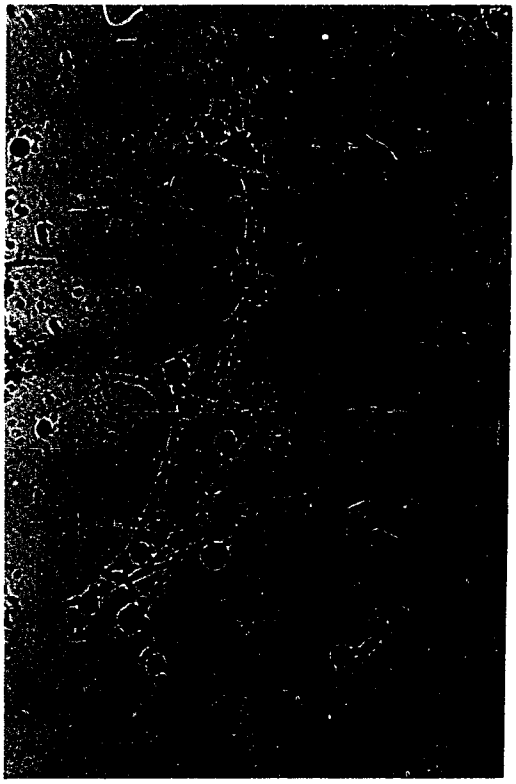

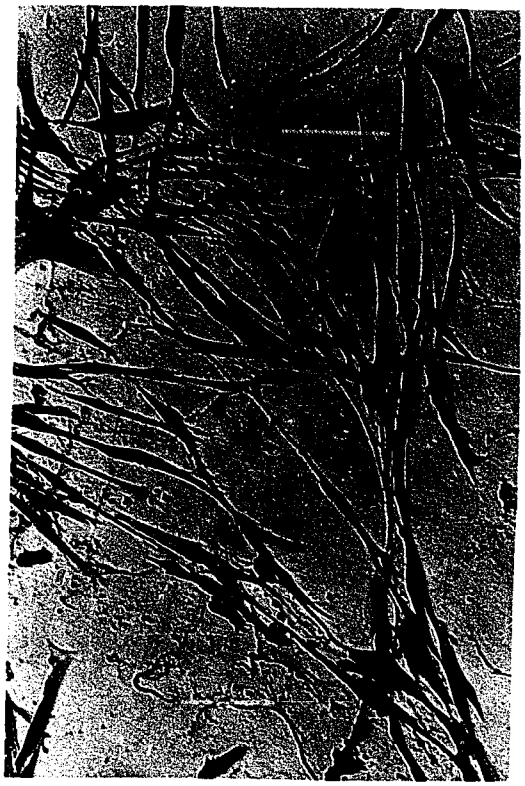

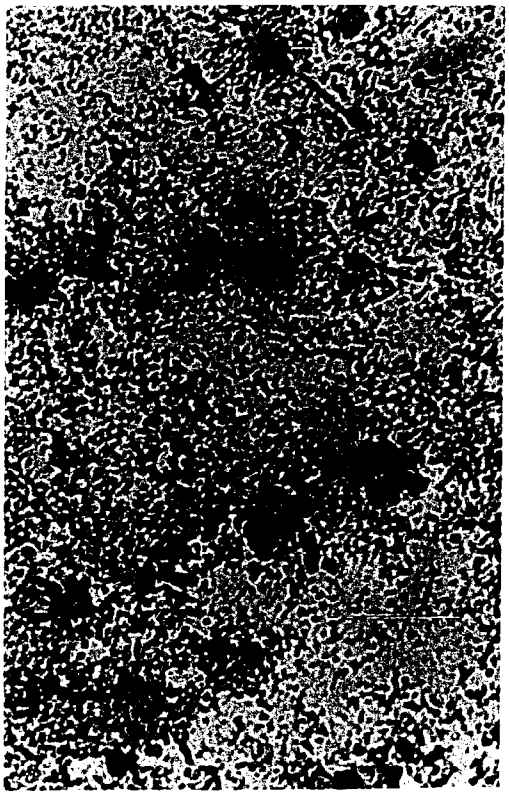

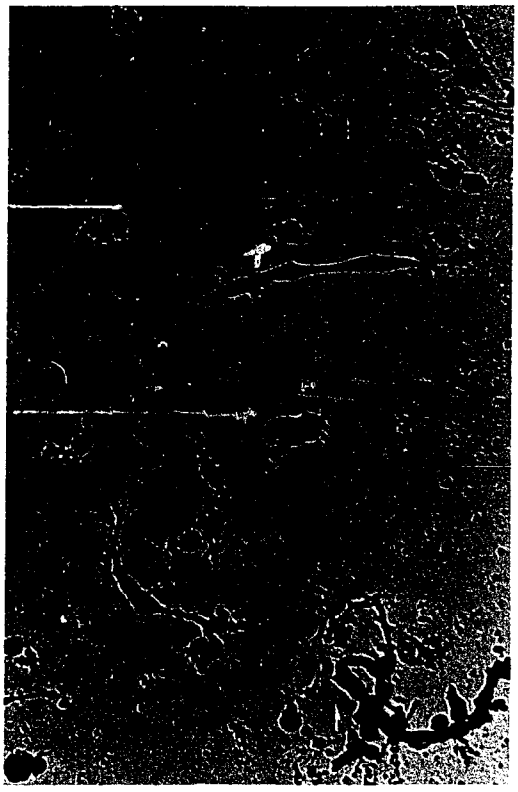

0.75 ppm displayed altered morphologies but when concentrations of 0.375 ppm were added more normal morphologies were observed. Thus it appeared that a chromium concentration of 0.375 ppm might be a threshold level for these experiments. If the stainless steel or Co-Cr-Mo solutions contained amounts of chromium greater than 0.375 ppm, toxic responses were observed, but if the solutions contained chromium concentrations less than 0.375 ppm, more normal cellular morphologies were observed. It appeared that the amount of chromium was critical in assessing the toxicity of the stainless steel or Co-Cr-Mo alloys. In contrast, the Ti-6Al-4V solution was toxic to the cells at 6.25 ppm but normal morphologies were observed at a 3 ppm concentration. At 6.25 ppm Ti-6Al-4V the solution contained 5.6 ppm Ti, 0.375 ppm Al, and 0.25 ppm V. Individually, all of these concentrations should be nontoxic. Thus a combination of the ions may have resulted in the toxic effects observed at 6.25 ppm Ti-6Al-4V.

In the cell culture analyses of this investigation, two parameters were investigated, cellular growth rates and cellular morphologies versus concentrations of metallic ions. It would be interesting to expand this investigation to determine why one element demonstrated toxic effects and another did not at the same concentration. Certain assays could be employed to determine: 1) the ability of the fibroblasts to synthetize proteins, 2) the ability of the Golgi apparatus to function normally, 3) the ability of the cell membrane to transport ions or 4) the ability of mitochondria to phosphorylate ADP (107). From these analyses, it could be possible to form an interpretation of the status of

cellular function resulting from exposure to individual and combinations of metallic ions.

C. In Vivo Animal Model Analyses

Tissue response to implant materials has often been investigated by implanting alloy specimens in nonhuman species. Alloy specimens were implanted in the back muscles of rabbits in this study. After implant removal, tissue adjacent to the implants was embedded in parafin blocks, sectioned, and stained with H and E for light microscopy. Three criteria were used to analyze the tissue reaction: fibrous capsule thickness, extent of cellular reaction and the presence of a granuloma at the implant site. Each of these criteria was scored as a function of the specimen's compositon (Appendix G) and the concentration of corrosion products injected at the implant to capsule interfaces (Appendix H). A score of 3 represents the most toxic response observed whereas a score of 0 represents the most benign response observed.

Of the three criteria chosen for judging the tissue response to implant materials, the fibrous capsule thickness is used more often than the other criteria. The problem with using this as a criterion is that the thickness of the capsule is also a function of the implant's mechanical stability. This effect is especially true when an alloy is implanted into soft tissues. Therefore, a thick capsule could be the result of a unstable implant. Also a thick capsule could be a result of a sharp edge on the implant site. However, these effects were minimized by sectioning the tissue transversely around the middle of the specimen. The capsules of this investigation ranged from 8 μm to 80 μm in thickness. This range can be seen in Figure 37A-B.

Figure 37: Tissue Response to 316L Stainless Steel Implants (120X):

A. Minimal tissue response

B. Adverse tissue response

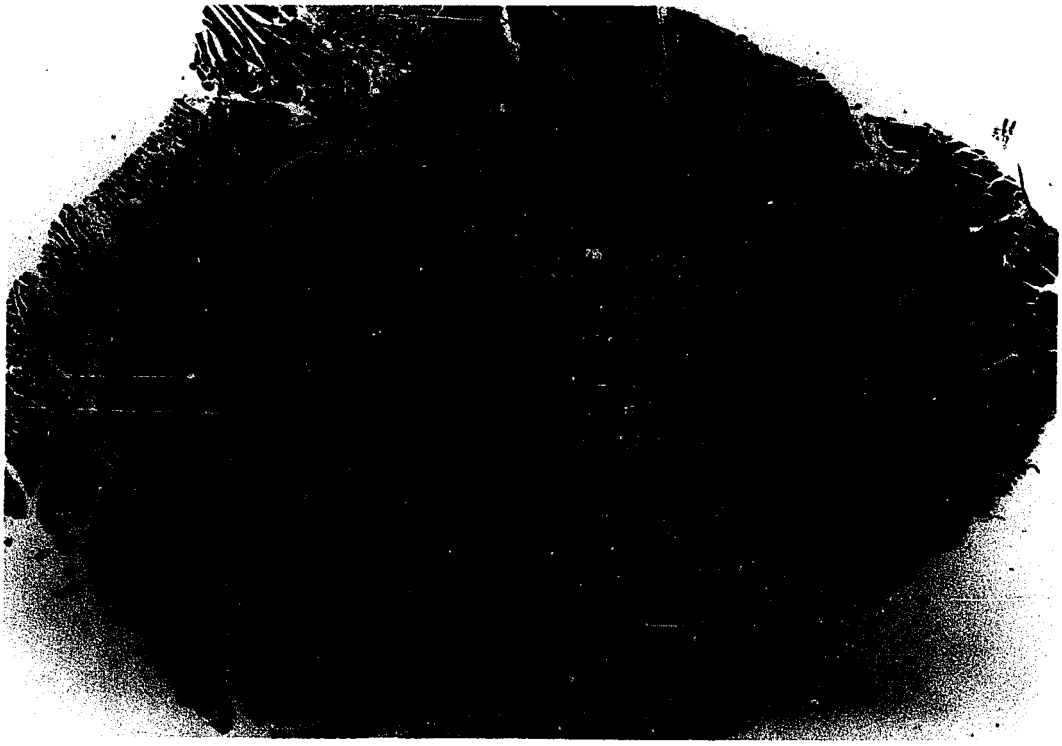

The second criterion was the extent of local phagocytic cellular response to the implant materials. The capsule in Figure 37B displays much more cellular infiltration in the capsule than the capsule shown in Figure 37A. The capsule in Figure 38A was exposed to a 3 ppm synthetic product solution of Ti-6A1-4V. The area adjacent to the capsule had an increased cellularity that spread into the muscle area. A similar situation is shown in Figure 38B. This capsule was exposed to 100 ppm Co-Cr-Mo corrosion product solution. Between the muscle bundles some granulation tissue is evident. One significant feature of Figure 38B is the blood vessel entering the capsule area. This provides a nearby source for granulocytes for engulfing foreign debris. The role of these cells is clearly demonstrated in Figure 38C. This capsule was exposed to a 100 ppm Ti-6A1-4V solution. The phagocytic cells at the edge of the capsule all contain intracellular pigments. This pigmentation was most often seen around the Ti-6A1-4V implants. The final criterion was the presence of granulamotous reactions at the implant site. Figure 38D shows a granuloma formation at the fibrous capsule. Several granulomas were observed with most forming at the proximal implantation sites. This site was subjected to more mechanical movement that the other sites.

After scoring each of these criteria, a correlaton between the quantity of corrosion products injected of a specific alloy and the tissue response elicited could not be made, Appendix H. For example, the score of the tissue response resulting from injecting corrosion products around Ti-6A1-4V alloys implanted in Rabbit #4521, was similar for a 3 ppm and a 100 ppm solution. To

Figure 38: Tissue Response to Implant Alloys:

A. 3 ppm Ti-6Al-4V (325X)

B. 100 ppm Co-Cr-Mo (650X)

C. 100 ppm Ti-6Al-4V (162X)

D. 0 ppm (Control) Ti-6Al-4V (325X)

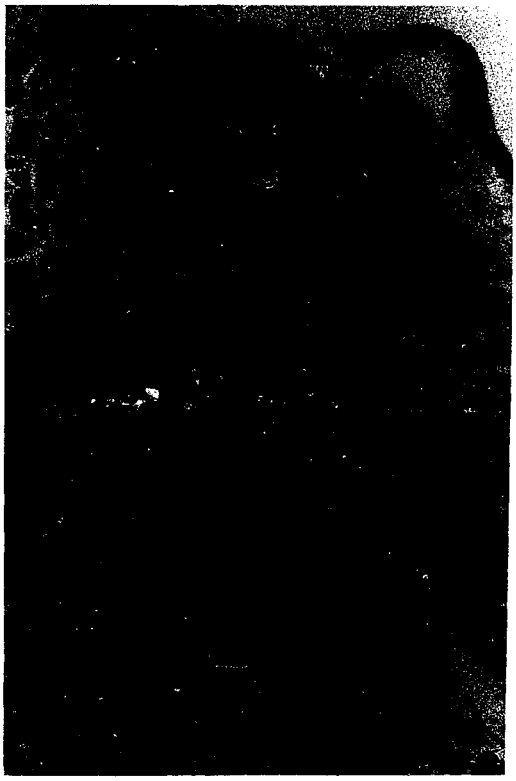

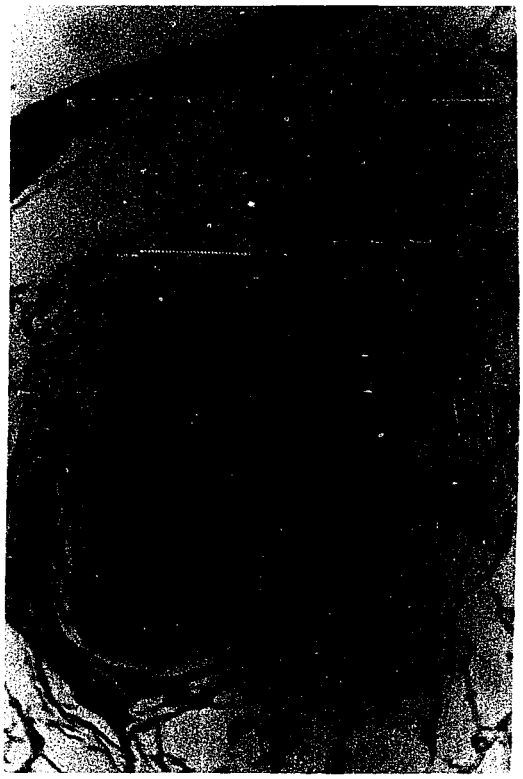

illustrate further, refer to Figures 37A and B. These figures both show tissue responses elicited due to a 25 ppm stainless steel corrosion product injection at the implant/capsule interface. The responses were significantly different even though the alloy, implant site, and quantity of corrosion products were all the same. Figure 37A shows a response that was quite minimal: thin fibrous capsule formation, minimal phagocytic reaction, and no granulomatous reaction. In contrast, Figure 37B, shows the formation of a thick fibrous capsule, an extensive phagocytic reaction, and the presence of a granuloma. Even keeping all experimental parameters constant, the host's response to an implant material can be significantly different.

There did exist a correlation between the tissue response and the implant composition, Appendix G. For each composition examined 3, 25 and 100 ppm, the total score of the tissue response for the titanium base alloy was less than for the cobalt base and stainless steel surgical alloys. Thus the chromium containing alloys resulted in more extensive tissue responses.

The histological examinations of tissue samples in this investigation were influenced by a number of variables other than the experimental parameters of corrosion product concentration and implant to composition. Some obvious variables were the implant geometry and degree of mechanical movement of the implant. Other variables could occur as a result of experimental proceudres used for this model. The corrosion products were injected at the implant/capsule interface. These injections were difficult to make due to locating the implant with the syringe needle. Sometimes

several needle placements were required before the implant interface could be found. This could have locally traumatized the tissue. When contact was made and it was certain the needle was at the interface, the corrosion products were released to the capsule area. The overall absorption of the corrosion products in the capsule was not known. Some tissue areas were most likely exposed to higher corrosion product concentrations than other areas. There always existed the possibilities of short-term infections even though sterile procedures were always followed. The experiment would be improved if a method of continually releasing the corrosion products internally could be developed. The corrosion products would be added to the tissues uniformly, without trauma and with less change of causing infections.

Light histology can be used to judge overall toxic or benign responses; however, in this study the more subtle differences could not be discerned. Too many variables were associated with the overall in vivo tissue resonse. This variety of responses can certainly be observed from Figures 37-38. This is not to say that implant materials should not be tested in animal models prior to human implantation. It is saying that when the tissue responses to implanted alloys are evaluated, care should be taken to remember the large number of factors that can affect the observed responses.

D. Electron Microscopic Analyses of Cellular Ultrastructures

The ultrastructures of in vivo cells from the fibrous capsules adjacent to 316L stainless steel implants and in vitro cultured

cells exposed to stainless steel synthetic corrosion products were examined. Fibrous capsules prepared for transmission electron microscopy (TEM) analyses were exposed to stainless steel corrosion products of the following concentrations: 100, 25 and 3 ppm per injection. Two injections were made at each implant site. A capsule having had no injections was also prepared and served as a control. The cellular organelles were observed and any deviations from normal morphology were recorded. The results are shown in Table 11. The events recorded range from normal to minor deviations of cellular ultrastructures to extensive alterations resulting in cellular death. The cellular events were divided into 3 phases: normal to early, middle, and late.

Cells in the normal to early phase experienced only slight deviations from normal morphology. The cells had a normal quantity of RER with a normal morphology. However, some of the RER did have a slightly dilated appearance with some detached ribosomes. The plasma membrane was continuous for the most part with only a few diffuse areas. The remaining organelles listed were typical of a normal and healthy fibroblasts. The events representative of this phase were seen in 80% of the control cells, 50% of the cells exposed of 3 ppm and 7% of the cells exposed to 25 ppm.

Cells in the middle phase experienced more cellular alterations than in the previous phase. These alterations included decreased amounts of RFR, increased vaculozation, dense staining around the nuclear membrane, swollen mitochondria and a diffuse plasma membrane often containing membrane blebs (small extrusions from the membrane). These events occurred in 20% of the control

Table 11

Phases of Cellular Necrosis for In Vivo Cells

Phase (Observed Event)	Concentration	Frequency
I. Normal to Early:		
(Normal rough endoplasmic reticulum (RER), dilated RER, detached ribosomes, continuous membrane, normal vaculozation, normal mitochondria)	Control 3 ppm 25 ppm 100 ppm	80% 50% 7.0% 0%
II. Middle:		
(Decreased RER, increased vaculozation, dense staining staining around nuclear membrane swollen mitochondria, diffuse membrane, membrane blebs)	Control 3 ppm 25 ppm 100 ppm	20% 33.3% 36% 28%
III. Late:		
(No RER, extensive vaculozation, extensive clumping around nuclear membrane, swollen mitochondria, loss of cellular organization)	Control 3 ppm 25 ppm 100 ppm	0% 16.7% 57% 72%

cells, 33.3% of the cells exposed to a 3 ppm stainless steel solution, 36% of cells exposed to 25 ppm solution and 28% of cells exposed to 100 ppm solution.

Cells in the late phase experienced extensive cellular alterations. These included a total loss of RER, extensive vaculozation, extensive clumping around the nuclear membrane, swollen and rounded mitochondria, and a total loss of cellular organization. These events occurred in 16.7% of the cells exposed to a 3 ppm solution, fifty-seven percent of the cells exposed to a 25 ppm solution, and 72% of the cells exposed to a 100 ppm solution.

These phases were not distinct and overlapping did occur. The previously listed events are shown in Figures 39 and 40. Figure 39A shows a portion of a fibroblast from the capsule of a stainless steel implant having no injections. This represented a control condition. The overall spindle shape of the cell and its nucleus was typical of the fibroblasts. The cytoplasm contained normal RER and the cellular membrane was without discontinuities. The area around the cell contained a significant amount of collagen fibers.

Figures 39B and 39C are photomicrographs of cells from the capsule having injections of 3 ppm corrosion product solutions. Figure 39B represented an early phase of cellular necrosis. The cell contained normal RER with some detached ribosomes. There was not a significant amount of dense staining around the nuclear membrane and only a small amount of cytoplasmic vaculozation was present. The membrane appeared discontinuous at the lower left corner. This was not a normal feature and indicated that the cell was beginning to experience difficulties in continuing normal functions. Figure 39C also shows a cell exposed to 3 ppm stainless steel corrosion solution. This cell represented an early-to-middle phase. Normal RER existed, however, the amount of RER was less than the cell shown previously in Figure 39B. Unusual features included a dilated nucleolus, rounded vaculoes containing dark staining pigment, and a diffuse plasma membrane.

Figures 39D, 40A and 40B show cells from capsules exposed to 25 ppm corrosion product solutions. Figure 39D represents a cell in the middle phase. The RER was dilated and discontinuous. Also the amount of RER was less than in the normal cell and the extent

Figure 39: In Vivo Cellular Ultrastructures Resulting from Exposure to the Following 316L Stainless Steel Corrosion Product Solutions (12,000X):

A. 0 ppm (control) B. 3 ppm S.S.

C. 3 ppm S.S. D. 25 ppm S.S.

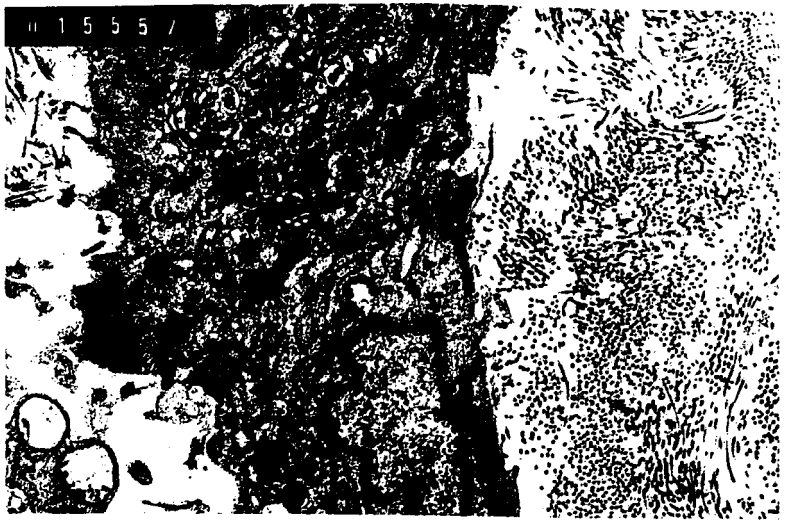
1555


15513

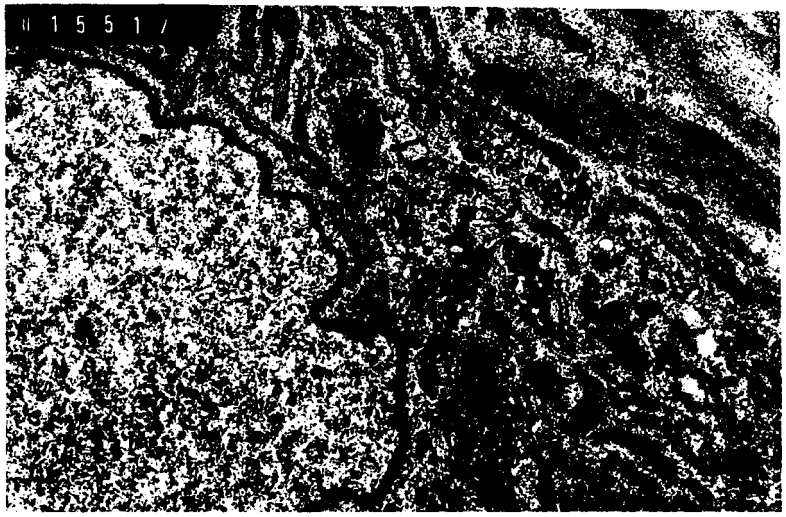
1551

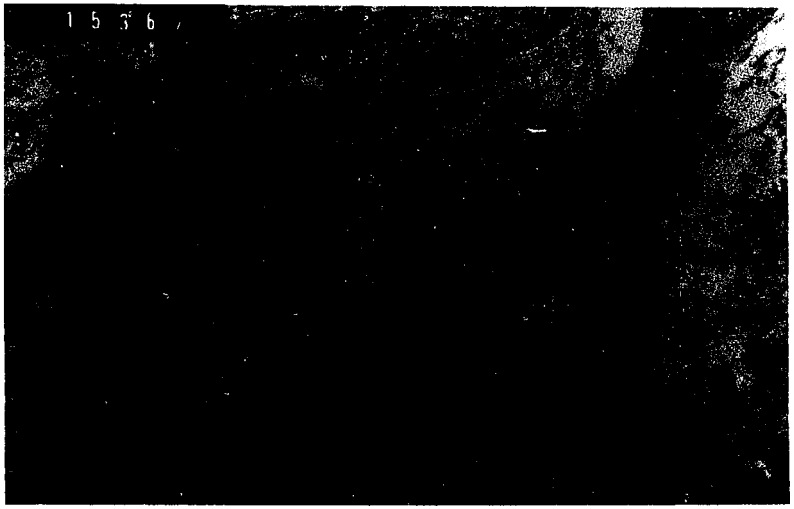
1536

Figure 40: In Vivo Cellular Ultrastructures Resulting from Exposure to the Following 316L Stainless Steel Corrosion Product Solutions (12,000X):

A. 25 ppm S.S.

B. 25 ppm S.S.

C. 100 ppm S.S.

D. 100 ppm S.S.

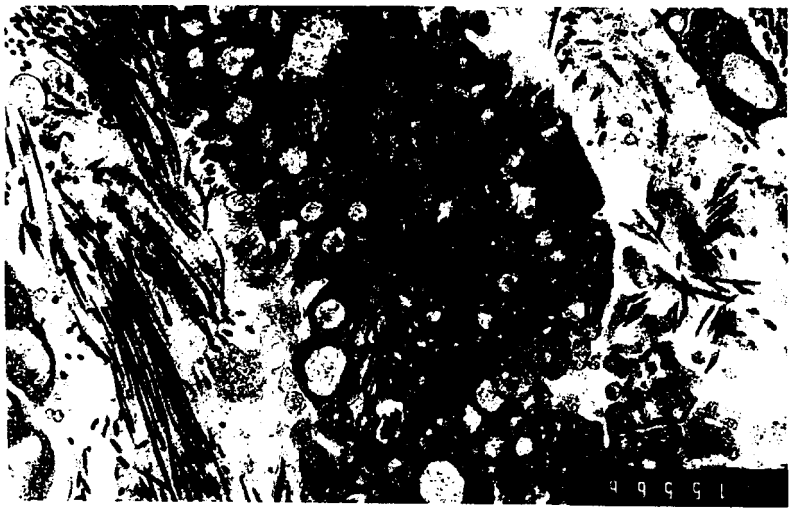

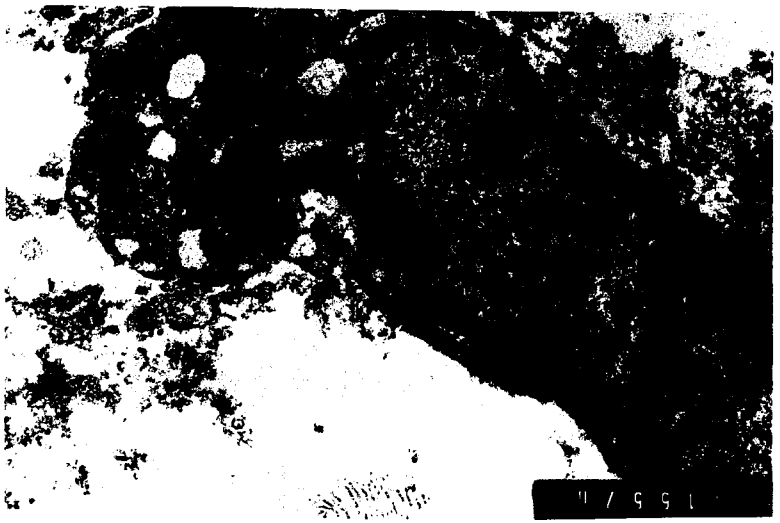

of vaculozation had increased. The nucleus was small in relation to the cytoplasm of the cell and the plasma membrane was diffuse in many areas. Figures 40A and 40B shows cells in the late phase. The cell shown in Figure 40A had a large amount of vaculozation. There no longer existed any RER, normal mitochondria or a discrete plasma membrane. The nucleus was irregularly shaped and showed a significant amount of dense staining around its membrane. The nucleus of the cell shown in Figure 40B was darkly stained almost completely. The cytoplasm of the cell in Figure 40B contained no RER and some vaculozation was present in the center of the cell. A most interesting and meaningful feature of this cell was the swollen and degenerating mitochondria. The spherical shape of the mitochondria was abnormal as was the mitochondrion's cristae. Both cells, Figures 40A and 40B, were in a necrotic state.

Figures 40C and 40D represent cells exposed to 100 ppm corrosion product solutions. The cells shown in Figure 40C represents a middle-to-late phase. It contained dilated RER, swollen mitochondria, a diffuse membrane and dense staining regions along the nuclear membrane. The cell in Figure 40D contained all the features of the late phase - swollen mitochrondria, no RER, increased vaculozation, diffuse membrane, dense staining around the nuclear membrane and total lack of cellular organization. Examination of the ultrastructure of cells in the fibrous capsule showed more direct correlations than the histological evaluations. The severity of response correlated with an increased corrosion product solution injection. Referring to Table 11 and Figures 39 and 40,

several trends are evident. When a greater concentration of corrosion products was injected into the capsule area, a more severe tissue response was observed. When a low concentration, 0 to 3 ppm, was injected, a much milder response was observed. In Table 11, the normal to early phase was observed mostly in cells receiving a 0 to 3 ppm stainless steel corrosion product solution. The late phase was seen mostly in cells receiving a 25 to 100 ppm injections. As the severity of the tissue response increased, there was a decrease in the amount of RER, an increase in vaculozation, an increase in altered organelles such as the mitochondria, and a general loss of cellular organization. Clearly a cell experiencing structural changes of this magnitude will be having extreme difficulty in functioning normally.

The ultrastructure of cultured human gingival fibroblasts (HGF) was also examined. As with the examination of the *in vivo* cells exposed to stainless steel corrosion product solutions, the cultured HGF also had been exposed to stainless steel corrosion solutions of the same concentrations, 3, 25 and 100 ppm. Cells were also examined which had been exposed only to Waymouth's complete medium. After examination of the ultrastructure of the cultured cells, it was determined that a sequence of events leading to cellular necrosis existed for the *in vitro* cells that was quite similar to the sequence found for the *in vivo* cells. Table 12 shows the sequence of events for the *in vitro* cells. This table was constructed in the same manner as Table 11. Similar trends were observed in the *in vitro* cells as were seen with *in vivo* cells. One trend was the relationship between the amount of RER

Table 12

Phases of Cellular Necrosis for In Vitro Cells

Phase (Observed Event)	Concentration	Frequency
I. Normal to Early:		
(Normal RER, normal mitochondria continuous plasma membrane, some increase in vaculozation, some decrease in RER)	Control	100%
	3 ppm	50%
	25 ppm	0%
	100 ppm	0%
II. Middle:		
(Decrease in RER, increase in vaculozation whorls)	Control	0%
	3 ppm	50%
	25 ppm	50%
	100 ppm	0%
III. Late:		
(No RER, extensive vaculozation, whorls)	Control	0%
	3 ppm	0%
	25 ppm	50%
	100 ppm	100%

and the degree of vaculozation, as the amount of RER decreased, the extent of vaculozation increased significantly. The vaculoes also contained a dark staining pigment. These trends can be seen in Figures 41A-D.

Figure 41A shows a cultured HGF exposed only to Waymouth's complete medium. The cytoplasm contained a significant amount of RER and only a small amount of vaculozation. The cultured cells had a more rounded appearance due to trypsinizing the cells prior to fixation. This cell is representative of the normal to early phase. The cell shown in Figure 41B was exposed to a 3 ppm

Figure 41: In Vitro Ultrastructures Resulting From Exposure to the Following 316L Stainless Steel Corrosion Product Solutions (12,000X):

A. 0 ppm (Control)

B. 3 ppm S.S.

C. 25 ppm S.S.

D. 100 ppm S.S.

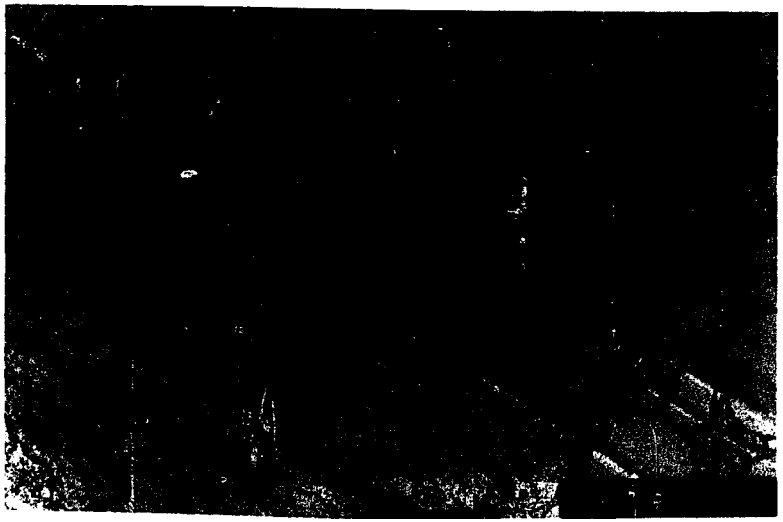

corrosion product solution. The amount of RER was less and discontinuous. Some vaculozation could be seen and the mitochondria had a swollen appearance. These features represented an early phase of cellular necrosis. Figure 41C shows a cell exposed to a 25 ppm solution. In the cell, there was a significant decrease in RER and a definite increase in vaculozation with dark staining pigment. The nucleus contained some dense staining around the nuclear membrane and the mitochondria had a swollen and spherical appearance. This represented a middle phase of cellular necrosis. The cell shown in Figure 41D represented a late phase. In this cell, there was a tremendous amount of vaculozation to the extent that it consumed the entire cytoplasm. The overall appearance of the cell's cytoplasm had a washed out look.

The events experienced by the in vitro cells were similar to the events experienced by the in vivo cells of the fibrous capusle around the implants. For both groups, increasing the concentration of corrosion products resulted in reduced quantities of RER, swollen mitochondria, diffuse plasma membranes and general lack of cellular organization mainly due to the extensive vaculozation that occurred. This similarity of events at the ultrastructura level may increase the basic understanding of cellular reactions under controlled conditions.

CHAPTER IV

SUMMARY AND CONCLUSIONS

Three major alloys used for surgical applications are 316L stainless steel (ASTM F138), Co-Cr-Mo (ASTM F75) and Ti-6Al-4V (ASTM F136). Their corrosion resistance is one reason for being chosen as implant alloys. The overall objective of this investigation was to determine by atomic absorption spectrophotometry the elemental constituents released under passive and accelerated forms of corrosion and to study the tissue response elicited by these constituents utilizing in vitro and in vivo testing procedures.

In vitro testing involved exposing a human gingival fibroblast cell line (HGF) to varying concentrations of synthetic corrosion product solutions based on the alloy's chemical composition. Solutions of the individual elements comprising the alloys were also exposed to the HGF at the same concentrations. The effect of the solutions on the growth rates and the cellular morphologies of the HGF were observed. Alterations of cellular morphologies were examined with optical and transmission electron microscopy.

In vivo testing involved implanting alloy specimens into the back muscles of rabbits and injecting varying concentrations of synthetic corrosion product solutions at the implant to capsule

interface. The tissue responses were examined by optical and transmission electron microscopy.

The following conclusions were made:

1. The in vitro cell culture analyses of synthetic stainless steel corrosion product solutions based on the chemical composition of the alloy demonstrated toxic responses (inhibited growth rates and altered cellular morphologies) at concentrations as low as 3.0 ppm. This solution represents 2 ppm Fe, 0.6 ppm Cr, and 0.42 ppm Ni. Synthetic corrosion product solutions of Co-Cr-Mo demonstrated toxic responses at 1.5 ppm which represents 1.0 ppm Co, 0.45 ppm Cr and 0.09 ppm Mo. Neither Fe, Ni, Co or Mo when tested individually demonstrated toxic responses at these low concentrations. However, chromium demonstrated abnormal morphologies above 0.375 ppm. Chromium was the most toxic element in these two alloys.

   Altered cellular morphologies were demonstrated for the 6.25 ppm Ti-6Al-4V alloy solution which represents in ppm 5.6 ppm Ti, 0.378 ppm Al and 0.25 ppm V. Improved cellular morphologies were observed for the 3 ppm Ti-6Al-4V solution. Individually, the elemental concentrations of the 6.25 ppm solution were nontoxic to the cells, whereas collectively a toxic response was observed. Of the individual elements, vanadium was most toxic and demonstrated abnormal morphologies above a concentration of 0.75 ppm.

2. Transmission electron microscopic analyses of tissue culture cells (in vitro) and cellular capsules (in vivo) showed a correlation between the ultrastructural features of the cells and concentration of corrosion products exposed to the cells. With increasing concentration, the cells showed a decrease in rough endoplasmic reticulum, a more diffuse plasma membrane, an increase in cytoplasmic vaculozation, and a decrease in cellular organization. This trend was consistent for the in vitro and in vivo studies.

3. Histological examinations of fibrous tissue capsules adjacent to alloys revealed a variety of tissue responses. It was not possible to corrleate the severity of tissue response using criteria of fibrous capsule thickness, extent of phagocytic response, and presence of a granuloma with the corrosion product concentration injected at the implant to capsule interface for a particular alloy. However, comparing the tissue response versus implant composition at a particular concentration revealed a more direct correlation. The stainless steel and cobalt base surgical alloys elicited more toxic responses than the titanium base alloys for all of the concentrations investigated.

4. Atomic absorption analyses revealed that the stainless steel and cobalt base alloys corroded preferentially under accelerated corrosion conditions of 0.80 volt vs SCE applied potential for times up to 24 hours. The

stainless steel alloy showed lower chromium concentrations (12.7% vs alloy composition of 19.3%). The cobalt alloy showed lower chromium (22.8% vs alloy composition of 28.4%) and higher cobalt concentrations (74.2% vs alloy composition of 66%). The Ti-6Al-4V alloy did not breakdown at an applied potential of 1.8 volts vs SCE over a period of two weeks.

CHAPTER V

RECOMMENDED FUTURE RESEARCH

The following areas of research are recommended:

1. The valence state of the ions released from alloys investigated could be critical to the tissue responses observed. Investigations should be conducted to determine *in vivo* valence states of released ionic constituents and compare these valence states to the various *in vitro* states.
2. The effects of the corrosion products on the cultured HGF were rated by growth inhibition studies and also by observing alterations in cellular morphologies. A number of enzyme assays are available for determining alterations in metabolic functions. Some of these assays would be beneficial in these studies.
3. Further TEM investigations would be beneficial also. The toxic effects demonstrated by stainless steel and cobalt base surgical alloys were mainly due to the presence of chromium. It would be interesting to observe ultrastructural changes due to chromium and compare these ultrastructural changes with those observed for the stainless steel and cobalt base alloys. Vanadium was the most toxic element investigated for the Ti-6Al-4V alloy.

TEM analyses of tissue exposed to vanadium would be of added value. This could give added insight into the ultrastructural effect these individual ions have on cells.

4. It would be interesting to conduct assays for determining cellular damage and to correlate this information with TEM analyses of the cellular ultrastructures. Combining this information could lead to the formation of a mechanism of cellular injury.
5. Further investigations need to be conducted concerning the corrosion of the alloys under passive conditions. This could be done by increasing the surface area of the alloy under controlled metallurgical conditions and exposing the materials to the electrolyte for longer periods of time. This should increase the quantity of ions released to the electrolyte for the atomic absorption analyses.
6. From this investigation, it was predicted that the cobalt and stainless steel alloys corroded preferentially under accelerated corrosion conditions. More extensive metallurgical investigations with emphasis on surface analyses need to be conducted.
7. The elemental compositions of corrosion products generated in saline were investigated in this study. It has been suggested that organic constituents can alter the corrosion process. The analyses of corrosion products

generated in serum could provide additional information in this area.

BIBLIOGRAPHY

1. T. Albrektsson, P. I. Branemark, H. A. Hansson, and S. Lindstrom, "Osseointegrated Titanium Implants," Acta Orthop. Scanda., 52, 155 (1981).

2. ASTM Designation F75-76, "Standard Specification for Cast Cobalt-Chromium-Molybdenum Alloy for Surgical Implant Applications," Annual Book of ASTM Standards, Part 46, American Society for Testing and Materials, Philadelphia, Pa., 534 (1978).

3. ASTM Designation F138-76, "Stainless Steel Bar and Wire for Surgical Implants (Special Quality)," Annual Book of Standards, Part 46, American Society for Testing and Materials, Philadelphia, Pa., 504 (1978).

4. ASTM, "Report on Stress Corrosion Cracking of Austenitic Chromoium-Nickel Stainless Steels," American Society for Testing and Materials Specification Technical Publications, Philadephia, Pa., 264 (1960).

5. J. Autian, "Toxicologic Aspects of Implants," Journal of Biomedical Materials Research, 1, 433 (1967).

6. D. I. Bardos and H. A. Luckey, "Microstructural Analysis of Biomaterials," Microstructural Science, Part B, American Elsvier Publishing Company, Inc., New York, New York, 951 (1975).

7. V. P. Barranco and H. Schaman, "Eczematous Dermatitis From Nickel," Journal of the American Medical Association, 220, 1244 (1972).

8. A. Baumhammers, H. H. Langkamp, R. K. Matta, and K. Kilbury, "Scanning Electron Microscopy of Epithelial Cells Grown on Enamel, Glass and Implant Materials," Journal of Periodontology, 49, 592 (1978).

9. L. J. Bearden, "The Toxicity of Two Prosthetic Metals (Cobalt and Nickel) to Cultured Fibroblasts," Ph.D. Dissertation, Clemson University, May 1976.

10. O. E. Beder and E. Gilbert, "An Investigation of Tissue Tolerance to Titanium Metal Implants in Dogs," Surgery, 39, 420 (1955).

11. O. E. Beder, J. K. Stevenson, and T. W. Jones, "A Further Investigation of the Surgical Application of Titanium Metal in Dogs," Surgery 41, 1012 (1956).

12. M.K.D. Benson, P. G. Goodwin, and J. Brostoff, "Metal Sensitivity in Patients with Joint Replacement Arthroplastics," British Medical Journal, 4, 374 (1975).

13. J. Black, Biological Performance of Materials, Fundamentals of Biocompatibility, Marcel Decker, Inc., New York, New York, 1981.

14. R. T. Bothe, L. E. Beaton, and H. A. Davenport, "Reaction of Bone to Multiple Metallic Implants," Surgery, Gynecology and Obstetrics, 71, 598 (1940).

15. G. C. Brown, M. D. Lockshin, E. A. Smith, and P. G. Bullough, "Sensitivity to Metal as a Possible Cause of Sterile Lossening After Cobalt-Chromium Total Hip Arthroplasty," Journal of Bone and Joint Surgery, 59-A, 164 1977).

16. S. A. Brown, M. B. Mayor, and K. Merrit, "Metal Sensitivity and Implants; An In Vitro Test," Transactions of the Fifth Annual Meeting of the Society for Biomaterials, 3, 123 (1979).

17. R. M. Browne and M. J. Tyas, "Biological Testing of Dental Restorative Materials In Vitro - A Review," Journal of Oral Rehabilitation, 6, 365 (1979).

18. R. A. Buchanan, J. E. Lemons, C. D. Griffin, N. G. Thompson and L. C. Lucas, "Effects of Carbon Coupling on the In Vitro Corrosion of Cast Surgical Cobalt-Base Alloy," Journal of Biomedical Materials Research, 15, 611 (1981).

19. R. A. Buchanan and J. E. Lemons, "In Vivo Corrosion-Polarization Behavior of Titanium-Base and Colbalt-Base Surgical Alloys," Transactions of the Eight Annual Meeting of the Society for Biomaterials, 5, 110 (1982).

20. J. R. Cahoon, "On the Corrosion Products of Orthopaedic Implants," Journal of Biomedical Materials Research, 7, 375 (1973).

21. J. R. Cahoon, R. Bandyopadhya, and L. Tennese, "The Concept of Protection Potential Applied to the Corrosion of Metallic Orthopaedic Implants," Journal of Biomedical Materials Research, 9, 259 (1975).

22. J. R. Cahoon and H. W. Paxton, "Metallurgical Analyses of Failed Orthopaedic Implants," Journal of Biomedical Materials Research, 2, 1 (1968).

23. E. Campbell, A. Meirowsky, and G. Hyde, "Studies on the Use of Metals in Surgery," Annals of Surgery, 114, 472 (1941).

24. J. Cohen, "Corrosion Testing of Orthopaedic Implants," Journal of Bone and Joint Surgery, 44, 307 (1962).

25. J. Cohen and B. Lidenbaum, "Fretting Corrosion of Orthopaedic Implants," Clinical Orthopaedics and Related Research, 61, 167 (1968).

26. J. Cohen and J. Wulff, "Clinical Failure Caused by Corrosion of a Vitallium Plate," Journal of Bone and Joint Surgery, 54-A, 617 (1972).

27. V. J. Colangelo and N. D. Greene, "Corrosion and Fracture of Type 316 SMO Orthopaedic Implants," Journal of Biomedical Materials Research, 3, 247 (1969).

28. C. L. Comar and F. Brunner, Mineral Metabolism, Part B., Academic Press, Inc., New York, New York, 1962.

29. A. Cornet, D. Muster, and J. H. Jaeger, "Fatigue-Corrosion of Endoprosthesis Titanium Alloys," Biomaterials Medical Devices and Artificial Organs, 7, 155 (1979).

30. M. Cramers and U. Lucht, "Metal Sensitivity in Patients Treated for Tibial Fractures with Plates of Stainless Steel," Acta Orthopaedica Scandanavia, 48, 245 (1977).

31. M. Daniel, J. T. Dingle, M. Webb, and S. C. Heath, "The Biological Action of Cobalt and Other Metals," British Journal of Experimental Pathology, 64, 163 (1963).

32. G. den Otter, "Total Prosthetic Replacement of Arioventricular Valves in the Dog," Thorax, 27, 105 (1972).

33. R. Deutman, J. Mulder, R. Brian, and J. P. Nater, "Metal Sensitivity Before and After Total Hip Arthroplasty," Journal of Bone and Joint Surgery, 59-A, 842 (1977).

34. A. Dooms-Goossens, A. Ceuterick, N. Vanmaele, and H. Degreef, "Follow-up Study of Patients with Contact Dermatitis Caused by Chromates, Nickel, and Cobalt," Dermatologica, 160, 249 (1980).

35. N. W. Elves, J. N. Wilson, J. T. Scales, and H.B.S. Kemp, "Incidence of Metal ensitivity in Patients with Total Joint Replacements," British Medical Journal, 4, 376 (1975).

36. H. Emnéus, "Metal as Material for Osteosynthesis," Acta Orthop. Scanda., 38, 368 (1967).

37. H. Emnéus, U. Stenram, and J. Baecklund, "An X-Ray Spectrographic Investigation of the Soft Tissue Around Titanium and Cobalt Alloy Implants," Acta Orthop. Scanda., 30, 226 (1960).

38. F. Escalas, J. Galante, W. Rostoker, and P. Coogan, "Biocompatibility of Materials for Total Joint Replacement," Journal of Biomedical Materials Research, 10, 175 (1976).

39. E. M. Evans, M.A.R. Freeman, A. S. Miller, and B. Vernon-Roberts, "Metal Sensitivity as a Cause of Bone Necrosis and Loosening of the Prosthesis in Total Joint Replacement," Journal of Bone and Joint Surgery, 56-B, 676 (1974).

40. A. B. Ferguson, Y. Akahoshi, P. Laing, and E.S. Hodge, "Characteristics of Trace Ions Released from Embedded Metal Implants in the Rabbit," Journal of Biomedical Materials Research, 44-A, 323 (1962).

41. A. B. Ferguson, P. G. Laing, and E. S. Hodge, "The Ionization of Metal Implants in Living Tissues," Journal of Bone and Joint Surgery, 42-A, 77 (1960).

42. M. Fontana and N. Greene, Corrosion Engineering, McGraw-Hill, New York, New York, 1978.

43. S. Fregert and H. Rorsman, "Allergy to Chromium, Nickel, and Cobalt," Acta Derm-Vernereol., 46, 144 (1966).

44. J. Galante and W. Rostoker, "Corrosion-related Failures in Metallic Implants," Clinical Orthopaedics and Related Research, 86, 237 (1972).

45. R. S. Gray, "Metallographic Examination of Retrieved Intramedullary Bone Pins and Bone Screws from the Human Body," Journal of Biomedical Materials Research Symposia, 5, 27 (1974).

46. C. D. Griffin, "An In Vitro Electrochemical Corrosion Study of Coupled Surgical Implant Materials," M.S.E. Thesis, University of Alabama in Birmingham, 1979.

47. C. D. Griffin and R. A. Buchanan, "An In Vitro Electrochemical Corrosion Stdy of Coupled Surgica Implant Materials," Transactions of the Twenty-Seventh Annual Orthopaedic Research Society, 6, 167 (1981).

48. T. A. Gruen, and H. C. Amstutz, "A Failed Vitallium/Stainless Steel Total Hip Replacement: A Case Report with Histological and Metallurgical Examination," Journal of Biomedical Materials Research, 9, 465, 1975.

49. D. S. Halpin, "An Unusual Reaction in Muscle in Association with a Vitallium Plate: A Report of Posible Metal Hypersensitivity," Journal of Bone and Joint Surgery, 57-B, 451 (1975).

50. J. W. Harrison, D. L. McLain, R. B. Hohn, G. P. Wilson, J. A. Chalmers, and K. N. MacGowan, "Osteosarcoma Associated with Metallic Implants, Report of Two Cases in Dogs," Clinical Orthopaedics and Related Research, 116, 253 (1976).

51. J. C. Heath, "The Production of Malignant Tumors by Cobalt in the Rat," British Journal of Cancer Research, 10, 668 1956).

52. J. C. Heath and M. R. Daniel, "The Production of Malignant Tumors by Nickel in the Rat," British Journal of Cancer, 18, 261 (1964).

53. J. C. Heath, M.A.R. Freeman and S.A.V. Swanson, "Carcinogenic Properties of Wear Particles From Prostheses Made in Cobalt-Chromium Alloy," Lancet, 1, 564 (1971).

54. L. L. Hench and E. C. Ethridge, "Biomaterials - The Interfacial Problem," Advances in Biomedical Engineering, 5, 35 (1975).

55. A. Hensten-Petersen, "Metal Senstivity," Seminar at University of Alabama in Birmingham, 1982.

56. A Hensten-Petersen and K. Heldgeland, "Evaluation of Biologic Effects of Dental Materials Using Four Different Cell Culture Techniques," Scandanavia Journal of Dental Research, 85, 291 (1977).

57. R. Hicks, P. J. Hewitt, and H. F. Lam, "An Investigation of the Experimental Induction of Hypersensitivity in the Guinea Pig by Material Containing Chromium, Nickel, and Cobalt from Arc Welding Fumes," Archives of Allergy and Applied Immunology, 59, 265 (1979).

58. T. P. Hoar and D. C. Mears, "Corrosion-Resistant Alloys in Chloride Solution: Materials for Surgical Implants," Proceedings of the Royal Society of London, A294, 486 (1966).

59. L. L. Hopkins, "Distribution in the Rat of Physiological Amounts of Injected $Cr^{51(III)}$ with Time," American Journal of Physiology, 209, 731 (1965).

60. W. C. Hueper, "Experimental Studies in Metal Cancerigenesis. I. Nickel Cancers in Rats, Experimental Studies in Metal Cancerigenesis," Texas Report on Biological Medicine, 10, 167 (1952).

61. W. C. Hueper, "Experimental Studies in Metal Cancerigenesis. I. Cancer Produced by Parenterally Induced Metallic Nickel," Journal of the National Cancer Institute, 16, 55 (1955).

62. A. N. Hughes and B. A. Jordan, "Metallurgical Observations on Some Metallic Surgical Implants Which Failed In Vivo," Journal of Biomedical Materials Research, 6, 33 (1972).

63. S. F. Hulbert and J. J. Klawitter, "A Quick Screening Test of Biomaterials by Means of Chick Embryo Techniques," Journal of Biomedical Materials Research, 8, 137 (1974).

64. D. A. Jones, H. K. Lucas, M. O'Driscoli, G.H.G. Price, and B. Wibberley, "Cobalt Toxicity After McKee Hip Arthroplasty," Journal of Bone and Joint Surgery, 57-B, 289 (1975).

65. S. W. King, J. Savory, and M. R. Willis, "Aluminum Toxicity in Relation to Kidney Disorders," Annals of Clinical and Laboratory Science, 11, 337 (1981).

66. W. R. Lacefield and L. L. Hench, "The Bonding of Bioglass to a Cobalt-Chromium Surgical Implant Alloy," Transactions of the Seventh Annual Meeting of the Society for Biomaterials, 4, 74 (1979).

67. P. G. Laing, "Compatibility of Biomaterials," Orthopaedic Clinics of North America, 4, 249 (1973).

68. P. G. Laing, A. B. Ferguson, and E. S. Hodge, "Tissue Reaction in the Rabbit Muscle Exposed to Metallic Implants," Journal of Biomedical Materials Research, 1, 135 (1967).

69. J. Leirskar and K. Helgeland, "A Methodologic Study of the Effect of Dental Materials on Growth and Adhesion of Animal Cells In Vitro," Scandanavia Journal of Dental Research, 80, 120 (1972).

70. J. E. Lemons, L. C. Lucas, R. A. Buchanan, and R. C. Compton, "Metallographic Investigations of Ti-6Al-4V Alloy Total Hip Components," accepted for publication by the American Society for Testing and Materials, 1982.

71. J. E. Lemons, K. M. W. Neimann, and G. H. Adams, "Investigations of Long Term Implant Devices," Transactions of the Seventh Annual Meeting of the Society for Biomaterials, 4, 143 (1981).

72. G. S. Leventhal, "Titanium, A Metal for Surgery," Journal of Bone and Joint Surgery, 33A, 473 (1951).

73. D. L. Levine and R. W. Staehle, "Crevice Corrosion in Orthopeadic Implant Metals," Journal of Biomedical Materials Research, 11, 553 (1977).

74. L. C. Lucas, "An Investigation on the Corrosin Susceptibilities of Multi-Alloy Total Hip Replacements," M.S.E. Thesis, University of Alabama in Birmingham, 1980.

75. L. C. Lucas, R. A. Buchanan, and J. E. Lemons, "Investigations on the Galvanic Corrosion of Multialloy Total Hip Prostheses," Journal of Biomedical Materials Research, 15, 731 (1981).

76. L. C. Lucas, R. A. Buchanan, and J. E. Lemons, "Susceptibility of Surgical Cobalt-Base Alloy to Localized Corrosion," Transactions of the Seventh Annual Meeting of the Society for Biomaterials, 4, 79 (1981).

77. A. McDougall, "Malignant Tumour at Site of Bone Plating," Journal of Bone and Joint Surgery, 38-B, 709 (1956).

78. G. Meachim and D. F. Williams, "Changes in Nonosseous Tissue Adjacent to Titanium Implants," Journal of Biomedical Materials Research, 7, 555 (1973).

79. D. C. Mears, "Electron-Probe Microanalysis of Tissue and Cells From Implant Areas," Journal of Bone and Joint Surgery, 48-B, 567 (1966).

80. V. A. Memoli, J. L. Woodman, R. M. Urban, and J. O. Galante, "Malignant Neoplasms Associated with Orthopeadic Implant Materials," Transactions of the Twenty-Eighth Annual Meeting of the Orthopaedic Research Society, 7, 164 (1982).

81. A. M. Mirza, M. G. Perera, C. A. Maccia, and O. G. Dziubynsky, "Leukocyte Migration Inhibition in Nickel Dermatitis," International Archives of Allergy and Applied Immunology, 49, 782 (1975).

82. M. Mital and J. Cohen, "Toxicity of Metal Particles in Tissue Culture - Part II," The Journal of Bone and Joint Surgery, 50-A, 547 (1968).

83. H. J. Mueller and E. H. Greener, "Polarization Studies of Surgical Materials in Ringers Solution," Journal of Biomedical Materials Research, 4, 29 (1970).

84. B. S. Oppenheimer, E. T. Oppenheimer, I. Danishefsky, and A. P. Stout, "Carcinogenic Effects of Metals in Rodents," Cancer Research, 16, 439 (1956).

85. R. Owen, G. Meachim, and D. F. Williams, "Hair Sampling for Chromium Content Following Chainley Hip Arthroplasty," Journal of Biomedical Materials Research, 10, (1 (1976).

86. A. M. Pappas and J. Cohen, "Toxicity of Metal Particles in Tissue Culture - Part I," Journal of Bone and Joint Surgery, 50-A, 535 (1968).

87. J. S. Pegum. "Nickel Allergy," Lancet, 1, 674 (1974).

88. V. Pirila and K. Kajanne, "Sensitization to Cobalt and Nickel in Cement Eczema," Acta Derm-Venereol, 45, 9 (1965).

89. D. Powell, W. H. Lawrence, and J. Autian, "Development of a Toxicity Evaluation Program for Dental Materials and Products. I. Screening for Irritant Responses," Journal of Biomedical Materials, 4, 583 (1970).

90. T. Rae, "A Study of the Effects of Particulate Metal of Orthopaedic Implants on Marine Macrophages, In Vitro," Journal of Bone and Joint Surgery, 57B, 444 (1975).

91. R. M. Rose, A. L. Schiller and E. L. Radin, "Corrosion-Accelerated Mechanical Failure of a Vitallium Nail Plate," Journal of Bone and Joint Surgery, 54A, 854 (1972).

92. S. A. Rosenbluth, G. R. Weddington, W. L. Guess, and J. Autian, "Tissue Culture Method for Screening Toxicity of Plastic Materials to be Used in Medical Practice," Journal of Pharmaceutical Sciences, 54, 156 (1965).

93. W. Rostoker, C. W. Pretzel, and J. O. Galante, "Couple Corrosion Among Alloys for Skeletal Prostheses," Journal of Biomedical Materials Research, 8, 407 (1974).

94. M. H. Samitz and S. A. Katz, "Nickel Dermatitis Hazards from Prostheses, In Vivo and In Vitro Solubilization Studies," Journal of Dermatology, 92, 287 (1975).

95. J. T. Scales, G. D. Winter, and H. T. Shirley, "Corrosion of Orthopaedic Implants," Journal of Bone and Joint Surgery, British Volume, 41-B, 810 (1959).

96. R. F. Sisca, J. C. Thonard, D. A. Lower, and W. A. George, "Responses of Epithelial-like Cells in Tissue Culture to Implant Materials," Journal of Dental Research, 46, 248 (1967).

97. G. S. Sohal and T. A. Weidman, "Ultrastructural Sequence of Embryonic Cell Death in Normal and Periperally Derived Trachlear Nucleus," Experimental Neurology, 61, 53 (1978).

98. R. S. Solar, S. R. Pollack, and E. Korostoff, "In Vitro Corrosion Testing of Titanium Surgical Implant Alloys: An Approach to Understanding Titanium Release from Implants," Journal of Biomedical Materials Research, 13, 217 (1979).

99. H. Spenser, L. Kramer, P. Osis, E. Wiatrowski, N. Clemontain, and M. Lender, "Effects of Calcium, Phosphorous, Magnesium, and Aluminum on Floride metabolism of Man," Annals of New York Academy of Sciences, 355, 181 (1980).

100. N. Stinson, "The Tissue Reaction Induced in Rats and Guinea Pigs by Polymethylmethacrylate (Acrylic) and Stainless Steel (18/8 MO)," British Journal of Experimental Pathology, 45, 21 (1963).

101. F. W. Sunderman, "Carcinogenic Effects of Metals," Federation Proceedings, 37, 40 (1978).

102. P. Süry and M. Semlitsch, "Corrosion Behavior of Cast and Forged Cobalt-Based Alloys for Double-Alloy Joint Endoprostheses," Journal of Biomedical Materials Research, 12, 723 (1978).

103. S. A. V. Swanson, M. A. R. Freeman, and J. C. Heath, "Laboratory Tests on Total Joint Replacement Prostheses," Journal of Bone and Joint Surgery, 55B, 759 (1973).

104. B. C. Syrett and S. S. Wing, "Pitting Resistance of New and Conventional Orthopaedic Implant Materials - Effect of Metallurgical Condition," Corrosion-NACE, 34, 138 (1978).

105. N. G. Thompson, R. A. Buchanan, and J. E. Lemons, "In Vitro Corrosion of Ti-6Al-4B and 316L Stainless Steel When Galvanically Coupled with Carbon," Journal of Biomedical Materials Research, 13, 35 (1979).

106. D. A. Tilsley and H. Rotstein, "Sensitivity Caused by Internal Exposure to Nickel, Chrome and Cobalt," Contact Dermatitis, 6, 175 (1980).

107. B. F. Trump, J. M. Valigorsky, J. H. Dees, W. J. Mergner, K. M. Kim, R. T. Jones, R. E. Pendergrass, J. Garbos, and R. A. Cowley, "Cellular Change in Human Disease," Human Pathology, 4, 89 (1973).

108. E. J. Underwood, Trace Elements in Human and Animal Nutrition, 3rd ed. Academic Press, New York, New York, 1971.

109. H. vonHolst, P. Collins and L. Steiner, "Titanium, Silver, and Tantalum Clips in Brain Tissue," Acta Neurochirurgica, 56, 239 (1981).

110. C. N. J. Wagner, A. H. Shabaik, D. J. Schurman, and H. C. Amsutz, "Preparation and Characterization of Wear Debris of Orthopaedic Materials for Biocompatibility Studies," Journal of Biomedical Materials Research, 10, 653 (1976).

111. E. D. Weinberg, "Iron and Susceptibility to Infectious Disease," Science, 184, 952 (1974).

112. A. Weinstein, H. Amstutz, G. Pauon, and V. Franceschini, "Orthopaedic Implants - A Clinical and Metallurgical Analysis," Journal of Biomedical Materials Research Symposium, 4, 297 (1973).

113. S. Weisman, "Metals for Implantation in the Human Body," Annals of New York Academy of Sciences, 121, 67 (1959).

114. A. Wennberg, G. Hasselgren, and L. Tronstad, "A Method for Toxicity Screening of Biomaterials Using Cells Cultured on Millipore Filters," Journal of Biomedical Materials Research, 13, 109 (1979).

115. B. E. Wilde, "A Critical Appraisal of Some Popular Laboratory Electrochemical Tests for Predicting the Localized Corrosion Resistance of Stainless Alloys in Sea Water," Corrosion, 28, 283 (1972).

116. H. G. Willert, "Reactions of the Articular Capsule to Wear Products of Artificial Joint Prostheses," Journal of Biomedical Materials Research, 11, 157 (1977).

117. D. F. Williams, "The Reaction of Tissues to Materials, Part III," Biomedical Engineering, 6, 152 (1971).

118. D. F. Williams, "The Selection of Implant Materials" in Implants in Surgery, D. F. Williams and R. W. Roaf, W. B. Sanders Company, Philadelphia, Pennsylvania, (1973).

119. D. F. Williams, "The Deterioration of Materials in Use" in Implants in Surgery, D. F. Williams and R. W. Roaf, W. B. Sanders Company, Philadelphia, Pennsylvania, (1973).

120. D. F. Williams, "The Response of the Body Environment to Implants" in Implants in Surgery, D. F. Williams and R. W. Roaf, W. B. Sanders Company, Philadelphia, Pennsylvania, (1973).

121. D. F. Williams, "Biomaterials and Biocompatibility," Medical Progress Through Technology, 4, 3 (1976).

122. D. F. Williams, "Titanium as a Metal for Implantation, Part I: Physical Properties," Journal of Medical Engineering and Technology, 1, 195 (1977).

123. D. F. Williams, "Titanium as a Metal for Implantation, Part 2: Biological Properties and Clinical Applications," Journal of Medical Engineering and Technology, 1, 266 (1977).

124. D. F. Williams, Biocompatibility of Clinical Implant Materials, Volume I, CRC Press, Inc., Boca Raton, Florida, 1981.

125. D. F. Williams and G. Meachim, "A Combined Metallurgical and Histological Study of Tissue-Prosthesis Interactions in Orthopaedic Patients," Journal of Biomedical Materials Research Symposia, 5, 1 (1974).

126. R. E. Wilsneck, "Quantitative Cell Culture Biocompatibility Testing of Medical Devices and Correlation to Animal Tests," Biomaterials, Medical Devices, and Artificial Organs, 4, 235 (1976).

127. G. O. Winter, "Tissue Reactions to Metallic Wear and Corrosion Products in Human Patients," Journal of Biomedical Materials Research, 5, 11 (1974).

128. C. A. Zapfle, "Human Body Fluids Affect Stainless Steel," Metallurgical Progress, 68, 95 (1955).

APPENDICES

APPENDIX A

Atomic Absorption Parameters

Varian Flame Atomic Absorption Unit

Element	Flame	Wavelength (nm)	Slit Width (μm)	Lamp Current (mA)
Fe	Air-acetylene	248.3	80	10
Ni	Air-acetylene	232	40	10
Cr	Nitrous oxide	357.9	160	7
Co	Air-acetylene	240.7	80	10

Varian and/or Perkin Elmer Graphite Furnace

Element	Flame	Wavelength	Slit Width	Current
Mo	Graphite Furnace	313.3	160	8
Mn	Graphite Furance	279.5	160	5
Ti	Graphite Furnace	364.3	80	10
Al	Graphite Furnace	318.5	160	8
V	Graphite Furnace	309.3	320	10

APPENDIX B, PART I

Calibration Standards for 316L Stainless Steel Corrosion Products Generated Under Pitting Conditions

Fe standards (ppm)	Absorption	r = 0.9995
12.5 ppm	3.0	
25.0	6.0	
50.0	13.0	
100.0	25.0	

Ni standards (ppm)	Absorption	r = 0.9998
6.25	10.0	
12.5	20.0	
25.0	38.5	

Cr standards (ppm)	Absorption	r = 0.9999
2.5	9.0	
5.0	18.0	
10.0	35.0	
25.0	90.0	

Mn standards (ppm)	Absorption	r = .09892
0.75	69.0	
1.5	124.0	
3.0	223.0	

Mo standards (ppm)	Absorption	r = 0.9924
0.1	47.0	
0.25	119.0	
0.5	193.0	
1.0	336.0	
3.0	701.0	

APPENDIX B, PART II

Calibration Standards for 316L Stainless Steel Corrosion Products Generated Under Passive Conditions

Fe standards (ppm)	Absorption	r = 0.9990
0.025	26.0	
0.05	43.0	
0.25	149.0	
0.5	268.0	
1.0	449.0	

Cr standards (ppm)	Absorption	r = 0.9986
0.01	16.0	
0.025	55.0	
0.05	110.0	
0.1	209.0	

Ni standards (ppm)	Absorption	r = 0.9990
0.025	29.0	
0.05	53.0	
0.10	106.0	
0.25	213.0	
1.0	710.0	

Mo standards (ppm)	Absorption	r = 0.9948
0.025	38.0	
0.05	71.0	
0.10	158.0	
0.25	554.0	

Mn standards (ppm)	Absorption	r = 0.9982
0.025	7.0	
0.05	16.0	
0.1	26.0	
0.25	90.0	
0.50	176.0	

APPENDIX B, PART III

Calibration Standards for Co-Cr-Mo Corrosion Products Generated Under Accelerated Conditions

Co standards (ppm)	Absorption	r = 0.9971
6.25	15.0	
12.5	29.0	
25.0	55.0	
50.0	95.0	

Cr standards (ppm)	Absorption	r = 0.9999
2.5	9.0	
5.0	18.0	
10.0	35.0	
25.0	90.0	

Mo standards (ppm)	Absorption	r = 0.9924
0.1	47.0	
0.25	119.0	
0.50	193.0	
1.0	336.0	
3.0	701.0	

APPENDIX B, PART IV

Calibration Standards for Co-Cr-Mo Corrosion Products Generated Under Passive Conditions

Co standards (ppm)	Absorption	r = 0.9986
0.05	55.0	
0.10	106.0	
0.25	280.0	
0.50	512.0	

Cr standards (ppm)	Absorption	r = 0.9986
0.01	16.0	
0.023	55.0	
0.05	110.0	
0.10	209.0	

Mo standards (ppm)	Absorption	r = 0.9948
0.025	38.0	
0.05	71.0	
0.10	158.0	
0.25	554.0	

APPENDIX B, PART V

Calibration Standards for Ti-6A1-4V Corrosion Products Generated Under Accelerated and Passive Conditions

Ti standards (ppm)	Absorption	r = 0.9987
0.1	43.0	
0.25	101.0	
0.5	207.0	
1.0	371.0	

Al standards (ppm)	Absorption	r = 0.9890
0.1	73.0	
0.25	174.0	
0.50	285.0	
1.0	448.0	

V standards (ppm)	Absorption	r = 0.9991
0.025	17.0	
0.05	36.0	
0.10	81.0	
0.25	189.0	

APPENDIX C

Growth Media for HGF Cell Culture Analyses

Waymouths Balanced Salt Solution

50 ml	Waymouth's 10X solution (MB 752/1-Gibco Lab)	
450 ml	Sterile - double-glass distilled H_2O	
5 ml	L-glutamine	(1 ml per 100 ml medium)
5 ml	Antibody	(1 ml per 100 ml medium)
15 ml	7.5% $NaHCO_3$	

Waymouths Complete Medium

450 ml	Waymouths Balanced Salt Solution
50 ml	Heat Inactivated Calf Serum

APPENDIX D

Splitting Cells for Propagation (Sterile Procedure)

1. Start with a confluent monolayer in the tissue culture flask.
2. Decant or aspirate medium from flask.
3. Dilute any remaining serum by rinsing with Waymouth's balanced salt solution - Pour off.
4. Add trypsin (37°C) to cover the bottom of the flask.
5. Incubate the flask in the CO_2 continuous flow incubator (37°C). Check often for monolayer peeling.
6. When cells have become dislodged, centrifuge 10 min at 1000 rpm in 50 ml Falcon tubes.
7. Pour off trypsin.
8. Resuspend pellet in 10 ml Waymouth's complete media.

For tissue culture flasks: Put 2-3 ml of cell suspension in sterile tissue culture flasks and bring the volume up to 20 ml with Waymouth's complete medium.

For 96-well tissue culture plates: Dilute a volume of the cell suspension 1:10 with Waymouth's complete medium. Dispense into each well a 0.2 ml aliquot of the diluted cell suspension.

APPENDIX E

Karnovsky Fixative
(Paraformaldehyde (2%) - Glutaraldehyde (2%) Fixative)

Paraformaldehyde powder:

Dissolve 10 gm powder in 125 ml H_2O by heating to 60-70°C and stiring. Add 5-15 drops IN NaOH while stirring until solution clears. Cool.

25% Charcoal filtered glutaraldehyde - 40 ml

Norit A Charcoal (sigma)
25% Glutaraldehyde (if pH is below 3 do not use)
Put 10 g Norit charcoal in 100 ml of glutaraldehyde
Filter 3 times through the charcoal or until pH is above 5.
After pH > 5, add 0.1N HCl to decrease pH back to 5.

0.15M Phosphate buffer, wash* pH 7.4-7.6 q.s. 500 ml

Final pH = 7.2
Must be used same day prepared.

---

*Buffer Wash (300 mO_sm)

0.15M phosphate buffer$^+$ ph 7.4	1 part
0.3M sucrose (102.69 gm/l DHOH)	1 part

$^+$0.15M Phosphate buffer

23.77 g. $NaH_2\ PO_4\ H_2O$ (monobasic) in 570 ml H_2O

102.44 g. Na_2HPO_4 (dibasic) in 2430 ml H_2O

Combine and bring to 6 liters

APPENDIX F

a. Fibrous Capsule Preparation for TEM Analysis

1. Fix tissues in 2.5% glutaraldehyde solution for 1½-2 hours. All tissues should be cut as thin as possible.

2. Remove glutaraldehyde and store tissues in a 0.1M cacodylate buffer for 4 hours. The buffer should be changed 3 times to ensure complete removal of the glutaraldehyde fixative.

3. The following solution treatments are added after removal of the cacodylate buffer.

1% OsO_4 (osmium oxide)	1 hour
20% alcohol	5 min.
50% alcohol	5 min.
70% alcohol	10 min.
90% alcohol	10 min.
100% alcohol	10 min.
100% alcohol	30 min.
100% alcohol	10 min.

4. After tissue dehydration, these changes of propylene oxide are added.

Propylene oxide	15 min.
Propylene oxide	30 min.
Propylene oxide	15 min.

5. Remove propylene oxide and add a 1:1 propylene oxide to Spurr* mixture for 2 hours.

6. Remove and add a 1:2 propylene oxide to Spurr* mixture and let stand overnight.

*Spurr Medium (All ingredients from Ladd Research Industries, Burlington, Vermont)

Spurr Medium: Ingredients	Amount
VCD (vinylcyclohexene dioxide)	10 gm
D.E.R. 736 (diglycidyl ether of polypropylene glycol epoxy)	6 gm
N.S.A. (nonenyl succinic anhydride)	26 gm+
Dimethylaminoethanol (DMAE)	0.4 gm

+Prior to adding DMAE, the mixture is stirred vigorously.

7. The next day add a full Spurr mixture for 4 hours.

8. Finally, the tissue samples are put into labeled capsules and filled with fresh Spurr medium. The capsules are placed in an oven at 60°C and left overnight. This allows the Spurr Medium to cure for thin sectioning at a later time.

b. Preparation of In Vitro Cells for TEM Analysis

1. Remove Waymouth's controls and synthetic corrosion product solutions.

2. Add 0.5 ml of trypsin (IX) and place in 37C incubator until the monolayer of HGF cells have detached from the bottom of the cell plate.

3. Spin at 500 rpm for 2 min. Remove the trypsin.

4. Add 2.5% gulataraldehyde fixative for 1½ hours.

5. Spin of 1000 1 pm for 5 minutes to remove the glutaraldehyde fixative.

6. Store the cells in 0.1M cacodylate buffer for 4 hours. Change out the buffer 3 times to ensure complete removal of the glutaraldehyde fixative.

7. The remainder of the preparation is the same as steps 3-8 of the fibrous capsule preparation.

APPENDIX G

Fibrous Capsules Ranked as a Function of Specimen Composition

3 ppm Concentrations

Alloy	Implant Site	Fibrous Capsule	Cellular Reaction	Granuloma	Total	Total/ Alloy
Ti-6Al-4V	Left Middle	1.5	1.5	0	3.0	7.0
Ti-6Al-4V	Left Middle	2.0	2.0	0	4.0	
Co-Cr-Mo	Left Proximal	1.5	1.5	0	3.0	8.5
Co-Cr-Mo	Left Middle	2.0	1.5	2.0	5.5	
316L S.S.	Left Middle	1.5	2.0	0	3.5	12.5
316L S.S.	Left Middle	3.0	3.0	3.0	9.0	

25 ppm Concentrations

Alloy	Implant Site	Fibrous Capsule	Cellular Reaction	Granuloma	Total	Total/ Alloy
Ti-6Al-4V	Right Proximal	1.0	2.5	0	3.0	6.5
Ti-6Al-4V	Right Proximal	1.0	2.6	0	3.5	
Co-Cr-Mo	Right Proximal	1.0	1.0	0	2.0	9.0
Co-Cr-Mo	Right Proximal	2.0	2.0	3.0	7.0	
316L S.S.	Right Proximal	1.0	1.5	0	2.5	11.5
316L S.S.	Right Proximal	3.0	3.0	3.0	9.0	

APPENDIX G
(Continued)

Fibrous Capsules Ranked as a Function of Specimen Composition

100 ppm Concentrations

Alloy	Implant Site	Fibrous Capsule	Cellular Reaction	Granuloma	Total	Total/ Alloy
Ti-6Al-4V	Left Distal	2.0	2.0	0	4.0	4.0
Ti-6Al-4V	Left Distal	1.5	2.0	0	3.5	
Co-Cr-Mo	Left Distal	1.5	1.5	0	3.0	6.5
Co-Cr-Mo	Left Distal	2.0	1.5	0	3.5	
316L S.S.	Left Distal	1.5	1.5	0	3.0	10.5
316L S.S.	Left Distal	2.6	3.0	2.0	7.5	

APPENDIX H

Fibrous Capsules Ranked as a Function of Corrosion Product Concentration

Rabbit #4521

Alloy	Implant Site	Concentration of Corrosion Product Injected	Fibrous Capsule Thickness	Cellular Reaction	Granolma	Total
Ti-6Al-4V	Left Proximal	0 ppm (control)	2.5	1.5	0	4.0
Ti-6Al-4V	Left Middle	3 ppm	2.5	1.5	0	4.0
Ti-6Al-4V	Left Distal	100 ppm	2.0	2.0	0	4.0
Ti-6Al-4V	Right Proximal	25 ppm	2.0	1.5		3.5
Ti-6Al-4V	Right Middle	Saline only	-	-	-	-
Ti-6Al-4V	Right Distal	Roughened sample	1.5	3.0		4.5

Rabbit #5048

Alloy	Implant Site	Concentration of Corrosion Product Injected	Fibrous Capsule Thickness	Cellular Reaction	Granolma	Total
Ti-6Al-4V	Left Proximal	0 ppm (control)	1.0	1.0	1.0	3.0
Ti-6Al-4V	Left Middle	3 ppm	1.5	1.5	0	3.0
Ti-6Al-4V	Left Distal	100 ppm	2.0	1.5	0	3.5
Ti-6Al-4V	Right Proximal	25 ppm	2.0	2.0	0	4.0
Ti-6Al-4V	Right Middle	Saline only	2.0	2.0	0	4.0
Ti-6Al-4V	Right Distal	Roughened sample	1.0	2.0	0	3.0

APPENDIX H
(Continued)

Fibrous Capsules Ranked as a Function of Corrosion Product Concentration

Rabbit #4521

Alloy	Implant Site	Concentration of Corrosion Product Injected	Fibrous Capsule Thickness	Cellular Reaction	Granolma	Total
Co-Cr-Mo	Left Proximal	0 ppm (control)	1.5	3.0	3.0	7.5
Co-Cr-Mo	Left Millde	3 ppm	2.0	2.0	2.0	6.0
Co-Cr-Mo	Left Distal	100 ppm	1.5	2.0	0	3.5
Co-Cr-Mo	Right Proximal	25 ppm	1.0	1.0	0	2.0
Co-Cr-Mo	Right Middle	Saline only	1.5	1.5	0	3.0
Co-Cr-Mo	Right Distal	Roughened sample	2.0	1.5	0	3.5

Rabbit #4522

Alloy	Implant Site	Concentration of Corrosion Product Injected	Fibrous Capsule Thickness	Cellular Reaction	Granolma	Total
Co-Cr-Mo	Left Proximal	3 ppm	2.0	2.5	0	4.5
Co-Cr-Mo	Left Middle	0 ppm (control)	2.0	2.0	0	4.0
Co-Cr-Mo	Left Distal	100 ppm	1.5	1.5	0	3.0
Co-Cr-Mo	Right Proximal	25 ppm	2.0	2.0	3.0	7.0
Co-Cr-Mo	Right Middle	Saline only	1.5	2.0	1.0	4.5
Co-Cr-Mo	Right Distal	Roughened sample	1.5	2.6	0	4.0

APPENDIX H
(Continued)

Fibrous Capsules Ranked as a Function of Corrosion Product Concentration

Rabbit #5506

Alloy	Implant Site	Concentration of Corrosion Product Injected	Fibrous Capsule Thickness	Cellular Reaction	Granolma	Total
316L S.S.	Left Proximal	0 ppm (control)	3.0	3.0	2.0	8.0
316L S.S.	Left Middle	3 ppm	3.0	2.6	2.0	7.5
316L S.S.	Left Distal	100 ppm	2.6	2.0	2.0	6.5
316L S.S.	Right Proximal	25 ppm	3.0	3.0	3.0	9.0
316L S.S.	Right Middle	Saline only	1.5	1.5	0	3.0
316L S.S.	Right Distal	50 ppm				

Rabbit #5710

Alloy	Implant Site	Concentration of Corrosion Product Injected	Fibrous Capsule Thickness	Cellular Reaction	Granolma	Total
316L S.S.	Left Proximal	0 ppm (control)	1.0	2.5	0	3.5
316L S.S.	Left Middle	3 ppm	1.5	1.5	0	3.5
316L S.S.	Left Distal	100 ppm	1.5	1.5	0	3.0
316L S.S.	Right Proximal	25 ppm	1.0	1.5	0	2.5
316L S.S.	Right Middle	Saline only	1.0	1.0	0	2.0
316L S.S.	Right Distal	50 ppm	1.0	1.5	0	2.5

GRADUATE SCHOOL
UNIVERSITY OF ALABAMA IN BIRMINGHAM
DISSERTATION APPROVAL FORM

Name of Candidate Linda Chambers Lucas

Major Subject Biomedical Engineering

Title of Dissertation Biocompatibility Investigations of Surgical Implant Alloys

Dissertation Committee:

[signature], Chairman

[signature]

[signature]

[signature]

[signature]

Director of Graduate Program [signature]

Dean, UAB Graduate School [signature]

Date August 9, 1982

PS-1428